Alma Mater Studiorum – Università di Bologna
Libera Università di Bolzano

DOTTORATO DI RICERCA CONGIUNTO IN

Colture Arboree ed Agrosistemi Forestali e Ornamentali

Ciclo XXIV

Settore Concorsuale di afferenza
07/B2 - SCIENZE E TECNOLOGIE DEI SISTEMI ARBOREI E FORESTALI

Settore Scientifico disciplinare
AGR 03 - ARBORICOLTURA GENERALE E COLTIVAZIONI ARBOREE

TITOLO TESI

Carbon fluxes and allocation pattern in an apple orchard

Presentata da: Damiano Zanotelli

Coordinatore Dottorato
Prof. Luca Corelli Grappadelli

Relatore
Prof. Massimo Tagliavini

Correlatore
Dr. Leonardo Montagnani

Esame finale anno 2012

to my mother

INDEX

CHAPTER 1 1

General Introduction 1

1. Overview of the global carbon cycle 2
2. Atmospheric CO_2 and climate change 3
3. The role of terrestrial ecosystems 4
4. General objectives of the thesis 8

References 9

FIGURE captions 12

CHAPTER 2 15

Net primary productivity, allocation pattern and carbon use efficiency in an apple orchard assessed by integrating eddy-covariance, biometric and continuous soil chamber measurements .. 15

1. INTRODUCTION 16
2. MATERIALS AND METHODS 18
   - 2.1 Site description 18
   - 2.2.Experimental set-up 18
   - 2.3 Measurement techniques 19
   - 2.4. R_a assessment 24
   - 2.5 NPP, GPP and CUE estimates 24
   - 2.6 Statistical analysis 25
3. RESULTS 26
   - 3.1 The ecosystem carbon stocks and fluxes 26
   - 3.2 The seasonal C allocation pattern 27
   - 3.3 Independent assessment of NPP, R_a and GPP 28
   - 3.4 CUE: seasonal trend and yearly value 29
4. DISCUSSION 30

4.1 Magnitude of C fluxes 30

4.2 Annual and seasonal C allocation pattern 32

4.3 Independent assessment of NPP, R_a and GPP 33

4.4 Annual and seasonal CUE 34

5. CONCLUSIONS 37

References 38

FIGURE captions 44

TABLES 52

CHAPTER 3 57

Environmental and physiological factors governing C fluxes in an apple orchard 57

1. INTRODUCTION 58

2. MATERIALS AND METHODS 60

2.1 Study Site description 60

2.2 Continuous measurements 61

2.3 Periodic measurements 62

2.4 Gap filling and flux partitioning of CO_2 fluxes 63

2.5 Light response curve 65

2.6 Interaction of C fluxes with environmental variables 65

3. RESULTS 68

3.1 Environmental conditions 68

3.2 NPP and LAI trends 68

3.3 Energy balance (evaluation of eddy covariance measurements) 69

3.4 Diurnal trend of NEE and environmental variables 70

3.5 Light response curve 70

3.6 Interaction of C fluxes with environmental variables 71

3.7 Seasonal and interannual C fluxes 74

4. DISCUSSION 76

4.1 Environmental conditions, NPP and LAI over the considered period 76

4.2 Variation of C fluxes over the season and response to light 77

4.3 Light response curve 78

4.4 Multiple regression approach 79

4.5 Cumulative C fluxes 80
5. CONCLUSIONS 81
References 82
FIGURE captions 88
TABLES 105

CHAPTER 4 109
General conclusions 109
Conclusions 110

Summary 111
Riassunto 113
Zusammenfassung 115
Acknowledgements 117

CHAPTER 1

General Introduction

1. Overview of the global carbon cycle

Carbon (C) on Earth is distributed among four major pools: the atmosphere, oceans, land (soils and vegetation) and sediments and rocks (IPCC 2007, Fig. 1).

Atmospheric carbon, which consists primarily by CO_2, is the smallest but most dynamic of these pools since it is completely replenished every 3-4 years primarily through its removal by photosynthesis and return by respiration.

In the oceans C is present the form of dissolved organic and inorganic carbon and particulate organic carbon, which consists of both living organisms and death material. Most of the carbon is in inorganic forms which are in a pH-dependent equilibrium. The marine biota account for only 3 Gt of C, but they cycle a comparable amount of carbon as do terrestrial ecosystems (Fig. 1, IPCC 2007).

The terrestrial biosphere contains the largest biological reservoir of carbon (Chapin III et al., 2002). There is nearly as much C in the terrestrial vegetation as in the atmosphere, while C in soils is twice as much as in the atmosphere. Terrestrial plant C has a turnover time of about 11 years, compared to 2 to 3 weeks in the oceans and an average time of 25 years for the C in soil. These average turnover times mask large differences among the diverse components of the carbon cycle. Photosynthetically fixed C turns over on a time scale of seconds trough photorespiration. Leaves and roots are replaced over weeks to years and the turnover of wood takes decades to centuries. Components of soil organic matter also have quite different turnover times, with labile forms being respired within minutes and humus having a turnover times of decades to thousands of years (Chapin III et al., 2002).

Carbon in rocks and surface sediments account for well over 99% of Earth´s carbon (Schlesinger, 1997), but cycles of this pools are extremely low, being governed by geological processes associated with the rock cycle which has a turnover time of millions of years.

Anthropogenic activities play a significant role on the global carbon cycle, contributing in increasing the atmospheric carbon pool mainly through the combustion of fossil fuels, the release of CO_2 from carbonate rocks during cement production, through the biomass burning and the decomposition consequent to land use conversion. Together, this three fluxes have a magnitudes of about 6 to 7 Gt C y^{-}

[1], making the human activities the third largest biotically controlled flux of C to the atmosphere (Chapin III et al., 2002, Houghton, 2007)

2. Atmospheric CO_2 and climate change

Atmospheric CO_2 has changed dramatically in Earth´s history, and concentration greater than 3000 ppmv likely have occurred several times in the last hundred of million years. Carbon dioxide concentrations have also been below 300 ppmv, starting from 20 million years ago and most recently just before the beginning of the Industrial Revolution, 150 years ago (Pearson and Palmer, 2000; Siegenthaler et al., 2005). Although there is still disagreement on what was the most significant control factors on CO_2 concentration over long time scale, it is hypothesized that abrupt changes are mainly caused by geological forces which altered atmospheric CO_2 inputs, with process such as volcanism and hydrothermal outgassing, and outputs, through processes such as weathering of silicate minerals and limestone formation or organic carbon burial (Pearson and Palmer, 2000; Chapin III, 2002).

Burning of fossil fuels returns C captured by plants in Earth´s geological history to the atmosphere (IPCC, 2007). New ice core records show that the Earth system has not experienced current atmospheric concentrations of CO_2, as well as other green house gasses (GHG), for at least 650 000 years, that is six glacial-interglacial cycles. During that period the atmospheric CO_2 concentration remained between 180 ppmv (glacial maxima) and 300 ppmv in warm interglacial periods (Sigman and Boyle, 2000; Siegenthaler et al., 2005). It is generally accepted that during glacial maxima, the CO_2 removed from the atmosphere was stored in the ocean. Several causal mechanisms have been identified connecting CO_2 and other greenhouse gases concentration to astronomical, climate, ocean circulation and temperature changes, to biological productivity and nutrient supply, and to interaction with ocean sediments (Sigman and Boyle, 2000). Anthropogenic emissions have caused atmospheric CO_2 to increase exponentially since the beginning of the industrial revolution (Friedlingstein et al., 2010; Peters et al., 2011). CO_2 increase causes an increment of the greenhouse potential of the atmosphere (IPCC, 2007) and makes the emissions of CO_2 the main contributor of anthropogenic climate change (Friedlingstein et al., 2010).

To balance the incoming radiation from the Sun, the Earth must, on average, radiate the same amount of energy to the space and, because of its temperature, it radiates at much longer wavelengths, primarily in the infrared part of the spectrum. Much of this thermal radiation emitted by the land and ocean is absorbed by the atmosphere, including clouds, and reradiated back to the Earth, causing the so-called green-house effect (IPCC, 2007). Greenhouse effect comes from molecules that are more complex and less common respect to the two most abundant gases in atmosphere (N_2 and O_2). Water vapor is the most important greenhouse gas, followed by CO_2 and then by other gases such as methane, nitrous oxide, ozone and several others present in small quantities in the atmosphere but contributing to the total greenhouse effect.

3. The role of terrestrial ecosystems

A comparison between the annual increment in carbon content of the atmosphere and the known emissions shows that only about half of the anthropogenic C that is emitted to the atmosphere remains there. The remaining part is taken up on land or in the oceans and it is referred as the “missing sink” (Schimel, 1995; Chapin III et al., 2002).

Four processes control the uptake of carbon by the world´s oceans: the ocean´s carbon chemistry, the air-sea exchange, the mixing between surface and deep waters, and ocean biology (Houghton et al., 2007). The mechanisms responsible for carbon sinks on land are not as clear as they are for the oceans, and two competing mechanisms have been hypothesized:

- Physiological or metabolic factors affecting rates of photosynthesis, respiration, growth and decay;
- Changes in land use, or management, affecting the mortality of forest stands, the age structure of the forests and hence their rate of assimilation or release of carbon.

The first mechanism implies an interaction effect among several factors that may cause an imbalance between photosynthesis and the release of carbon through respiration which is supposed to lead to an increase in carbon storage. This factors include: *a)* the CO_2 fertilization effect, with several studies reporting an increase in photosynthesis and water use efficiency at high CO_2 levels (e.g. Luo et al., 2006); *b)* the Nitrogen fertilization effect, with the increase of biologically active forms of nitrogen due to huma activities expected to increase net primary production and, hence, terrestrial carbon storage (Magnani et al., 2007; Elser et al., 2007; deVries et al., 2009); *c)* the climate change, with warmer temperatures and changes in soil moisture that may favor an increase in productivity and carbon storage especially at high latitudes (Myneni at al., 1997; Houghton, 2007). However, due to the close interconnection of these processes, it is extremely difficult to attribute the missing sink effect to a single or a combination of these factors (Hyvonen et al., 2007). Moreover, terrestrial sinks also result from the recovery of ecosystems disturbed in the past (Schimel et al., 2000) and up to date there is a lack in the investigation of the combined effect of these two classes of mechanisms: the effects of changing environmental conditions have been ignored in analysis of land use change, and physiological models have generally ignored changes in land use (Houghton, 2007).

Plant ecophysiology is the experimental science which aims to provide causal, mechanistic explanation for ecological question relating to survival, distribution, abundance and interactions of plants with other organisms and environmental factors, including questions originating from agriculture, horticulture, forestry and environmental sciences. Techniques that measures the microenvironments of plants, their water relations and their pattern of carbon exchange became typical tools in plant ecophysiology (Lambers et al., 2008).

The eddy covariance techniques is the most widely used and accepted method to continuously measure CO_2, water and energy exchange between atmosphere and a plant canopy. Nowadays, more than four hundred eddy-covariance sites are recorded as active worldwide, providing defensible estimates of carbon exchange over a wide range of ecosystems (Baldocchi et al., 2003, Luyssaert et al., 2007, FLUXNET). An overview of the basic principles and assumptions of the eddy covariance methodology is given in box 1.

To my knowledge, no eddy covariance site has been established in an apple orchard and only few papers report the use of such technique in fruit tree ecosystems (Rossi et al., 2007; Testi et al., 2008, Navarro et al., 2008). Agricultural ecosystems are estimated to be the largest source of carbon lost to the atmosphere in Europe each year (Janssens et al., 2003) although cropland estimates are the most uncertain among all the land-use type (Smith, 2004). Ciais et al (2010) substantially revised this statement reporting a more neutral role of croplands in carbon emission but confirming that the sequestration of carbon in soils per unit of input is much less efficient in croplands than in other biomes such as grassland and forests, possibly as a result of soil tillage. A conceptual model illustrating C fluxes in agroecosystems is presented in figure 2.

Box 1

Overview of the eddy covariance methodology

The Earth´s surface has a dominating influence on the lowest 100 to 3000 m of the atmosphere, creating the so called boundary layer: a relatively shallow portion of air with rather peculiar characteristics respect to the free atmosphere. The boundary layer may be defined as that part of the troposphere that is directly influenced by the presence of the Earth´s surface, and responds to surface forcing with a time scale of about an hour or less (Stull, 1988). It is the ground that, warming and cooling in response to the solar radiation, forces changes in the boundary layer causing transport processes such as wind, turbulence and wave. The occurrence of turbulence near the ground, very effective in transporting material, is one of the characteristics that make the boundary layer different from the rest of the atmosphere. Turbulence can be visualized as consisting of irregular swirls of motion called eddies, which have different size and are superimposed each other. The relative strengths of these different scales eddies define the turbulence spectrum (Stull, 1988).

The eddy covariance technique samples these turbulent motions to determine the net difference of material moving across the canopy-atmosphere interface (Fig. 1). In practice, this task is accomplished by statistical analysis of the instantaneous vertical mass flux density using Reynolds rules of averaging. The product of this operation is a relationship that expresses the mean flux density of CO_2 (F, µmol $m^{-2}s^{-1}$) averaged over a time span (usually 30 or 60 minutes), resulting from the covariance between fluctuations in vertical velocity (w) and the CO_2 mixing ratio ($c = \rho_c / \rho_a$ where ρ_a is air density and ρ_c is CO_2 density (Baldocchi, 2003)):

$$F = \overline{\rho_a} \cdot \overline{w'c'} \qquad (1)$$

Where the overbars denote time averaging and primes represent fluctuations from the mean (i.e. $w' = w - \overline{w}$). For a micrometeorological convention, a positively signed covariance represent net CO_2 transfer into the atmosphere, and a negative value denotes the opposite.

Eddy covariance is commonly used to measure sensible heat, latent heat and carbon exchange between a specific land surface and the atmosphere. In the case of assessing turbulent transfer of CO_2, the conservation equation is used to deduce the exchange of carbon in and out of the plant–soil system on the basis of eddy covariance measurements made in the surface boundary layer a few meters above the plant canopy. Since turbulence fluctuations occur very rapidly, measurements require sophisticated instrumentation: changes in concentration, density, temperature and wind velocity are often small and need to be measured very fast and with great accuracy (Burba and Anderson, 2011).

In practice, several assumptions are made in the Eddy Covariance method. First, over flat and vast spaces, density fluctuations are safely assumed negligible. Secondly, the mean vertical flow is assumed negligible for horizontal homogeneous terrain so that the classical equation for eddy flux (eq 1) is true.

Older instruments usually do not measure mixing ratio (c') so another assumption is made in the practical formula:

$$F_c = \overline{w'\rho_c'} \qquad (2)$$

That is eq 1 is assumed to be equal to the mean covariance between deviations in instantaneous vertical wind speed and gas density. F_c may then be corrected for heat and water vapor density fluctuations (WPL, Webb et al., 1980; Leuning, 2004). Other assumptions regards the fact that measurements at a point are assumed to represent an upwind area, measurements are assumed to be done inside the boundary layer of interest and fetch and footprint are assumed to be adequate, so that flux is measured only from the area of interest. The degree to which these assumptions hold true depend in part on proper site selection and experiment setup, and in part on atmospheric conditions and weather (Montagnani et al., 2009; Burba and Anderson, 2011).

Flux measurements are affected by several types of errors which needs to be properly corrected. A complete treatment of errors is outside the purposes of this box, however it is worth to mention that there are two families of errors: the first is called frequency response errors and the second which includes errors due to time delay, spike and noises and unleveled instrumentation.

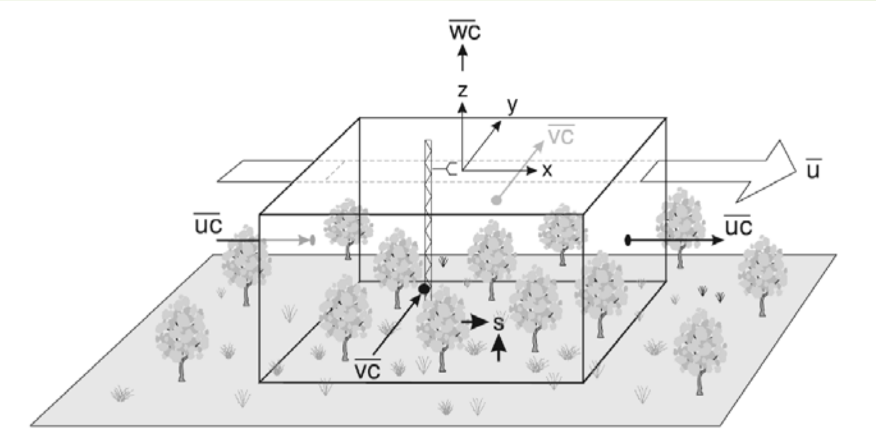

Figure 1. Cartesian control volume placed over a vegetates surface (from Leuning, 2004).

References

Baldocchi D.D., 2003. Assessing the eddy covariance technique for evaluating carbon dioxide exchange rates of ecosystems: past, present and future. *Global Change Biology*, 9: 479-492.

Burba G., Anderson D., 2011. A Brief Practical Guide to Eddy Covariance Measurements: Principle and Workflow Examples for Scientific and Industrial Applications. *LI-COR Biosciences*, Nebraska, USA.

Leuning R., 2004. Measurements of trace gas fluxes in the atmosphere using eddy covariance: WPL correction revisited. In: *Handbook of Micrometorology, A Guide for Surface Gas Measurements and Analysis* [Lee X., Massman W., Law B.], Chapter 6, 139-132. Atmospheric and Oceanographic Sciences, *Kluwer Academic Publishers,* the Netherlands.

Montagnani L., Manca G., Canepa E., Georgieva E., Acosta M., et al., 2009. A new mass conservation approach to the study of CO_2 advection in an alpine forest. *Journal of Geophysical Research-Atmospheres*. 114, D07306.

Stull R.B., 1988. An introduction to Boundary Layer Meteorology. Eds. Atmospheric Sciences Library; *Kluwer Academic Publisher*, The Netherlands.

Webb E. K., Pearman G. I., Leuning R., 1980. Correction of flux measurements for density effects due to heat and water-vapor transfer, *Q. J. Roy. Meteor. Soc*. 106, 85–100.

4. General objectives of the thesis

Despite the large amount of information obtained through continuous eddy covariance measurements on natural ecosystems, less knowledge is available for intensively managed ecosystems, particularly woody-agroecosystems, although some cropping system may assume great importance especially at regional scale (Rossi et al., 2007, Testi et al., 2008). Application of this micrometeorological approach on agricultural stands may be of great help in understanding not only the patterns of agro-ecosystems carbon fluxes, but also their physiological response to environmental parameters and human management practices, thus favoring the transition of agricultural sector toward a higher degree of sustainability.

In the present study, an apple orchard located in the Province of Bolzano (Italy, Fig. 3) was investigated with ecophysiological and micrometeorological approaches. Eddy covariance measurements were carried out for three years (starting in march 2009) and were supported by soil respiration and biometric measurements.

The experimental part of the present work is divided in two chapters (chapter 2 and 3). The main objectives of the first part (chapter 2) are to assesses the magnitude of the carbon fluxes of the apple orchard and compare it with those of natural deciduous forest growing in similar environmental condition, using carbon use efficiency as a comparison index. The differences in the C allocation pattern are also analyzed. In the second part (chapter 3), objectives are to quantitatively assess the carbon exchange fluxes of the apple orchard at different time scales (daily, seasonal and interannual), to partition the net carbon exchange, between its downward (photosynthesis) and upward (ecosystem respiration) components and assess the influence of the main environmental and physiological parameters on the daily values of the three C fluxes.

References

Baldocchi D.D., 2003. Assessing the eddy covariance technique for evaluating carbon dioxide exchange rates of ecosystems: past, present and future. *Global Change Biology*, 9: 479-492.

Buchmann N., Schulze E.D., 1999. Net CO_2 and H_2O fluxes of terrestrial ecosystems. *Global biochemical cycles*, 13(3): 751-760.

Chapin III F. S., Matson P.A., Mooney H.A., 2002. Principles of Terrestrial Ecosystem Ecology, *Springer-Verlag New York*, Inc.

De Vries W., Solberg S., Dobbertin M., Sterba H., Laubhann D., van Oijen M., Evans C., Gundersen P., Kros J., Wamelink G.W.W., Reinds G.J., Sutton M.A., 2009. The impact of nitrogen deposition on carbon sequestration by European forests and heatlands. Forest Ecology and Management, 258(8): 1814-1823.

Elser J.J., Bracken M.E.S., Cleland E.E., Gruner D.S., Harpole W.S., Hillebrand H., Ngai J.T., Seabloom E-W., Shurin J.B., Smith J.E., 2007. Global analysis on nitrogen and phosphorous limitation of primary producers in freshwater, marine and terrestrial ecosystems. *Ecology Letters*, 10: 1135-1142.

FLUXNET, A Global Network Integrating Worldwide CO_2, Water and Energy Measurements. {HYPERLINK http://www.fluxnet.ornl.gov/}

Friedlingstein P., Houghton R.A., Marland G., Hackler J., Boden T.A., Conway T.J., Canadell J.G., Raupach M.R., Ciais P., Le Quére C., 2010. Update on CO_2 emissions. *Nature Geosciences*, 3: 811-812.

Houghton, 2007. Balancing the global carbon budget. *Annual Review Earth Planet Science*, 35: 313-347.

Hyvönen R., Agren G.I., Linder S., Persson T., Cotrufo M.F., Ekblad A., Freeman M., Grelle A., Janssens I.A., et al., 2007. The likely impact of elevated CO_2, nitrogen deposition, increased temperature and management on carbon sequestration in temperate and boreal forest ecosystems: a literature review. *New Phytologist*, 173: 463-480.

IPCC, 2007: Summary for Policymakers. In: *Climate Change 2007: The Physical Sciences Basis*. Contribution of Working Group I to the Fourth Assessment Report of the Intergovernmental Panel on Climate Change [Solomon S., Qin D., Manning M., Chen Z., Marquis M., Averyt K.B., Tignor M., Miller H.L. (eds)] . Cambridge University Press, Cambridge, United Kingdom and New York, NY, USA.

Lambers H. , Chapin III F.S., Pons T.S., 2008. Plant Physiological Ecology. Second Edition. *Springer Science + Businness Media*, LLC, New York.

Luo Y., Hui D., Zhang D., 2006. Elevated CO_2 stimulates net accumulations of carbon and nitrogen in land ecosystems: a meta-analysis. *Ecology*, 87(1): 53-63.

Luyssaert S., Inglima I., Jung M., Richardson A.D., Reichstein M., Papale D., Piao S.L., Schulze E.D., Wingate L., Matteucci G., Aragao L., Aubinet M., et al., 2007. CO_2 balance of boreal, temperate, and tropical forests derived from a global database. *Global Change Biology*, 13: 1-29.

Magnani F, Mencuccini M, Borghetti M, et al., 2007. The human footprint in the carbon cycle of established temperate and boreal forests. *Nature,* 447: 848-850.

Myneni R.B., Keeling C.D., Tucker C.J., Asrar G., Nemani R.R., 1997.Increased plant growth in the northern high latitudes from 1981 to 1991. *Nature*, 398: 698-702.

Navarro M.N.V., Jourdan C., Sileye T., Braconnier S., Mialet-Serra I., Saint-Andre L., Dauzat J., Nouvellon Y., Epron D., Bonnefond J.M., Berbigier P., Rouziere A., Bouillet J.P., Roupsard O., 2008. Fruit development, not GPP, drives seasonal variation in NPP in a tropical palm plantation. *Tree Physiology*, 28:1661-1674.

Pearson P.N., Palmer M.R., 2000. Atmospheric carbon dioxide concentrations over the past 60 million years. *Nature*, 406: 695-699.

Peters G.P., Marland G., Le Quére C., Boden T., Canadell J.G., Raupach M.R., 2011. Rapid growth in CO_2 emissions after the 2008-2009 global finalcial crisis. *Nature Climate Change*, 2: 1-3.

Rossi F., Facini O., Georgiadis T., Nardino M., 2007. Seasonal CO_2 fluxes and energy balance in a kiwifruit orchard. *Italian Journal of Agrometeorology*, 2007(1): 44-56.

Schimel, D. S., 1995. Terrestrial ecosystems and the carbon cycle. *Global Change Biology*, 1: 77–91.

Schimel D., Melillo J., Tian H., McGuire A.D., Kicklinghter D., et al., 2000. Contribution of Increasing CO_2 and Climate to Carbon Storage by Ecosystems in the United States. *Science*, 287: 2004-2006.

Schlesinger W.H., 1997. Carbon balance in terrestrial detritus. *Annual Review of Ecology and Systematics*, 8: 51-81.

Siegenthaler U., Stocker T.F., Monnin E., Lüthi D., Schwander J., Stauffer B., Raynaud D., Barnola J.M., Fischer H., Delmotte V.M., Juzel J., 2005. Stable Cycle-Climate Realtionship During the Late Pleistocene. *Science*, 310: 1313-1317.

Sigman D.M., Boyle E.A., 2000. Glacial/Interglacial variations in atmospheric carbon dioxide. *Nature*, 407: 859-869.

Testi L., Orgaz F., Villalobos F., 2008. Carbon exchange and water use efficiency of a growing, irrigated olive orchard. *Environmental and Experimental Botany*, 63: 168-177.

Smith P., 2004. Carbon sequestration in croplands: the potential in Europe and the global contest. *European Journal of Agronomy*, 20: 229-236.

Ciais P., Wattembach M., Vuichard N., Smith P., Piao S.L., Don A., Luyssaert S., Janssen A., et al., 2010. The European carbon balance. Part 2: croplands. *Global Change Biology*, 16: 1409-1428.

Janssens I.A., Freibauer A., Ciais P., Smith P., Nabuurs G.J., Folbert G., et al., 2003. Europe´s terrestrial biorphere absorbs 7-12 % of European anthropogenic CO_2 emission. *Science* 300: 1538-1542.

FIGURE captions

Figure 1. The global carbon cycle: the natural or unperturbed exchanges (estimated to be those prior to 1750) are shown in black arrows; red arrows represent “anthropogenic” fluxes (from IPCC, 2007). Data of stocks and fluxes are in Gt C y^{-1} (1 Gt = 1 Pg = 10^{15} g).

Figure 2. Conceptual model of the main ecosystem carbon fluxes (adapted for fruit agro-ecosystem from Buchmann and Schulze, 1999). The literal meaning for the common acronyms is also shown.

Figure 3. and geographical location of the experimental orchard where measurements were carried out. The apple production area in the Alto Adige Province is shown in the upper map.

List of figures

Fig. 1

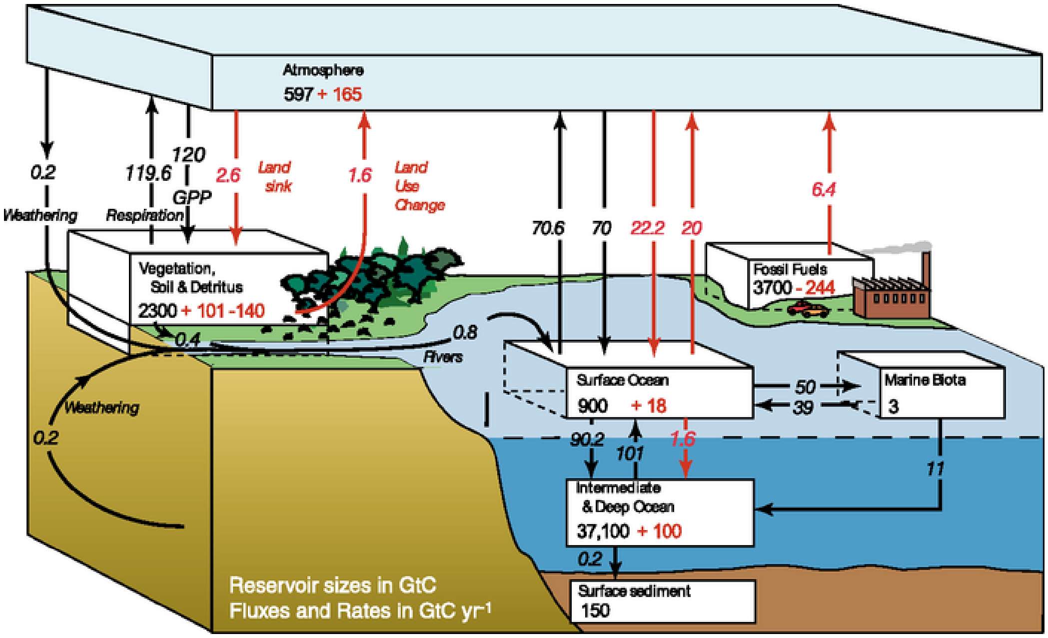

Fig. 2

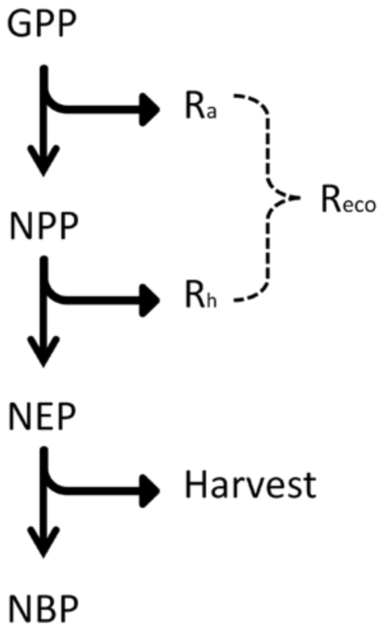

GPP: *Gross Primary Productivity*

NPP: *Net Primary Productivity*

NEP: *Net Ecosystem Productivity*

NBP: *Net Biome Productivity*

R_a: *autotrophic Respiration*

R_h: *heterotrophic Respiration*

R_{eco}: *ecosystem Respiration*

Harvest: *exported fruit production*

Fig. 3

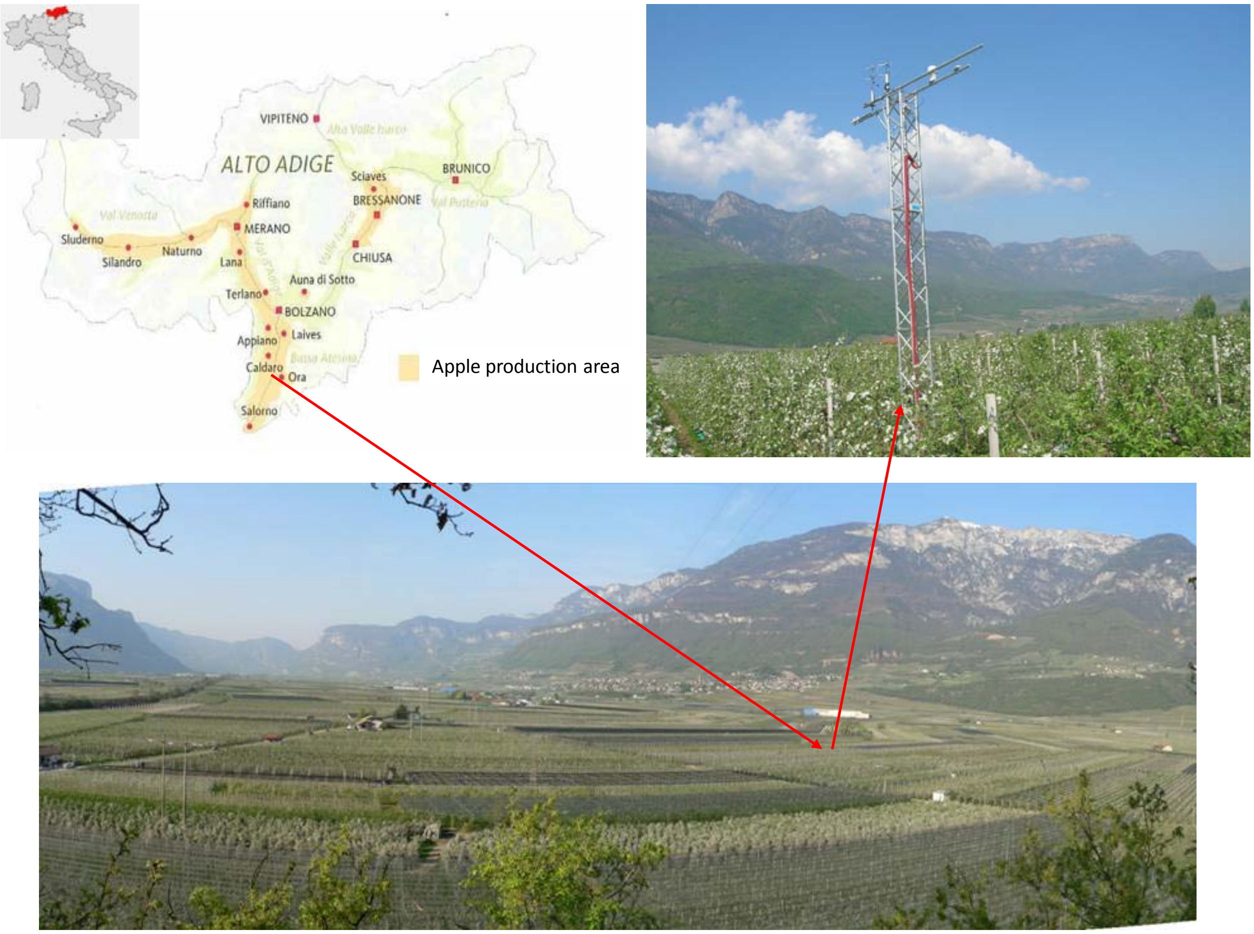
VIPITENO
Alta Valle Isarco
ALTO ADIGE
Sciaves
BRUNICO
BRESSANONE
Val Pusteria
Val Venosta
Riffiano
MERANO
Sluderno
Silandro
Naturno
Lana
Val d'Adige
Valle Isarco
CHIUSA
Auna di Sotto
Terlano
BOLZANO
Laives
Appiano
Caldaro
Bassa Atesina
Ora
Salorno
Apple production area

CHAPTER 2

Net primary productivity, allocation pattern and carbon use efficiency in an apple orchard assessed by integrating eddy-covariance, biometric and continuous soil chamber measurements

1. INTRODUCTION

Global greenhouse gas (GHG) concentration in atmosphere has been growing since pre-industrial times due to anthropogenic forcing, in particular fossil fuel combustion and land use change (Canadell et al., 2007, Le Quere et al., 2009), with carbon dioxide (CO_2) being the most important anthropogenic GHG (IPCC-AR4, 2007; Peters et al., 2011). By sequestering a large amount of atmospheric carbon (C), terrestrial ecosystems are thought to offer a mitigation strategy to reduce global warming (Schimel et al., 2001). This is confirmed by the observation that annual increment of atmospheric CO_2 is substantially smaller than the increment in anthropogenic emission and, on a global scale, it has been estimated that the terrestrial biosphere is able to take up annually about 30% of anthropogenic CO_2 emission (Schulze, 2006; Canadell et al., 2007).

Several studies have been carried out to assess the capacity of ecosystems in different natural biomes to sequester C from atmosphere, most of which related to FLUXNET synthesis activity (Baldocchi, 2008; {HYPERLINK http://www.fluxnet.ornl.gov/}) and results have been recently reviewed in a global dataset (Luyssaert et al. 2007; Schulze et al., 2010). An effective way to compare the ability of different ecosystems to sequester CO_2 from the atmosphere is to determine their carbon use efficiency (CUE). CUE, the ratio of gross primary productivity (GPP) to net primary productivity (NPP), is indeed an intuitive and easily comparable index to assess the capacity of an ecosystem to transfer C from the atmosphere to terrestrial biomass (DeLucia et al., 2007). Increase our knowledge on the magnitudes and spatial distribution of CUE and heterotrophic respiration (R_h), could allow a better linkage of the GPP estimates with those of net ecosystem productivity (NEP), for which reliable climatic and biological predictors at the global scale are still not available.

Despite the great effort carried out on natural ecosystems, less knowledge is available from this ecological point of view regarding intensively managed ecosystems, particularly woody-agroecosystems, although some cropping system may assume great importance especially at regional scale (Testi et al., 2007). Agricultural practices such as soil tillage, fertilization, irrigation and the reduced biodiversity occurring in non-natural ecosystems, may alter significantly ecosystems capacity of exchange C with the atmosphere (Smith, 2004; Osborne et al., 2010) and thus their potential to act as a sink of C when confronted with natural ecosystems growing in similar environmental conditions.

Woody agro-ecosystems are among the least well quantified and most uncertain elements in the terrestrial biogeochemical cycle. In the present study we hypothesize that the main ecosystem carbon fluxes of a woody agro-ecosystem are of the same magnitudes with respect to those of a natural forested ecosystem of the same biome rank (temperate –humid deciduous forest), while the main differences between the two land use types take place in the allocation pattern of fixed C within tree organs.

We investigated an apple orchard (*Malus domestica* Borkh.) growing in a temperate-humid area and confronted with data taken from literature of temperate humid forests (Curtis et al., 2002, Luyssaert et al., 2007, DeLucia et al., 2007). We used CUE as a comparison index and we biometrically measured the NPP of the main ecosystems compartments to assess C allocation pattern. In order to test the robustness of the measured C fluxes involved in CUE determination (GPP, NPP and R_a), we adopted an experimental protocol which allowed us to obtain a double independent estimate of each flux.

2. MATERIALS AND METHODS

2.1 Site description

The study site is located in the intensively cultivated bottom Valley of the Adige river, municipality of Caldaro, South Tyrol, Italy (46°21’ N, 11°16’ E; 240 m a.s.l.). Apple trees (Malus domestica var. Fuji grafted on dwarfing M9 rootstock) have been planted in the year 2000 in a regular frame of 3x1 m, where 1 m is the distance between plants along the line and 3 m is the distance between two lines of trees. Average pruned tree height was 3.6 m. Budburst occurred in the second half of March, trees maximum LAI was 2.8 m^2 m^{-2} in July and major leaf fall started at the end of October. The 30 year average mean annual temperature was 11.5 °C, while mean annual temperature during 2010 was 11.6°C. Total water input for 2010 was 1770 mm, of which 1050 mm from precipitation and 720 mm from irrigation. The soil is a Calcaric Cambisols according to FAO Soil Taxonomy, with a pH of 7.4 and an organic carbon content of 1.74 % in the upper 20 cm. The soil bulk density is 1.49 In the upper 20 cm and 1.52 between 20 and 60 cm. Apple tree plantations with the same characteristics were present around the selected field for a minimum distance of 300 m in all directions.

2.2.Experimental set-up

The site was selected based on the favorable conditions for eddy-covariance (EC) measurement in term of regular terrain and homogeneity of land surface cover. An 8 meter tower was settled up at the beginning of 2009. Instruments for EC measurements were installed at the top of it (see section 2.3.1 for details). Additionally, the tower was equipped with a series of meteorological instruments. Solar radiation components were measured by CNR1, Kipp & Zonen, Delft, Holland; air temperature and relative humidity by CS215, Campbell Scientific Incorporated, Logan, Utah, United States (CSI hereafter), rainfall by a professional rain gauge (RAIN-O-MATIC, Pronamic, Silkeborg, Denmark) and soil water content by multiple TDRs (CS616, CSI). All meteorological data were logged by a CR3000 (CSI).

Close to the tower, 16 collars for soil respiration measurement were placed along a selected tree line, 8 on control plots and 8 on trenching plots. Practical limitation for expanding the survey area on other tree lines were experienced, mostly due to the necessity of not to impede the execution of the normal agricultural practices. This gap was overcome by carrying out a parallel independent campaign for assessing the spatial variability of soil respiration in the field (section 2.3.3 for details).

After a characterization of tree diameters that was conducted over the whole site, six groups of five plants each were selected in order to represent the observed tree diameter probability density distribution. Nets for litter collection were placed under selected trees and biometric measurements were carried out during the 2010 growing season to assess total NPP and carbon allocation within the studied ecosystem (section 2.3.2 for details). Along with measurements and litter collection, 9 branches (3 per plant level) were cut from randomly selected trees and brought to laboratory for analysis at each sampling date. The collected material was used to determine: the mean dry weight of each organ (after drying in oven to a constant weight at 65°C); the mean carbon and nitrogen content of each NPP component (FlashEA™ 1112 Elemental Analyzer, Thermo Fisher Scientific, Germany) and the mean leaf surface (LI-3000 + LI-3050 Portable Area Meters, Li-Cor Biosciences, Lincoln, Nebraska, USA).

2.3 Measurement techniques

2.3.1 Eddy-Covariance CO_2 flux tower measurements

Net Ecosystem Exchange (NEE) of CO_2 was measured continuously by the eddy covariance technique since March 2009. Measurements and calculation were performed following Euroflux methodology as described by Aubinet et al. (2000) with a 3D sonic anemometer (Gill R3-50, Gill-Instruments, Lymington, UK) at a height of 8 m above ground (4 m above the canopy) and a close path CO_2/H_2O infrared gas analyzer (IRGA, LI-7000, Li-Cor Biosciences, Lincoln, Nebraska, USA). Air was sampled trough a polyethylene tube (4 mm inner, 6 mm external diameter) at a distance of 0.3 m from the anemometer with a flux rate of 10 l min^{-1} provided by an external pump (N838 KNDC, KNF Nueberger GmbH, Freiburg, Germany). Calibration was performed bi-weekly with reference gases: Nitrogen and 380 ppm CO_2 flasks (produced by Messer, Grugliasco, Italy), were used to set the zero and the CO_2 span, respectively. Zero-level of CO_2 and H_2O in the reference cell of the analyzer was assured by the use of chemicals (respectively Ascarite II for CO_2 and magnesium perchlorate for water vapor), which were substituted bi-weekly. The software Eddysoft (Kolle and Rebmann, 2007; Mauder et al., 2008) was used to calculate eddy fluxes with the following criteria: no detrending, no high or low pass filtering corrections were used; a two-axis rotation of coordinates was applied each 30 minutes. The software automatically calculated the lag-time for CO_2 at each half-hour to maximize the covariance between fluctuations in vertical wind velocity and gas mole density. In addition, the analysis of stationary conditions for CO_2 turbulent flux and of Integral Turbulent Characteristic (ITC) following Foken and Wichura (1996) was performed.

Gaps in CO_2 flux time series were filled with look-up tables (LUT) based on meteorological and seasonal conditions. The whole year was separated into six bimonthly periods and for each period two different tables were compiled: one for night and one for day time. For both tables quality checked data only were used as input. Average flux for the night time table was calculated using a moving LUT with 15 days sliding windows, compiled for 21 classes of relative soil water content and 26 classes of air temperature. The ranging interval of a meteorological variable in a specific class depended on the ratio between the overall range of the variable in the bimonthly period and the number of classes. Gaps in the fifteen central days of the LUT were filled and then the temporal window of the LUT was moved 15 days ahead. For the daytime the moving LUT was compiled for 26 classes of air temperature and 26 classes of global radiation (Rg). Rg was also used to distinguish day from night (Rg > 20 W m^{-2}).

The partitioning of the observed NEE into gross primary productivity (GPP) and ecosystem respiration (R_{eco}) was achieved through night time LUT used for gap filling. Indeed, day time R_{eco} values during the central time period (15 days) of a nocturnal LUT come from the same LUT and they were chosen according to air temperature and soil humidity for the specific half–hour period.

As a form of control, gap-filling was also performed by the marginal distribution sampling method (Reichstein et al., 2005) using the on-line standard tool ({HYPERLINK http://www.bgc-jena.mpg.de/bgc-mdi/html/eddyproc/index.html}), which accounts for temporal autocorrelation of fluxes, replacing missing-data with the average value under similar meteorological conditions (Reichstein et al., 2005). GPP and R_{eco} calculation was performed using the same tool. The same procedure was also followed using the light response curve approach described by Lasslop and colleagues (2010) and following the selection of the maximal sum of turbulent and storage flux observed at the beginning of the night (van Gorsel et al., 2009).

2.3.2 Biometric measurements

Biometric measurements were conducted over six representative plots following Law et al. (2008). Six NPP components were considered separately: leaves (NPP*l*); fruits (NPP*f*); aboveground woody tissues ($NPPw_{ag}$) which include trunk, branches and shoots; belowground woody tissues ($NPPw_{bg}$) which include coarse roots and the belowground part of trunk; fine roots (NPP*fr*); understory production (NPP*u*). Each of these fluxes was assessed directly and independently. We did not consider in this budget the volatile organic compounds (VOC), non CO_2 carbon emission and root exudates production. Data and samples were collected once a month and the following equation was used to calculate the total NPP produced within each sampling date and in the whole season:

$$\Delta NPP = (L_{t+1} + Sb_{t+1}) - (Sb_t) \qquad (1)$$

Where *L* is the litter collected from the nets and *Sb* is the standing biomass. Variations in C storage within tree organs were not considered beside their relevance. Details on the sampling procedures for each NPP component are described below.

NPP*l* - One plant out of each plot for a total of 6 plants was selected. In April 2010 we divided the plants in 3 levels of height (low= 0 – 120 cm, medium = 120 – 240 cm, high=240-360 cm) to represent within tree vertical variability (e.g. Rayment et al., 2002); we numbered and tagged all the branches and we counted the number of leaves and flowers of each branch.

Three branches per plant level were then chosen, and in the following months, from May till November, number of leaves and fruits of these 9 branches per plant were monitored avoiding any sampling collection. We used the complete characterization done in April to determine a multiplicative factor, specific for each plant level, to upscale measured values to the whole plant. The derived total number of leaves per plant was multiplied by the mean leaf dry weight of that period and thus by leaf carbon concentration to determine the amount of C allocated to leaves.

Leaf abscission was monitored by collecting at the same sampling date the litter from nets placed under each selected plot. NPP*l* was thus calculated using equation 1.

NPP*f* - Once a month, flowers (April) and fruits (from May till October) were counted on the selected branches. The whole number of fruits per plant was counted at harvest (October) and a multiplicative factor calculated from selected branches was considered to account for fruit number reduction due to early drop occurring in the whole plant from fruit setting till harvest, and thus to have an estimate of total fruit number per plant throughout the season. In a similar way as done for the leaves, in order to assess C allocation to fruits, total number of fruits was multiplied with the mean fruit dry weight at each sampling date and for the mean C content. Equation 1 was applied to assess NPP*f*.

NPPw_{ag} and NPPw_{bg} - Monthly records of trees circumferences at 10 cm above grafting points were collected for each plant of the selected plots (n=30). Allometric ($y = ax^b$) equation parameters were determined by excavating 11 apple plants of the same age and size, grown in very similar environmental and soil conditions in a nearby orchard. Since apple trees are pruned each year during winter time, the same plant diameter may lead to a significant difference in aboveground (AG) woody biomass estimate depending on whether allometric equations are fitted over pruned or not pruned trees. To consider this effect, we built a first allometric equation with pruned trees (wood$_{\mathrm{AG\_p}}$) and a second equation with not pruned trees (wood$_{AG\_np}$, see respective parameters in table 1). Based on our measurements, pruning material was quantified in 11.5% of AG woody biomass. To calculate the NPPw_{ag} at monthly time-step, a third allometric equation (wood$_{AG}$, see table 1 for equation parameters) was determined with an initial value (April) on the ordinate set by the equation fitting pruned trees and the final value (November) on the ordinate set by equation fitting un-pruned trees:

$$NPPw_a = a(x_{t+1}{}^b - x_t{}^b) \qquad (2)$$

Where x is the diameter at 10 cm above grafting point, *a* and *b* are parameters of the fitting power equation and t is the time of biometric measurement. When considering wood production over more than one year, the overall procedure results in a saw-tooth diagram.

On the same excavated trees, the belowground (BG) biomass up to a horizontal distance of 15 cm, and up to a vertical depth of 1 m was also determined. This value was integrated in space by considering the coarse roots excavated through soil coring (see below). Coarse roots where considered if >2 mm diameter. Spatial interpolation was performed by ordinary kriging, assuming a maximum root depth of 1 m. A power allometric equation was established to relate diameter and below ground woody organs (wood$_{BG}$). The following equation was then used to estimate NPPw_{bg}

$$NPPw_b = c(x_{t+1}{}^d - x_t{}^d) \qquad (3)$$

Where x is the diameter at 10 cm above grafting point and *c* and *d* are the parameters of the best fitting power equation reported for wood$_{BG}$ in table 1.

NPP*fr* - In March 2010 an intensive soil sampling campaign was carried out in order to assess the mean root biomass and distribution. One plant per plot was selected and 17 soil cores were taken at each of the six plots, along two parallel lines across tree row at different distances from the tree trunk. Each soil core was divided into 3 depth levels: 0-20, 20-40 and 40-60 cm. Each soil sample (n=306) was sieved to extract roots, separating them into coarse (diameter > 2 mm) and fine (< 2 mm) roots. Interpolation in space of fine root density values was performed as for coarse roots.

In order estimate root contribution to detritus cycle, we assumed that all coarse root growth accounted for standing biomass increase and that a constant ratio between fine and coarse roots existed to estimate annual fine roots increment.

In summer 2009, several minirhizotrons were installed in the apple orchard, at a distance of 15, 35, 55 and 150 cm from the tree. They consisted in transparent Plexiglas tubes (8 cm diameter, length = 1 m) inserted into the soil with an angle of 45° for approximately 90 cm, thus exploring a soil depth of 60 cm. Starting from March 18, 2010, root growth was monitored by periodic images collected inside the minirhizotrons by a root scanner (CI-600 Root Scanner, CID-Inc, Camas, Wa, USA). After a first screening of the collected images, 8 representative minirhizotrons were considered for the analysis. To assess fine roots NPP, the relative growth rate was calculated by image analysis (WinRHIZOTRON software, Regent Instruments, Canada). The growth coefficient obtained was applied to the value of initial fine root biomass assessed biometrically. Grass and tree fine roots growing patterns were not distinguished.

NPP*u* - Apple trees were planted in rows. A soil stripe 1.2 m wide centered on the row was kept free of grasses trough periodic tillage. In the inter-row (1.8 m wide) grasses were free to grow, and were cut 3 times along the season. We selected 6 control plots of 1.8 m^2 in the inter row, close to the monitored plants, from which we monthly mowed the aboveground grass production. Root growth, observed with minirhizotrons, was considered together with trees fine roots as NPP_{fr} component (see above). The herbaceous biomass grown along the tree row in periods between tillage events was assumed to be negligible.

2.3.3 Soil respiration measurements

An automatic multichambers CO_2 soil flux measurement system (LI-8100 + LI-8150 with 8 chambers type LI-8100-104; Li-Cor Biogeosciences, Lincoln, Nebraska, USA) was used to measure soil respiration (R_s). Four chambers were kept on the same collars for the whole season, while the other 4 were rotated over 12 different positions on a weekly base. Fluxes in each chamber were taken every half hour. During measurements, CO_2 concentration values were taken every second for a measurement length set up to 2 min and 35 s. The first 45 s were considered as mixing period and excluded from the calculation of the soil CO_2 efflux, which was thus obtained from the linear regression of the increasing CO_2 concentration within the chamber during 1 min and 50 s.

Out of the total 16 positions, 8 were on control plots (to assess R_s) and 8 on trenched plots (to assess R_h). Overall, more than 26000 data points for both R_s and R_h were recorded. As quality control, we used the correlation coefficient of the linear relation between time and CO_2 concentration, discarding values with R^2 below 0.99. Gap-filling was performed on data collected at each collar via LUT method and total S_r and R_h were calculated by summing the gap-filled time series.

In June 2010 a parallel soil respiration measurement campaign has been carried out to assess spatial variability of soil respiration. Six collars (10 cm diameter) have been placed at different distances from the tree in each plot used for biometric measurements (36 total collars) and 7 measurement cycles have been performed for each collar by a second LI-8100 with a LI-8100-102 survey chamber. Observed relation with air temperature was used to upscale continuous soil respiration measurements, localized along a single tree line, to the whole plot.

2.4. R_a assessment

Autotrophic respiration was not measured directly but derived in three independent ways from measurements that relied on different methodologies. The first method follows the equation:

$$R_a = GPP - NPP \qquad (4)$$

where GPP is the EC derived and NPP is assessed biometrically.

The second method follows the equation

$$R_a = R_{eco} - R_h \qquad (5)$$

where the first term is EC-derived and the latter is measured with the soil chamber system.

The third method estimates total R_a multiplying belowground R_a (R_{a_bg}), obtained by subtracting R_h from R_s, per a coefficient ($K = 1+(R_{a\_ag}/R_{a\_bg})$) that accounts for the aboveground component of R_a (R_{a_ag}). The coefficient K was obtained following the model published by Reich et al. (2006) who observed a consistent near–isometric scaling of total and aboveground plant respiration to total and aboveground plant N content across different taxa, environments and experiments.

2.5 NPP, GPP and CUE estimates

Carbon Use Efficiency (CUE) is defined as the ratio between net (NPP) and gross (GPP) primary production. An objective of this work was to assess two independent estimates of this two Carbon fluxes in order to obtain four estimates of annual CUE of the study site.

2.5.1 NPP

NPP was assessed biometrically (NPP_{biom}), by adding together the cumulated values of each NPP component considered in the biometric measurements as explained in session 2.3.2, and by summing the yearly NEP and R_h (NPP_{flux}), thus involving respectively eddy-covariance and soil respiration chamber system. The daily carbon uptake rate was calculated dividing both the cumulated NPP_{biom} and NPP_{flux} at each sampling date per the number of days occurring from the actual sampling date to the previous one.

2.5.2 GPP

The first annual estimate of GPP (GPP_{EC}) was obtained from flux partitioning of eddy covariance detected NEE fluxes (section 2.3.1) while the second yearly GPP value ($GPP_{b\&sc}$) was calculated avoiding any involvement of the eddy covariance methodology by summing NPP_{biom} with the R_a assessed following the third method described in session 2.4. In this case it was possible to estimates the cumulated amount of GPP at each sampling date using only GPP_{EC} values.

2.5.3 CUE

On annual base, CUE was calculated dividing NPP_{biom} and NPP_{flux} per both GPP_{EC} and $GPP_{b\&sc}$, thus obtaining four independent estimates of this index. To assess the seasonal trend of CUE, NPP_{biom} and NPP_{flux} values at each sampling were divided by only the respective GPP_{EC} amount.

2.6 Statistical analysis

Additive and multiplicative errors in this study were calculated by means of the error propagation theory (Taylor, 1982). When two means (X and Y) with their standard error of the mean (SEMx and SEMy) were added yielding the value Z, the standard error of Z (SEMz) was calculated as follow:

$$SEM_z = \sqrt{(SEM_x)^2 + (SEM_y)^2} \tag{5}$$

While if X and Y were multiplied, the resulting SEMz was calculated as follow:

$$SEM_z = Z \times \sqrt{\frac{(SEM_x)^2}{X} + \frac{(SEM_y)^2}{Y}} \tag{6}$$

3. RESULTS

3.1 The ecosystem carbon stocks and fluxes

Data relative to the stocks of carbon in the apple orchard at the beginning of the growing season (March 2010) are reported in Table 2. Soil resulted by far the highest carbon pool, containing much more carbon than the standing biomass (17.2 vs. 1.0 kg C m^{-2}). Within the standing biomass, 60 % was above and 40 % was allocated belowground.

3.1.1 Fluxes from eddy covariance

Figure 1 shows the daily ecosystem carbon fluxes of the apple orchard for the year 2010 assessed via eddy-covariance. Budburst occurred the 18th of March and NEE started to become negative (sink of C) during the first decade of April. The maximum NEP was 7.21 g C $m^{-2}d^{-1}$ (25 June) while daily NEE returned to be positive (source of C) in the first decade of November, when leaf abscission was almost complete and only inter-row grasses were photosynthesizing. On a yearly basis, GPP, R_{eco}, and NEP accounted respectively for 1263 ± 189, 883 ± 160 and 380 ± 30 g C $m^{-2}y^{-1}$. For this study, gap-filling and flux partitioning were done with LUT method. Uncertainties were determined as standard error obtained from comparison with other interpolation algorithms and flux partitioning methods. Following Reichstein et al., 2005, NEP was 351, GPP 1074 and R_{eco} 723 g C $m^{-2}y^{-1}$. Following Lasslop et al., 2010, these values were respectively 512, 945, and 433 g C $m^{-2}y^{-1}$.

3.1.2 Fluxes from soil respiration system

Soil respiration (R_s) and its heterotrophic component (R_h) fluxes over the season are shown in Fig 2. Yearly cumulated R_s was 1118 ± 91 and R_h was 691 ± 156 (mean ± *se*) g C m^{-2}.

According to results from the spatial variability campaign (Fig. 3), we calculated a reduction factor of 0.768 to be applied to the flux values obtained with the fixed multiplexed chambers, and up-scaled R_s and R_h accounted respectively for 859 ± 70 and 530 ± 42 g C $m^{-2}y^{-1}$. To assess the robustness of these estimates, parameters of Q10 and Lloyd and Taylor model have been calculated (Tab. 3) and with both models the yearly amount of R_s and R_h where within the uncertainty expressed above.

3.1.3 Fluxes from biometric sampling

The total NPP assessed biometrically (Tab. 4) was 960 ± 70 g C $m^{-2}y^{-1}$ of which 52 % is represented by fruit component (495 ± 35 g C $m^{-2}y^{-1}$). Leaves, which are deciduous, represent 11% of total NPP (106 ± 5 g C $m^{-2}y^{-1}$). Fine roots production was 14% of NPP (130 ± 28 g C $m^{-2}y^{-1}$). Assuming that fine roots increment follows the same growth pattern of the coarse roots, C allocated to standing fine roots is 6 ± 1 g C $m^{-2}y^{-1}$ (4.5% of NPP*fr*), while the remainder 124 ± 27 g C $m^{-2}y^{-1}$is supposed to be shed annually and to feed the detritus cycle.

NPP allocated to above ground woody organs like trunk and branches (NPPw_{ag},) was 173 ± 53 g C $m^{-2}y^{-1}$ (18% of total NPP); the largest part of this component is given by pruned wood feeding the detritus cycle (147 ± 45 g C $m^{-2}y^{-1}$), while only 26 ± 8 g C $m^{-2}y^{-1}$ represent the increment of standing wood biomass.

Carbon allocated to belowground structural organs accounted for only 1% of total NPP (NPPw_{bg} = 13 ± 3 g C $m^{-2}y^{-1}$). Grass production of the understory (NPP*u*) was 42 ± 3 g C $m^{-2}y^{-1}$, 4 % of total NPP.

Summarizing the fate of NPP components, we obtained that 45 ± 9 g C $m^{-2}y^{-1}$ represent an increase in standing wood biomass, 471 ± 35 g C $m^{-2}y^{-1}$ are exported, and 444 ± 53 g C $m^{-2}y^{-1}$ are feeding the detritus cycle.

3.1.4 The carbon cycle

All the C fluxes measured on a yearly base within the ecosystem during 2010 are shown in Figure 4. The only flux not directly assessed in the present study was the autotrophic respiration (R_a), which was determined indirectly as described in session 2.4. The value reported in Fig. 4 (396 ± 166 g C $m^{-2}y^{-1}$) refers to the average ± *se* of the three models presented in table 5.

3.2 The seasonal C allocation pattern

Results of the biometric measurements of NPP are shown in Figure 5 and in Table 6 with related uncertainties. Right after budburst (from March 18th to April 20th), fine roots represented the most significant component of total observed growth (56% of total NPP), while when averaged over the whole year the incidence of this component (130 ± 28 g C m^{-2}) was 14% of total NPP.

Leaves growth occurred mostly between April and early June. From April 20th till May 11th were produced 50 ± 3 of 110 ± 5 g of C m^{-2}, 47% of total leaf biomass produced in the year. In that period, leaves represented 44 % of total NPP.

The relative growth of woody organs, which include trunk, branches and shoots, was larger during spring and early summer (21% of total NPP) and decreased to 8% from mid August till the end of the season. Parameters obtained by fitting the allometric equations were respectively 229.3 (a) and 1.61 (b) for un-pruned aboveground biomass, 202.9 (a) and 1.61 (b) for the pruned aboveground biomass; 46.7 (c) and 1.77 (d) for the below-ground biomass.

From June till the harvest, fruits represented the highest sink of C of the entire ecosystem. C allocation to this organ was more than 65% of total NPP in July and August and more that 75 % of total NPP in September and October. At harvest, carbon allocated to fruits was 495 ± 35 g C m^{-2}, 52% of total NPP.

Understory primary production was a significant component of total NPP, accounting for 42 ± 3 g C m^{-2}, the 5% of total NPP, with a relatively constant growth rate throughout the season.

3.3 Independent assessment of NPP, R_a and GPP

The equation NPP + R_a = GPP shows relation among these three fluxes and their importance for the determination of CUE (NPP: GPP ratio). In this study, the yearly amount of each of these three C fluxes was obtained following at least two independent pathways.

3.3.1 NPP_{biom} and NPP_{flux}

Results of biomass accumulation of the considered ecosystem components at each sampling date are reported in table 6, while in figure 6 are shown the daily carbon uptake rate of both NPP_{biom} and NPP_{flux}. Daily NPP_{biom} showed a less regular annual pattern of C uptake respect to NPP_{flux}, which was well bell shaped. Maximum daily NPP occurred from mid June till mid July for both NPP_{biom} (7.80 ± 2.18 g C $m^{-2}d^{-1}$) and for NPP_{flux} (6.76 g C $m^{-2}d^{-1}$).

Although some discrepancies emerge when confronting the two curves (NPP_{flux}-NPP_{biom}= -2.9 g C $m^{-2}d^{-1}$ in May, -1.5 g C $m^{-2}d^{-1}$ in September, + 1.3 C $m^{-2}d^{-1}$ in November) , we found a good agreement between these two independent methods of determining NPP, confirmed by the surprisingly close value of yearly NPP_{biom} and NPP_{flux} values, which were respectively 960 ± 68 and 910 ± 51 g C $m^{-2}y^{-1}$.

3.3.2 R_a

As mentioned above, R_a was the only element of the C cycle which was not measured directly. Each of the three equations applied implies the integration of different methodologies and lead to sensible different estimates of R_a (tab 5). Following model 1, R_a was 303± 201 g C $m^{-2}y^{-1}$, a value close to model 2 which leads to a R_a of 353 ± 165 g C $m^{-2}y^{-1}$. The third method, based on the up scaling of soil autotrophic respiration (R_s-R_h) and thus relying only on soil chamber methodology, is significantly higher respect to the previous two, resulting in an estimate of total R_a of 533 ± 132 g C $m^{-2}y^{-1}$.

3.3.3 GPP_{EC} and $GPP_{B\&S}$

On a yearly basis, it was possible to estimate GPP independently from EC measurements. $GPP_{B\&S}$ was obtained summing NPP_{biom} with R_a determined by model 3 of table 7, therefore relying only on biometric and soil chamber measurements. While GPP_{EC} was 1263 ± 189 g C $m^{-2}y^{-1}$, $GPP_{B\&S}$ resulted approximately 200 g C $m^{-2}y^{-1}$ greater (1493 ± 150 g C $m^{-2}y^{-1}$).

3.4 CUE: seasonal trend and yearly value

We assessed the seasonal trend of CUE in two partially independent ways (CUE_{biom} and CUE_{flux}, Fig 7). We obtained these CUE values by dividing respectively NPP_{biom} and NPP_{flux} by GPP derived from flux partitioning of EC measured NEE, that was the same in both the estimates.

Significant differences between the two estimates occurred at the beginning of the growing season and at its end, after harvest. When analyzed separately, CUE_{biom} showed an irregular pattern with a decreasing trend throughout the season, while CUE_{flux} showed its highest values during the summer months. In both cases, CUE was above 0.5 for the whole growing season. Based on results shown in the previous sections, on yearly basis we obtained four independent estimates of CUE (tab 7) that returned an average value of CUE for the apple orchard of 0.68 ± 0.10.

4. DISCUSSION

4.1 Magnitude of C fluxes

The first hypothesis of this study was that the main ecosystem C fluxes of a woody agro-ecosystem have the same order of magnitude of natural forest ecosystems growing in the same biome rank. Table 8 shows a comparison between meteorological and biological variables measured at the study site and at the temperate-humid deciduous forests reported in the global forests database published by Luyssaert et al. (2007). Regarding the mean stand characteristics, it appears clearly that apple trees are smaller in size (height, AG and BG biomass), which is reflected in a smaller LAI. Climate characteristics of the stand are very similar to the average observed in temperate-humid forests, with the exception of summer precipitation, that in the studied ecosystem is conditioned by irrigation, a practice that eliminates major stress due to drought in the summer period. Based on our results, EC ecosystems carbon fluxes (GPP, NEP and R_{eco}) obtained in the studied agro-ecosystem are quantitatively similar to a forested stand. We obtained GPP and R_{eco} values slightly smaller and a larger NEP, but differences where within 100 g C $m^{-2}y^{-1}$.

The estimate of R_h was obtained by measuring R_s from trenching plots. This methodology for separating microbial and root respiration is widely applied for its simplicity and low cost although it is affected by several disadvantages (Subke et al., 2006; Lamberty et al., 2011). Among them, the most important is probably the fact that part of the measured C may come from decomposition of roots that are excised during the trenching (Hanson at al., 2000). We avoided accounting for the “priming effect” due to an excess of decomposable matter (Kuzyakov et al., 2000) starting the measurements approximately 10 months after the trenching plots were set. Another problem could rise because of the higher soil water content of trenching respect to control soil, due the absence of root absorption. This may cause a change in the microbial community and in the rate of CO_2 emission (Dìaz-Pìnes et al., 2010) that we prevented starting from June 2010 by installing plastic shelter approximately 1 meter above trenching. Small trenching have also being indicated to act as a sink for CO_2 from surrounding soil (Rachpal et al., 2006), thus causing an overestimation of R_h. Despite all these limitations of the trenching approach and the assumptions that need to be made, the metaanalytical review published by Subke (et al., 2006) reports a general good agreement among different methodologies in soil respiration partitioning, reinforcing the reliability of our estimates.

A different source of error may be the limited amount of replicates from which we estimated R_h. Rodeghiero and Cescatti (2007) indicated in 30 the number of sampling points needed to properly account for the spatial variability of Rs. Since we had a limited number of trenched plots, we derived total Rh from the ratio between Rs and Rh observed by continuous chamber measurements, and then we extrapolated Rh to the whole stand based on an independent measurement campaign of Rs carried out over 42 collars from which we calculated a constant multiplicative factor of 0.768 to be applied to continuous measurements.

The ratio R_h/R_s obtained in the present study (0.62) is within the range of the studies carried out over temperate forests, as reviewed by Subke et al. (2006), while the absolute value of our average estimates of R_h (530 ± 42 g C $m^{-2}y^{-1}$) is higher respect to the average R_h obtained by Luyssaert (et al., 2007) for temperate humid deciduous forests (387 ± 4 g C $m^{-2}y^{-1}$, Tab.3). Besides uncertainties of the methodology itself, this fact may also be due to a relatively high soil organic carbon content and to the superficial soil tillage which was periodically carried out along apple trees stripe (1.2 m wide) to control the growth of grasses below the trees, a common practice in an organic production system (Reganold et al., 2001, Smith, 2004).

The protocol that has been used to biometrically assess NPP, accounts for four (out of 6) hierarchical levels of the framework for net primary production that were proposed by Luyssaert and colleagues (2007). We did not account for root exudates component and non-CO_2 carbon emission (VOC, CO, CH_4) and thus, besides uncertainties in the estimates of the other NPP components, the biometric value we found (960 ± 68 g C $m^{-2}y^{-1}$) is very likely to be an underestimation of the real NPP. There are few reliable estimation of the magnitude for root exudates component and non-CO_2 carbon emission on total NPP in literature (Grayston et al., 1996, Millard et al., 2007) and are often accounted as missing NPP due to the intrinsic difficulty of their direct assessment (Luyssaert et al., 2007) under field conditions. In the review of 14-C labeling studies on plant-soil interactions published by Farrar et al. (2003) it is suggested that exudation may account for 5-10 % of net C assimilation although Jones et al. (2004) revisited this estimation to 2-4% and other studies pose the accent on the dependency of root exudates amount to plant species, soil type and fertility and other climatic variables (Cheng et al., 2007, Jones et al., 2009). NPP found in this study, was about 200 g C $m^{-2}y^{-1}$ higher respect to natural forests of the same biome rank reported in table 8. The presence of a large amounts of fruits on an apple tree is known to enhance specific leaf photosynthesis as a consequence of their role of sink that allow a more rapid download of photosynthates from the phloem (Giuliani et al., 1997).

We conclude this section stating that if yearly C exchange of natural and not natural ecosystems is of comparable entities, net primary production in our fruit tree ecosystem was consistently higher respect to deciduous forest.

4.2 Annual and seasonal C allocation pattern

The second hypothesis of this study was that the main differences between natural and agricultural woody ecosystems are in the allocation pattern of fixed C instead of in a different magnitudes of C fluxes. Results from this study confirm that hypothesis, highlighting how this agro-ecosystem is strongly oriented to fruit production. While deciduous forest of temperate humid biomes allocate the fixed C primarily into leaves, wood and roots, with an incidence (based on data of tab 8, Luyssaert et al., 2007) on total NPP of 30, 43 and 27 %, respectively, these three NPP components in the studied orchard accounted for only 11, 18 and 15% of total NPP, with fruits being by far the major NPP contributor (495 ± 35 g C $m^{-2}y^{-1}$, 52% of total NPP). When analyzing the seasonal trend of C allocation pattern, it was noticed that roughly 70 % of the leaves are set within 2 months after bud burst, while aboveground woody organs show a constant growth until mid August. Most of root NPP is due to fine roots production, since apple tree are grafted on dwarfing rootstock and thus new coarse roots production is rather limited. Fine roots show a first peak of growth in April (55% of total NPP*fr*) and a second lower peak in June (21% of NPP*fr*). Their growth is very limited during summer while a third period of growth was observed in October after fruit harvest (16% of NPP*fr*). These results are consistent with findings published by Eissenstadt et al. (2006). Apple orchard is also interested by important lateral flows of C due to human activities which are occurring, with a different magnitude, in both input and output direction. As input lateral C input, we must consider the organic fertilization, a common agricultural practice repeated every year for ensuring the reintegration of exported mineral nutrients, which accounted for about 35 g C $m^{2}y^{-1}$. The output lateral C flow is quantitatively much more important since it is represented by the harvested apples (equal to 74 t ha^{-1} fresh weight) which are taken away from the ecosystem for commercial purposes. In 2010 this component has been quantified in 471 ± 35 g C $m^{-2}y^{-1}$ (95% of NPP*f*), while the remaining 5% is accounted by early drops and uncollected fruits (24 ± 3 g C $m^{-2}y^{-1}$) entering the detritus cycle. The estimated fruit production is consistent with the yields observed in this area of intense apple production. The fate of the C contained in the abscised leaves of apple trees during their decomposition on soil surface has been reported by Tagliavini et al. (2007) who showed that approximately 80% of initial amounts are lost in the first two years after leaf abscission. Ventura et al. (2009) reported that decomposition of peach leaf litter is complete after 3 years and about 10% of initial amounts of leaf C are likely to be transformed into more stable C forms in the soil.

Our findings are consistent with other studies on apple trees of different growing conditions and varieties (Palmer, 1988; Minchin et al., 1997; Faqi et al., 2008), while the incidence of fruit production on total NPP was found also in other agro-ecosystems as coconut palm plantation (Navarro et al., 2008), peach (Chalmers and van den Ende, 1975) orange (Liguori et al., 2009) and kiwifruits orchards (Rossi et al., 2007). For comparison with other croplands see Ciais et al. (2010).

The fate of allocated carbon is partially different from forests, with a fraction of C exported from the ecosystem through apple production representing nearly half of total net primary production. About 46% of annual NPP production feeds the detritus cycle, and this is similar to natural forests if tree mortality is not considered (e.g. Tan et al., 2010), giving an ample potential for the soil of the fruit tree ecosystem to act as a net carbon sink. The amount of NPP which increases the standing biomass, contributing to ecosystem C storage function (5% of total NPP), is conversely much lower than in forests. The value obtained strongly relies on assumptions done on fine roots mortality (Section 3.1.3) and not on a direct assessment. However, results obtained in studies on apple tree fine root turnover (Wells and Eissenstat, 2001) are quantitatively consistent, and give us confidence on the method used for computation.

4.3 Independent assessment of NPP, R_a and GPP

The methodological approach carried out in the present study gave the opportunity to assess C fluxes involved in CUE determination through independent pathways. This allowed a cross check of the estimated fluxes thus obtaining an important feedback on the robustness of the estimation.

NPP was assessed by using only biometric measurements of different ecosystem components (NPP_{biom}) and through the sum of CO_2 fluxes obtained by EC (NEP) and soil chamber (R_h) methodology (NPP_{flux}). Regarding the latter method, it is important to specify that we rely on the assumption that organic C content in trenching plots was constant throughout the season. The seasonal trend, as well as the yearly cumulated value, were very close each other, supporting the reliability of the methodological approach.

Since no direct measurements of R_a were carried out, a multiple approach was applied to assess this component of the carbon fluxes. As shown in table 5, R_a was estimated by coupling: (i) EC with biometric measurements (GPP-NPP), (ii) EC with soil chamber measurements (R_{eco}-R_h) and (iii) only via soil chambers measurements ($1.62*R_{a\_soil}$). The difference between the results of the latter method and the previous two, highlights the most important discrepancy we registered in the present study, which is due to the relatively higher amount of C fluxes obtained via soil chambers, respect to the EC derived

R_{eco}, problems which are reported also in other studies (Ryan et al., 1997, Law et al., 1999). EC measurements may be affected by a series of different systematic and random errors (Baldocchi 2003, Richardson et al., 2006) which may lead to uncertainties in the yearly NEE estimate as well as the derived R_{eco} and GPP. We tried several methodologies for the gap filling and flux partitioning procedure of our dataset ranging from MDS (Reichstein et al., 2005), light response curve (Lasslop et al., 2010), LUT (Moffat et al., 2007; Rossini et al., 2010 and present study) and the method described by van Gorsel et al. (2009). Since the yearly amount of R_s measured by our multiplexed system was consistent with other published data (Blanke et al., 1995; Koerber et al., 2009; Ceccon et al., 2011) and we are quite confident on the result from biometric measurements (NPP_{biom}), LUT was the methodology which gave the most reliable estimate of EC derived GPP and R_{eco} and we adopted it as the reference method using the estimates from other methods to assess flux uncertainty.

The third method to assess R_a allowed us to obtain a second estimate of yearly GPP, completely independent from eddy covariance measurements ($GPP_{B\&S} = Ra_s + NPP_{biom}$). This resulted to be higher respect to GPP_{EC} by approximately 200 g C m^{-2} y^{-1}, suggesting an underestimation of C fluxes with EC.

4.4 Annual and seasonal CUE

The hypothesis that CUE is constant among forests (Gifford, 1994, 2003; Dewar et al., 1998; Ryan et al., 1997) with a possible appropriate universal value of 0.47 (Waring et al., 1998), has been recently rejected by De Lucia and colleagues (2007) who reported a systematic large variation of CUE among forest types (from 0.23 to 0.83) over a wide range of published data. They conclude however that further studies which rely on independent estimates of NPP and GPP are needed to speculate on the ratio of R_a with photosynthesis or biomass. Amthor (2000) suggested a theoretical possible interval of CUE between 0.2 and 0.65, confirmed also by experimental results on herbaceous species by van Iersel (2003), with crops having generally a higher value respect to “natural” vegetation (Amthor, 1989). In the present study, two independent estimate of both NPP and GPP are provided, with CUE ranging from 0.61 to 0.76 (average = 0.68 ± 0.10).

The high CUE value found in this agro-ecosystem suggests that a relatively low value of plant respiration (R_a) is occurring. A possible explanation may be found in both structural characteristics of the orchard and climatic conditions of the site. Regarding the first aspect, despite understanding of plant R_a is still incomplete and poorly parameterized into current models (Piao et al, 2010), several studies (Ryan et al., 1997, Arneth et al., 1998, Law et al., 1999) highlighted the importance of the biomass composition of the forest stand in determining the total R_a, with foliage respiration having the greatest incidence on total Ra when considered over unit of biomass. In our case, leaves represent only the 11% of total NPP respect to the average value of 30% for deciduous forests (n=32) calculated from the database of Luyssaert et al. (2007). By contrast, a large fraction of growth and biomass in crops is allocated in storage organs such as seeds and tubers which have a relatively small growth respiration and a usually low maintenance respiration (Amthor, 2000). In our case, 52% of NPP was represented by fruits. Apples have a specific dark respiration rate which is high during early cell division period after bloom and rapidly decline as growth by cell expansion begins (Jones, 1981; Bepete and Lakso, 1997). Our findings confirm the hypothesis that apple trees have relatively low autotrophic respiration compared to many other plants due to low constructions costs of fruits (Lakso et al., 1999). The fact that apple trees grafted on dwarfing rootstocks like in our study orchard have a relatively small tree framework and root system, likely contributes to explain the high value of CUE. Additionally, the low Nitrogen content of apple fruits (0.29%) associated with their elevated incidence on total plant biomass (33 ± 7 %), supports the theory of Reich et al. (2006; see also Ryan et al., 1996) who observed an almost linear correlation between total plant nitrogen and total plant respiration, confirmed also considering only the aboveground plant nitrogen and respiration. The low respiratory costs observed in the orchard may be thus correlated with a relatively low nitrogen content of the orchard biomass compared with forests.

Regarding climatic conditions that may contribute to high CUE, following findings of Piao et al. (2010), and related debate (Enquist, 2011; Chen et al., 2011), the mean annual temperature (MAT) of our site (11.5°C) is very close to the MAT (~ 11°C) at which occurs, at global scale, the minimum Ra: GPP ratio over a wide range of ecosystems, thus suggesting a possible role of temperature in controlling autotrophic respiration. In addition, optimal conditions of water availability prevents CUE rise due to drought (Metcalfe et al., 2010).

This study allowed assessing the seasonal trend of CUE, using both NPP_{biom} and NPP_{flux} over the same GPP_{EC} respective value. According to Campioli et al. (2010), it is important to specify that the variability of GPP estimates over a short period depending on the selected partitioning method may have a great effect on the CUE value, thus making difficult to speculate on the absolute values observed along the season in each estimate, which in our case was occasionally above the unit. As shown in Figure 7, the greatest discrepancy between the two curves of CUE_{biom} and CUE_{flux} occurs in spring, particularly in the first two months after budburst where NPP_{biom} estimate was greater than NPP_{flux} and in autumn, when the opposite was observed (Fig. 6). Since the C stored in reserve organs was not measured, we interpreted this results as a clear sign remobilization (Mauler et al., 2004; Millard et al., 2007), with apple trees using stored carbohydrates in the first two months after budburst and likely re-allocating C to storage organs after harvest. Although a spring peak of CUE followed by a quick decline after May was observed by Campioli (et al., 2011) in a temperate beech forest, in our case the NPP: GPP ratio was high also throughout the summer mainly due to the continue biomass accumulation in fruits and thus suggesting a minor accumulation of nonstructural soluble carbohydrates respect to what is occurring in forests (Hoch et al., 2003).

5. CONCLUSIONS

This study carried out on an apple orchard allowed to demonstrate how the main ecosystem carbon fluxes of a fruit tree ecosystem have a comparable magnitude with respect to deciduous forest growing at the same climate conditions. The main difference between the two natural and agricultural ecosystems reside in the allocation pattern of fixed C, with fruits representing approximately half of total yearly NPP in the orchard while reproductive organs are often even not considered in forests. The high amount of fruit biomass may be a possible explanatory reason of the high CUE found for the orchard, because of both the low respiratory costs of fruits and their low nitrogen content. Other possible explanation may be the good environmental and cultural conditions of the orchard, given the optimal mean annual temperature and optimal water availability which occurred at the experimental study site. The seasonal trend of CUE obtained with two partially independent methods allowed to highlight the remobilization effect occurring in spring and in autumn.

We believe that the protocol adopted and the cross checked results obtained in this study are important in order to correct the C estimates and the modeling approach over woody agro-ecosystems in temperate areas.

References

Amthor J.S., 1989. Respiration and crop productivity. New York: Springer Verlag.

Amthor J.S., 2000. The Mc Cree-de Wit-Penning de Vries-Thornley respiration paradigms: 30 Years Later. *Annals of Botany*, 86: 1-20.

Arneth A., Kelliher F.M., McSeveny T.M., Byers J.M., 1998. Net ecosystem productivity, net primary productivity and ecosystem carbon sequestration in a *Pinus radiata* plantation subject to soil water deficit. *Tree Physiology*, 18: 785-793.

Aubinet M., Grelle A., Ibrom A., Rannik Ü., Moncrieff J. B., Foken T., Kowalski, A.S., Martin, P.H., et al., 2000. Estimates of the annual net carbon and water exchange of forests: The EUROFLUX methodology. *Advances in Ecological Research*, 30: 113–175.

Baldocchi D.D., 2008. 'Breathing' of the terrestrial biosphere: Lessons learned from a global network of carbon dioxide flux measurement systems. *Australian Journal of Botany* **56**(1) 1–26

Bepete M., Lakso A.N., 1997. Apple fruit respiration in the field: Relationship to fruit growth rate, temperature and light exposure. Acta Horticulture 451: 319-326.

Blanke M.M., 1995. Soil respiration in an apple orchard. *Environmental and Experimental Botany*, 36 (3): 339-348.

Campioli M., Gielen B., Gökede M., Papale D., Bouriaud O., Granier A., 2011. Temporal variability of the NPP-GPP ration at seasonal and interannual time scales in a temperate beech forest. *Biogeosciences*, 8: 2481-2492.

Canadell J.G., Le Quéré C., Raupach M.R., Field C.B., Buitenhuis E.T., Ciais P., Conway T.J., Gillett N.P., Hougton R.A., Marland G., 2007. Contributions to accelerating CO_2 growth from economic activity, carbon intensity and efficiency of natural sinks. *Proceeding of the National Academy of Sciences*, 104 (47): 18866-18870.

Ceccon C., Panzacchi P., Scandellari F., Prandi L., Ventura M., Russo B., Millard P., Tagliavini M., 2011. Spatial and temporal effects of soil temperature and moisture and the relation to fine root density on root and soil respiration in a mature apple orchard. *Plant and Soil*, 342: 195-206.

Chalmers D.J., van den Ende B., 1975. Productivity of Peach Trees: Factors Affecting Dry-weight Distribution During Tree Growth. *Annals of Botany*, 39: 423-432.

Chen A., Piao S., Luyssaert S., Ciais P., Janssen I.A., Friedlingstein P., Luo Y., 2011. Forest annual carbon cost: reply. *Ecology*, 92 (10): 1998-2002.

Cheng W., Gershenson A., 2007. Carbon fluxes in the rhizosphere. *The Rhizosphere, An ecological perspective*, chapter 2 , 29-54.

Ciais P., Wattenbach M., Vuichard N., Smith P., Piao S.L., Don A., Luyssaert S., Janssens I.A., Bondeau A., Dechow R., Leip A., Smith P.C., Beer C., van den Werf S., Gervois S., van Oost K., Tomelleri E., Freibauer A., Schulze E.D., 2010. The European carbon balance. Part 2: croplands. *Global Change Biology*, 16: 1409-1428.

Curtis P.S., Hanson P.J., Bolstad P., Barford C., Randolph J.C., Schmid H.P., Wilson K.B., 2002. Biometric and eddy-covariance based estimates of annual carbon storage in five eastern North American deciduous forests. *Agricultural and Forest Meteorology*, 113: 3-19.

De Lucia E., Drake J.E., Thomas R.B., Melers M.G., 2007. Forest carbon use efficiency: is respiration a constant fraction of gross primary production? *Global Change Biology*, 13: 1157-1167.

Dewar R.C., Medlyn B.E., McMurtrie R.E., 1998. A mechanistic analysis of light and carbon use efficiencies. *Plant, Cell and Environment*, 21: 573–588.

Dìaz-Pìnes E., Schindlbacher A., Pfeffer M., Jandl R., Boltenstern S.Z., Rubio A., 2010. Root trenching: a useful tool to estimate autotrophic soil respiration? A case study in an Austrian mountain forest. *European Journal of Forest Research*, 129: 101-109.

Eissenstat D.M., Bauerle T.L., Comas L.H., Lakso A.N., Neilsen D., Neilsen G.H., Smart D.R., 2006. Seasonal patterns of root growth in relation to shoot phenology in grape and apple. *Acta Horticulture*, 721: 21-26.

Enquist B.J., 2011. Forest annual carbon cost: comment. *Ecology*, 92 (10): 1994-1998.

Faqi W., Haibin L., Baosheng S., Jian W., Gale W.J., 2008. Net primary production and nutrient cycling in and apple orchard – annual crop system in the Loess Plateau, China: a comparison of Quinguan apple, Fuji apple corn and millet production subsystems. *Nutrient Cycling in Agroecosystems*, 81:95-105.

Farrar J., Haves M., Jones D.L., Lindow S., 2003. How roots control the flow of carbon to the rhizosphere. *Ecology*, 84 (4): 827-837.

Foken T., Wichura B., 1996. Tools for quality assessment of surface-based flux measurements. *Agricultural and Forest Meteorology*, 78: 83-105.

Gifford R.M., 1994. The global carbon cycle: a viewpoint on the missing sink. *Australian Journal of Plant Physiology*, 21(1): 1-15.

Gifford R.M., 2003. Plant respiration in productivity models: conceptualization, representation and issues for global terrestrial carbon-cycle research. *Functional Plant Biology*, 30: 171–186.

Giuliani R., Nerozzi F., Magnanini E., Corelli-Grappadelli L., 1997. Influence of environmental and plant factors on canopy photosynthesis and transpiration of apple trees. *Tree Physiology*, 17: 637-645.

Grayston S.J., Vaughan D., Jones D., 1997. Rhizosphere carbon flow in trees, in comparison with annual plants: the importance of root exudation and its impact on microbial activity and nutrient availability. *Applied Soil Ecology*, 5: 29-56.

Hanson P.J., Edwards N.T., Garten C.T., Andrews J.A., 2000. Separating root and microbial contribution to soil respiration. A review of methods and observations. *Biogeochemestry*, 48: 115-146.

Hoch G., Richter A., Körner C., 2003. Non-structural carbon compounds in temperate forests trees. *Plant, Cell and Environments*, 26: 1067-1081.

Intergovernmental Panel on Climate Change, 2007. AR-4, Climate Change, Synthesis Report. *Contribution of Working Groups I, II and III to the Fourth Assessment Report of the Intergovernmental Panel on Climate Change.* IPCC, Geneva, Switzerland, pp 104.

Jones D.L., Hodge A., Kuzyakov Y., 2004. Plant and mycorrhizal regulation of rhizodeposition. *New Phytologist*, 163: 459-480.

Jones D.L., Nguyen C., Finlay R.D., 2009. Carbon flow in the rhizosphere: carbon trading at the soil-root interface. *Plant Soil*, 321: 5-33.

Jones H.G., 1981. Carbon Dioxide Exchange of Developing Apple (Malus pumila Mill.) Fruits. *Journal of Experimental Botany*, 32(6): 1203-1210.

Koerber G.R., Jones G.E., Hill P.W., Canals L.M., Nyeko P., York E.H., Jones D.L., 2009. Geographical variantion in carbon dioxide fluxes from soils in agro-ecosystems and its implication for life cycle assessment. *Journal of Applied Ecology*, 46: 306-314.

Kolle O., Rebmann C., 2007. Eddysoft – Documentation of a Software Package to Acquire and Process Eddy Covariance Data. Technical Reports, pp. 88, Max-Planck Institut für Biogeochemie, Jena, Germany.

Kuzyakov Y., Friedel J.K., Stahr K., 2000. Review of mechanisms and quantification of priming effects. *Soil Biology & Biochemestry*, 32: 1485-1498.

Lakso A.N., Wünshe J.N., Palmer J.W., Grappadelli L.C., 1999. Measurement and modeling of carbon balance of the apple tree. Horticultural Science, 34(6): 1040-1047.

Lambert B.B., Bronson D., Bladyka E., Gower S.T., 2011. A comparison of trenched plots techniques for partitioning soil respiration. *Soil Biology & Biochemestry*, 43: 2108-2114.

Lasslop G., Reichstein M., Papale D., Richardson A.D., Arneth A., Barr A., Stoy P., Wohlfahrt G., 2010. Separation of net ecosystem exchange into assimilation and respiration using a light response curve approach: critical issue and global evaluation. *Global Change Biology*, 16: 187-208.

Law B., Arkebauer T., Campbell J.L., Chen J., Sun O., Schwartz M., van Ingen C., Verma S., 2008. Terrestrial Carbon Observations: Protocol for Vegetation Sampling and Data Submission. TCO panel of the Global Terrestrial Observing System (GTOS - 55), {HYPERLINK http://www.fao.org/gtos/ }.

Law B.E., Ryan M.G., Anthoni P.M., 1999. Seasonal and annual respiration of ponderosa pine ecosystem. Global Change Biology, 5: 169-182.

Le Quéré C., Raupach M.R., Canadell J.G., Marland G., Bopp L., Ciais P., Conway T., et al., 2009. Trends in the sources and sinks of carbon dioxide. *Nature geoscience*, advance online publication, DOI: 10.1038/NGEO689.

Liguori G., Gugliuzza G., Inglese P., 2009. Evaluating carbon fluxes in orange orchards in relation to planting density. *Journal of Agricultural Science*, 147: 637-645.

Luyssaert S., Inglima I., Jung M., Richardson A.D., Reichstein M., Papale D., Piao S.L., Schulze E.D., Wingate L., Matteucci G., Aragao L., Aubinet M., et al., 2007. CO_2 balance of boreal, temperate, and tropical forests derived from a global database. *Global Change Biology*, 13: 1-29.

Mauder M., Foken T., Clement R., Elbers J.A., Eugster W., Grünwald T., Heusinkveld B., Kolle O., 2008. Quality control of CarboEurope flux data – Part II: Inter-comparison of eddy-covariance software, *Biogeosciences,* 5: 451-462.

Maurel K., Leite G.B., Bonhomme M., Guilliot A., Rageau R., Pétel G., Sakr S., 2004. Trophic control of bub break in peach (Prunus persica) trees: a possible role of hexoses. *Three Physiology*, 24: 579-588.

Metcalfe D. B., Meir P., Aragao L. E. O. C., Lobo-do-Vale R., Galbraith D., Fisher R. A., Chaves M. M., Maroco J. P., da Costa A. C. L., de Almeida S. S., Braga A. P., Gonçalves P. H. L., de Athaydes J., da Costa M., Portela T. T. B., de Oliveira A. A. R., Malhi Y., William M., 2011. Shifts in plant respiration and carbon use efficiency at a large-scale drought experiment in the eastern Amazon. *New Phytologist* 187: 608–621.

Millard P., Sommerkorn M., Grelet G., 2007. Environmental change and carbon limitation in trees: a biochemical, ecophysiological and acosystem appraisal. *New Phytologist*, 175: 11-28.

Minchin P. E. H., Thorpe M.R., Wünshe J.N., Palmer J.W., Picton R.F., 1997. Carbon partitioning between apple fruits: short- and long-term response to availability of photosynthate. *Journal of Experimental Botany*, 48(312): 1401-1406.

Moffat A.M., Papale D., Reichstein M., Hollinger D.Y., Richardson A.D., Barr A.G., Beckstein C., et al., 2007. Comprehensive comparison of gap-filling techniques for eddy covariance net carbon fluxes. *Agricultural and Forest Meteorology*, 147: 209-232.

Navarro M.N.V., Jourdan C., Sileye T., Braconnier S., Mialet-Serra I., Saint-Andre L., Dauzat J., Nouvellon Y., Epron D., Bonnefond J.M., Berbigier P., Rouziere A., Bouillet J.P., Roupsard O., 2008. Fruit development, not GPP, drives seasonal variation in NPP in a tropical palm plantation. *Tree Physiology*, 28:1661-1674.

Osborne B., Saunders M, Walmsley D., Jones M., Smith P., 2010. Key questions and uncertainties associated with the assessment of the cropland greenhouse gas balance. *Agriculture Ecosystems & Environment*, 139-3, 293–301.

Palmer, J.W., 1988. Annual dry matter production and partitioning over the first 5 years of a bed system of Crispin-M27 apple trees at four spacings. *Journal of Applied Ecology*, 25: 569-578.

Peters G.P., Marland G., Le Quéré C., Boden T., Canadell J.G., Raupach M.R., 2011. Rapid growth of CO_2 emission after the 2008-2009 global financial crisis. *Nature climate change*, 2: 1-3.

Piao S., Luyssaert S., Ciais P., Janssen I.A., Chen A., Cao C., Fang J., Friedlingstein P., Luo Y., Wang S., 2010. Forest annual carbon cost: a global scale analysis of autotrophic respiration. *Ecology*, 91 (3): 652-661.

R Development Core Team, 2008. R: A language and environment for statistical computing. *R Foundation for Statistical Computing*. Vienna, Austria. ISBN 3-900051-07-0, {HYPERLINK http://www.R-project.org }.

Rachpal S.J. and T.A. Black, 2006. Estimating heterotrophic and autotrophic soil respiration using small area trenching plot technique: Theory and Practice. Agricultural and Forest Meteorology 140, 193-202.

Reganold J.P., Glover J.D., Andrews P.K., Hinman H.R, 2001. Sustainability of tree apple production systems. *Nature*, 410: 926-930.

Reich P.B., Tjoelker M.G., Machado J.L., Oleksyn J., 2006. Universal scaling of respiratory metabolism, size and nitrogen in plants. *Nature*, 439 (26): 457-461.

Reichstein M., Falge E., Baldocchi D., Papale D., Aubinet M., Berbigier P., Bernhofer C., Buchmann N., et al., 2005. On the separation of net ecosystem exchange into assimilation and ecosystem respiration: review and improved algorithm. *Global Change Biology*, 11: 1424-1439.

Rodeghiero M., Cescatti A., 2007. Spatial variability and optimal sampling strategy of soil respiration. *Forest Ecology and Management*, 255: 106-112.

Rossi F., Facini O., Georgiadis T., Nardino M., 2007. Seasonal CO2 fluxes and energy balance in a kiwifruit orchard. *Italian Journal of Agrometeorology*, 2007(1): 44-56.

Rossini M., Meroni M., Migliavacca M., Manca G., Cogliati G., Busetto L., Picchi V., Cescatti A., Seufert G., Colombo R., 2010. High resolution field spectroscopy measurements for estimating gross ecosystem production in a rice field . *Agricultural and Forest Meteorology*, 150: 1283-1296.

Rayment M.B., Lousau D., Jarvis P.G., 2002. Photosynthesis and respiration of black spruce at three organizational scales: shoot, branch and canopy. Tree Physiol. 22:219-229.

Ryan M. G., Lavigne M.B., Gower S.T., 1997. Annual carbon cost of boreal forest ecosystem in relation to species and climate. Journal of Geophysical Research, 102(D24) : 28871-28883.

Ryan M.G., Hubbard R.M., Pongracic S., Raison R.J., McMutrie R.E., 1996. Foliage, fine-root, woody tissue and stand respiration in *Pinus radiata* in relation to nitrogen status. *Tre Physiology*, 16: 333- 343.

Schimel D.S., House J.I., Hibbard K.A., Bousquet B., Ciais P., Peylin P., Braswell B.H., et al., 2001. Recent pattern and mechanisms of carbon exchange by terrestrial ecosystems. *Nature,* 414: 169-172.

Schulze E.D., 2006. Biological control of the terrestrial carbon sink. Biogeosciences 3: 147-166.

Schulze E. D., Ciais P., Luyssaert S., Schrumpf M., Janssens I.A., Thiruchittampalam B., Theloke J., et al., 2010. The European Carbon balance. Part 4: integration of carbon and other trace gas fluxes. *Global Change Biology*, 16: 1451-1469.

Smith P., 2004. Carbon sequestration in croplands: the potential in Europe and the global context. *European Journal of Agronomy*, 20: 229-236.

Subke J.R., Inglima I., Cotrufo M.F., 2006. Trends and methodological impacts of soil CO_2 efflux partitioning: a metaanalytical review. *Global Change Biology*, 12: 921-943.

Tagliavini M., Tonon G., Scandellari F., Quiñones A., Palmieri S., Menarbin G., Gioacchini P., Masia A., 2007. Nutrient recycling during the decomposition of apple leaves (*Malus domestica*) and mowed grassed in an orchard. *Agriculture, Ecosystem and Environment*, 118: 191-200.

Taylor J. R., 1982. An Introduction to Error Analysis, The Study of Uncertainties in Physical Measurements. *University Science Books*.

Tan Z., Yiping Z., Guirui Y., Liqing S, Jianwei T., Xiaobao D., Qinghai S., 2011. The carbon balance of a primary tropical seasonal rain forest. *Journal of Geophysical Research-Atmospheres*, 115: D00H26.

Testi L., Orgaz F., Villalobos F., 2008. Carbon exchange and water use efficiency of a growing, irrigated olive orchard. *Environmental and Experimental Botany*, 63: 168-177.

Van Gorsel E., Delpierre N., Leuning R., Black A., Munger J.W., Wofsy S., Aubinet M., et al., 2009. Estimating nocturnal ecosystem respiration from the vertical turbulent flux and change in storage of CO_2. *Agricultural and Forest Meteorology*, 149: 1919-1930.

Van Iersel M.W., 2003. Carbon use efficiency depends on growth respiration, maintenance respiration and relative growth rate. A case study with lettuce. *Plant ,Cell and Environment*, 26: 1441-1449.

Ventura M., Scandellari F., Bonora E., Tagliavini M., 2009. Nutrient release during decomposition of leaf litter in a peach (*Prunus persica L.,*) orchard. Nutrient Cycling in Agroecosystems, 87:115:125.

Waring R.H., Landsberg J.J., Williams M., 1998. Net primary production of forests: a constant fraction of gross primary production? *Three Physiology*, 18: 129-134.

Wells, Ch. E. and Eissenstat D. M., 2001. Marked differences in survivorship among apple roots of different diameters. *Ecology*, 82 (3): 882-892.

FIGURE captions

Figure 1. Eddy Covariance measured and derived C fluxes (g C $m^{-2}y^{-1}$). Blue dots show NEE, with negative values indicating day in which the ecosystems is acting as a sink of C. Red and green dots represent daily R_{eco} and GPP which were obtained from flux partitioning of NEE data via LUT method.

Figure 2. Average daily soil respiration (g C $m^{-2}d^{-1}$) measured in control (a) and trenching plots (b). Data from every single collar are plotted with gray *. Red and blue dots represent respectively daily Rs and Rh when at list 3 collars were available. Bars are standard deviation of the mean.

Figure 3. Comparison of R_s obtained in the same time period (24-28 June 2010) from the multiplexed system and the survey chamber (a). Multiplexed data are 58 half hourly average of 4 sampling collars (n tot= 232). Data from the survey chamber are 7 measurements replicates over 36 different positions (n=252). A two-sample t-test was carried out to compare R_s obtained from the 2 measurement system. R_s was significantly higher in multiplexed system (mean = 8.46 µmol CO_2 m^{-2} s^{-1}) than in survey chamber mode (mean = 6.36 µmol CO_2 m^{-2} s^{-1}; t=9.996, p < 0.001 (2-tailed), d.f. = 147). (b) The Q10 regression with temperature of both multiplexer and survey chamber´s soil respiration data with respective parameters showing the higher fluxes measured at the multiplexer stand.

Figure 4. The Carbon cycle of the studied agro-ecosystem for year 2010. Data express grams of C m^2y^{-1} for each component of the C cycle. Arrows size doesn´t reflect the size of flux.

Figure 5. NPP accumulation (g C m^{-2}) at each sampling date in the six considered ecosystem compartments. Bars width reflects the time (in days) occurred between successive biometric samplings.

Figure 6. Seasonal trend of daily NPP obtained from biometric measurements (NPP_{biom}, dotted line) and by summing the daily fluxes of R_h and NEP (NPP_{flux}, solid line showing a 15-days moving average of actual NPP_{flux}). Bars represent standard error (*se*) of the mean daily NPP_{biom} calculated at each sampling date and valid for period of time from the previous sampling to the actual.

Figure 7. Seasonal trend of the Carbon Use Efficiency obtained dividing NPP_{biom} and NPP_{flux} per the EC derived GPP and reported respectively as CUE_{biom} (dotted line) and CUE_{flux} (solid line, 15 days moving average). Time period considered is the growing season 2010, from DOY 77 till DOY 291.

Figure 1.

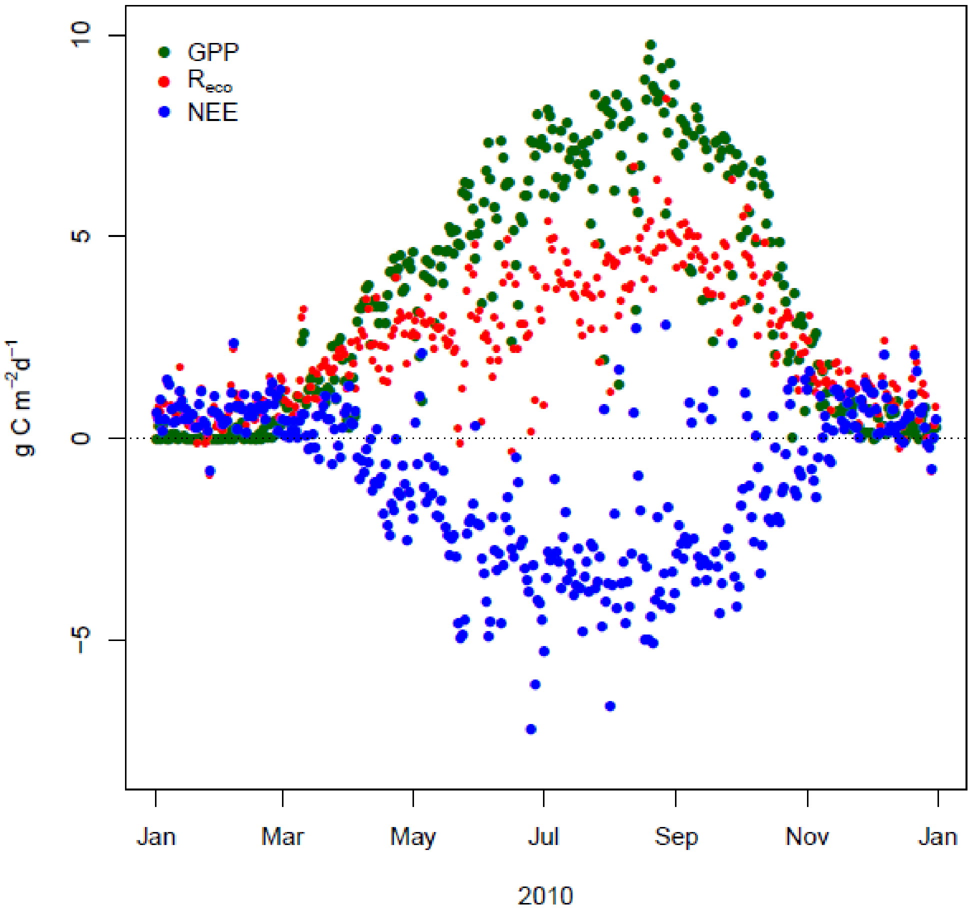

Figure 2

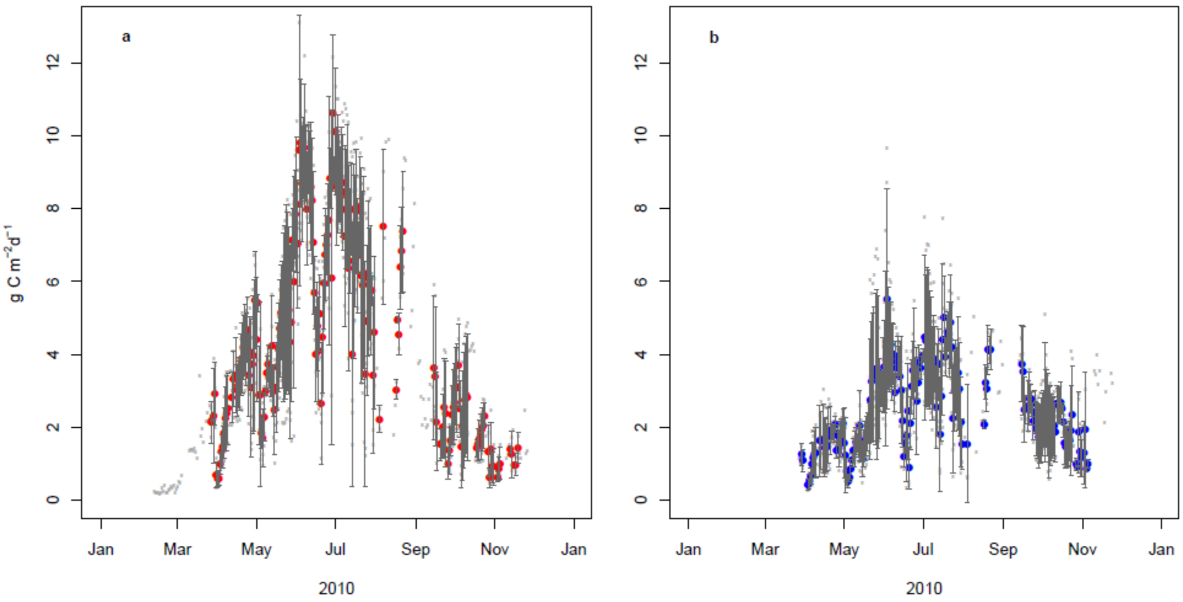

Figure 3a.

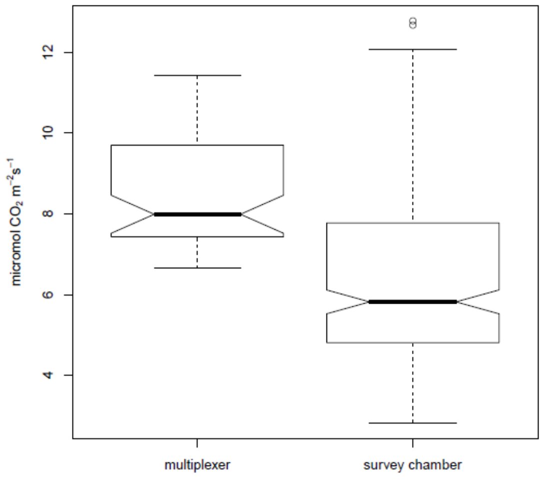

Figure 3b.

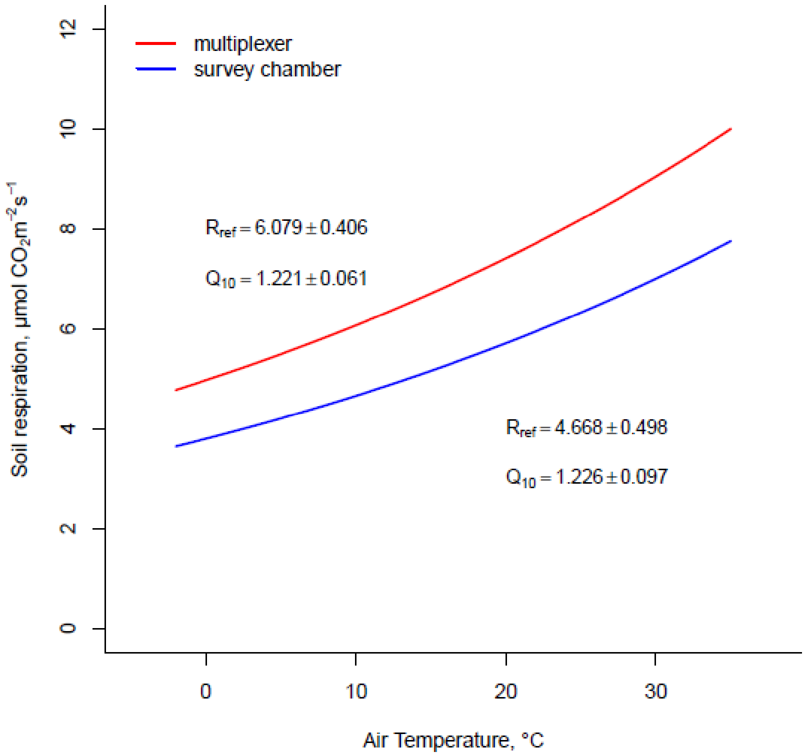

Figure 4.

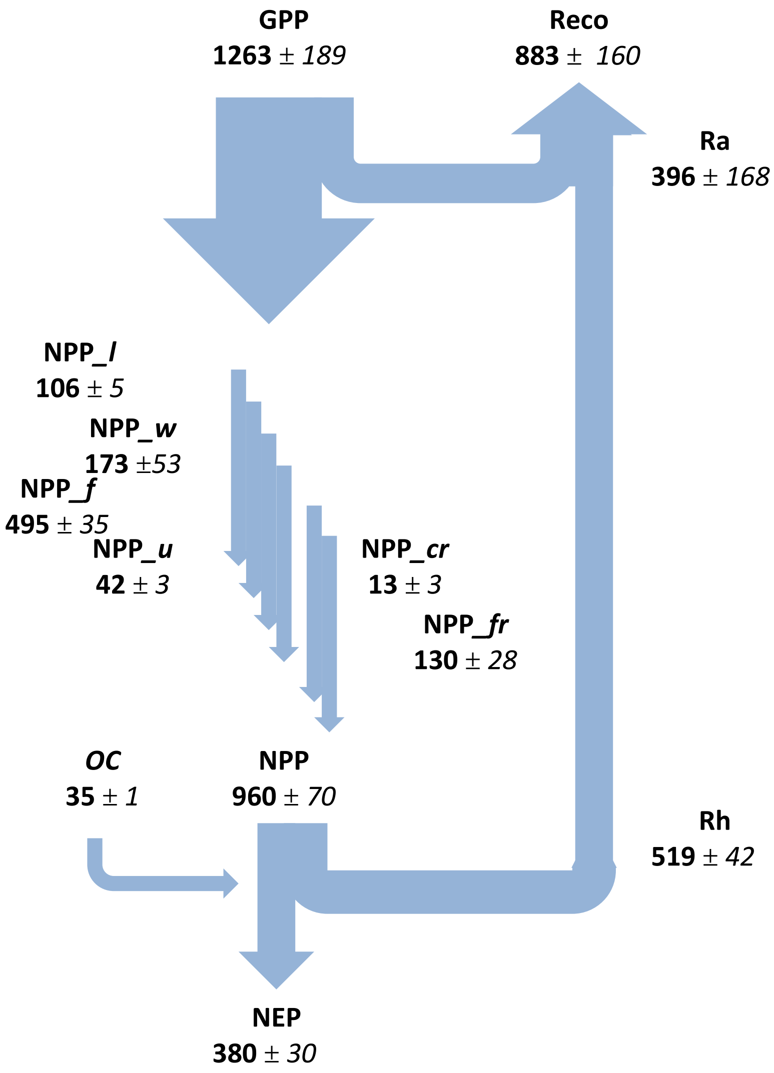
GPP
1263 ± *189*
Reco
883 ± *160*
Ra
396 ± *168*
NPP_*l*
106 ± *5*
NPP_*w*
173 ±*53*
NPP_*f*
495 ± *35*
NPP_*u*
42 ± *3*
NPP_*cr*
13 ± *3*
NPP_*fr*
130 ± *28*
OC
35 ± *1*
NPP
960 ± *70*
Rh
519 ± *42*
NEP
380 ± *30*

Figure 5.

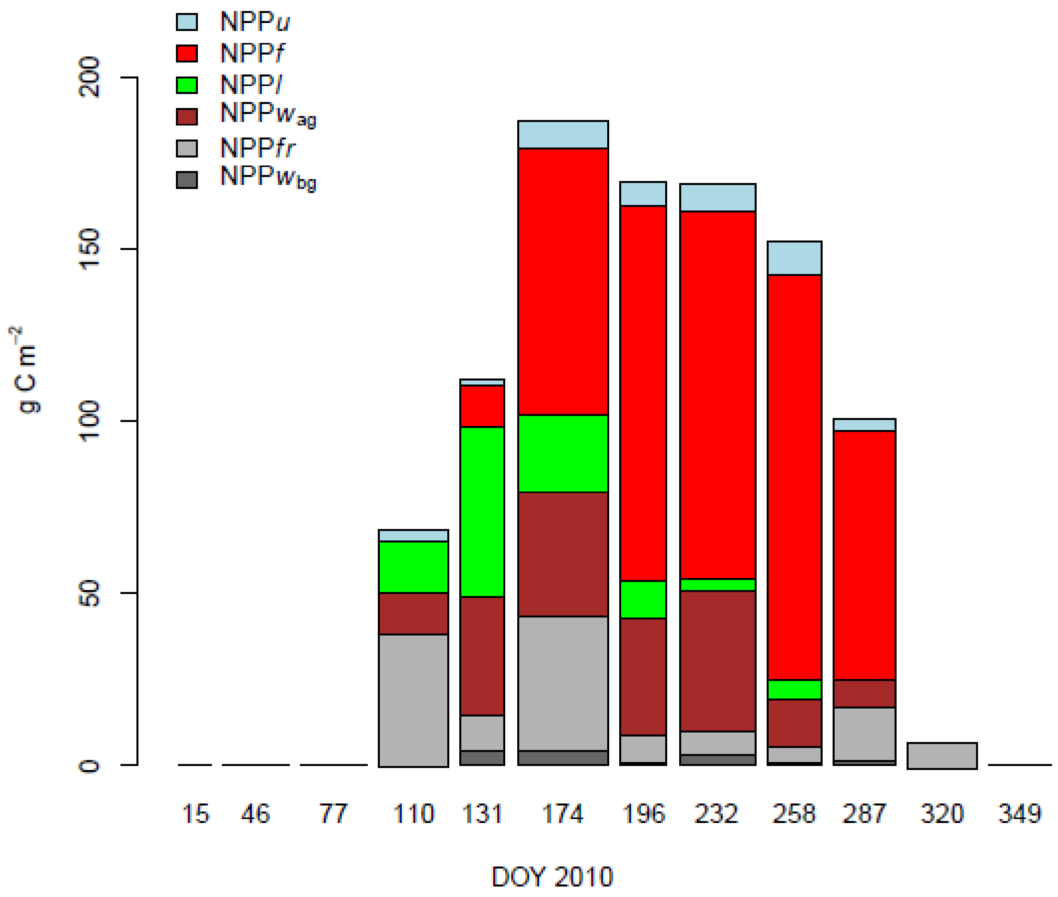
NPPu
NPPf
NPPl
NPPw_{ag}
NPPfr
NPPw_{bg}
g C m^{-2}
0
50
100
150
200
15
46
77
110
131
174
196
232
258
287
320
349
DOY 2010

Figure 6.

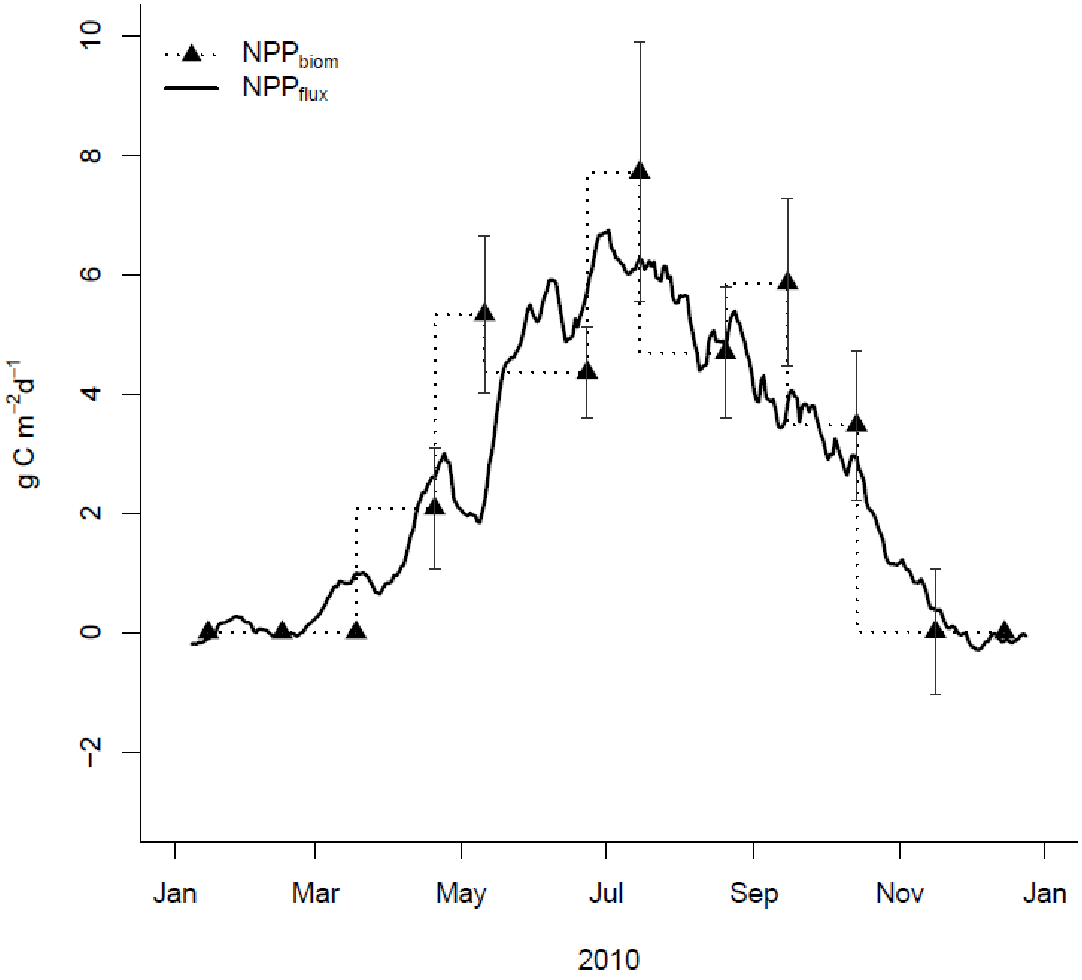

NPP$_{biom}$
NPP$_{flux}$
g C m^{-2}d^{-1}
10
8
6
4
2
0
-2
Jan
Mar
May
Jul
Sep
Nov
Jan
2010

Figure 7.

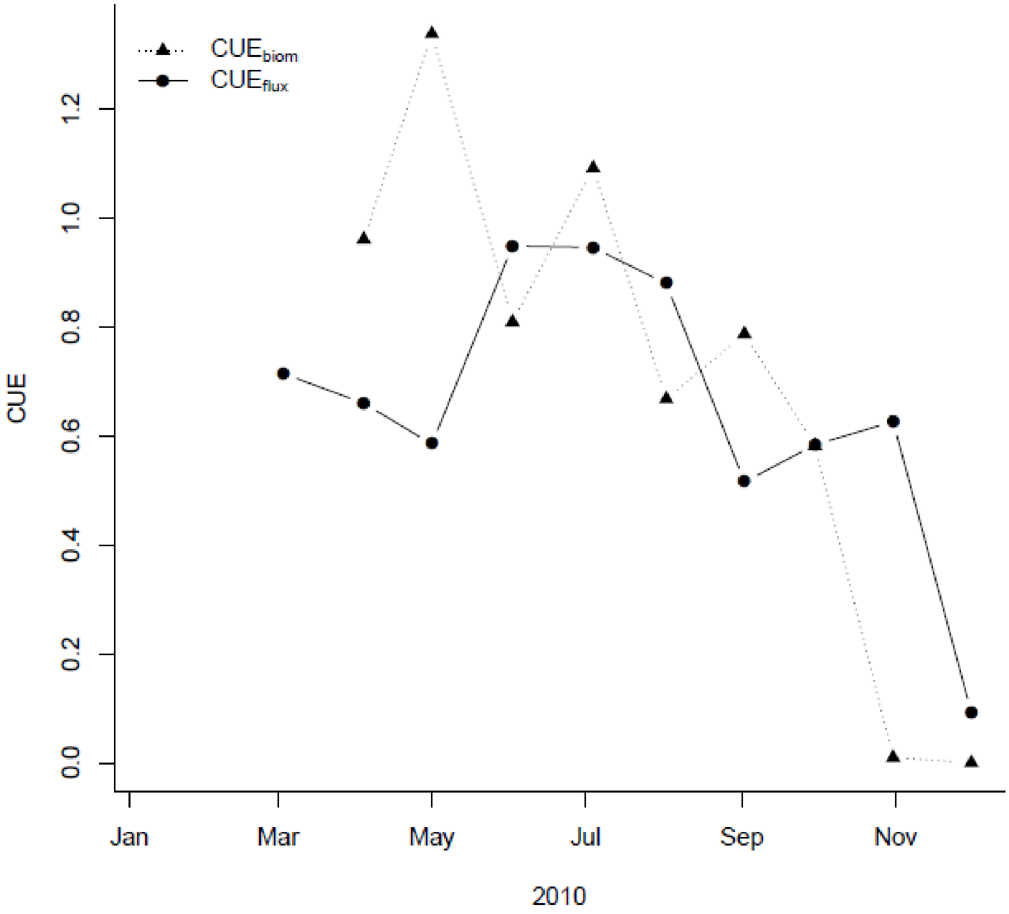
CUE_biom
CUE_flux
CUE
0.0
0.2
0.4
0.6
0.8
1.0
1.2
Jan
Mar
May
Jul
Sep
Nov
2010

TABLES

Table 1. Coefficients of the power allometric equation founded for aboveground woody biomass ($wood_{AG}$) and below ground woody biomass ($wood_{BG}$). The "$wood_{AG}$" equation is calculated using the "pruned above ground woody biomass" equation ($wood_{AG\_p}$) at the beginning of the season and the "not-pruned aboveground woody biomass" equation at the end of the season ($wood_{AG\_np}$), thus accounting for the pruning material. Reported are parameters with their relative standard errors.

Woody organs	**n**	**Intercept ± *se***	**Exponent ± *se***	**R^2**	**p-*value***
$wood_{AG\_np}$	11	229.3158 ± *1.3820*	1.6115 ± *0.1787*	0.9105	< 0.001
$wood_{AG\_p}$	11	202.9379 ± *1.3682*	1.6115 ± *0.1787*	0.9105	< 0.001
$wood_{AG}$	2	0.0384 ± *na*	6.2470 ± *na*	na	na
$wood_{BG}$	11	46.7026 ± *1.9599*	1.7694 ± *0.3716*	0.7391	0.0014

Table 2. Distribution of the C stocks within the ecosystem at the beginning of the season (march 2010). $Wood_{AG}$ includes trunks and pruned branches of different ages calculated with allometric equation number 2 of table 1; $Wood_{BG}$ are coarse roots (allometric ecquation number 3 of table 1); Fine roots were obtained by the intensive soil core sampling conducted in march 2010; The soil C pool was derived from data of soil organic carbon and bulk density for a profile of 1 m.

Components *(march 2010)*	**C** *kg m^{-2}*	distribution %
$Wood_{AG}$	0.6	3.4
$Wood_{BG}$	0.3	1.7
Fine roots	0.1	0.7
Soil	17.1	94.2
Total	18.2	100.0

Table 3. Parameters of Lloyd and Taylor and Q10 model for soil respiration. Reported are the estimated parameters ± their standard error.

model	parameter	R_s	R_h
Q_{10}	R	2.728 ± 0.016	1.601 ± 0.009
	Q_{10}	1.759 ± 0.007	1.636 ± 0.007
Llord and Taylor	R_{ref}	2.498 ± 0.017	1.515 ± 0.010
	T_o	220.886 ± 0.258	214.613 ± 0.337

Table 4. Yearly NPP values and relative weight of the ecosystem components measured biometrically (data expressed in $g\ m^{-2}\ y^{-1}$ of dry weight and C ± standard error of the mean) .

NPP component	**n**	**DW**	**DW % distr**	**C %**	**C**	**C % distr**
NPP*l*	6	232 ± *10*	10	0.458	106 ± *5*	11
NPP*f*	30	1239 ± *88*	55	0.400	495 ± *35*	52
NPPw_{ag}	30	382 ± *117*	17	0.454	173 ± *53*	18
NPPw_{bg}	30	29 ± *7*	1	0.453	13 ± *3*	1
NPP*fr*	8	292 ± *62*	13	0.444	130 ± 28	14
NPP*u*	6	103 ± *6*	5	0.410	42 ± *3*	4
NPP*total*		**2278 ± *160***	**100**		**960 ± *70***	**100**

Table 5. The three models applied for the indirect assessment of R_a. Data of C fluxes involved in model 1 and 2 are reported in Figure 4. R_a belowground (R_{a_bg}) is obtained subtracting R_h to R_s. K is calculated from model published by Reich (et al., 2006) and was 1.62.

	model	**methodology**	**R_a**	***se***
1	GPP - NPP_{biom}	EC - biometric	303	*202*
2	R_{eco} - R_h	EC - soil chamber	353	*165*
3	k*R_{a_bg}	soil chamber	533	*132*

Table 6. Biomass accumulation (g DW m^{-2} ± standard error) in the monitored tree organs at each sampling date

sampling date	**leaves**	**fruits**	**wood$_{ag}$**	**wood$_{bg}$**	**fine roots**	**Understory**	**Total**
20/04/2010	32.7 ± *1.7*	0	26.9 ± *59.1*	0	85.9 ± *45.6*	9.0 ± *1.2*	153.8 ± *74.7*
11/05/2010	108.2 ± *5.5*	29.4 ± *4.6*	75.8 ± *31.1*	9.6 ± *4.0*	22.7 ± *52.7*	4.3 ± *0.1*	250.1 ± *61.7*
23/06/2010	48.6 ± *6.2*	194.5 ± *41.2*	79.6 ± *21.4*	9.3 ± *1.7*	87.8 ± *59.0*	20.1 ± *4.4*	440.0 ± *75.4*
15/07/2010	22.8 ± *4.2*	273.5 ± *54.9*	75.1 ± *68.1*	1.9 ± *3.2*	17.9 ± *65.5*	17.3 ± *1.5*	408.5 ± *109.4*
20/08/2010	7.8 ± *2.5*	266.4 ± *57.7*	89.8 ± *54.1*	7.2 ± *1.9*	15.0 ± *48.0*	20.0 ± *2.6*	406.2 ± *92.6*
15/09/2010	12.4 ± *3.4*	294.3 ± *61.4*	30.4 ± *30.4*	1.1 ± *1.1*	10.8 ± *51.6*	24.3 ± *3.8*	373.3 ± *85.9*
14/10/2010	0	181.2 ± *33.7*	17.5 ± *9.3*	2.6 ± *1.2*	35.5 ± *75.2*	8.3 ± *2.3*	245.1 ± *83.0*
16/11/2010	0	0	0	0	16.3 ± *78.1*	0	16.3 ± *78.1*

Table 7. The four independent approaches used to assess the CUE of the studied apple orchard. (average =0.68 ± *10*)

Model	**CUE**	***se***
NPP_{biom}/GPP_{EC}	**0.76**	*0.13*
NPP_{flux}/GPP_{EC}	**0.71**	*0.11*
$NPP_{biom}/GPP_{B\&SC}$	**0.65**	*0.08*
$NPP_{flux}/GPP_{B\&SC}$	**0.61**	*0.07*

Table 8. Table of comparison between natural woody ecosystems of temperate humid biomes (dataset of Luyssaert et al., 2007) and the studied apple orchard, a woody agro-ecosystem.

stand characteristics (mean ± SD)	**Temperate humid deciduous forest**	**apple orchard (2010)**
Latitude (°)	44 ± 9	46
Max LAI (m2/m2)	6.1 ± 3.5	2.8
Tree height (m)	19 ± 7	4
Tree density (number/ha)	1723 ± 2439	3330
Stand age	75 ± 50	11
AG biomass (gC/m2)	10882 ± 5670	840 ± 180
BG biomass (gC/m2)	2565 ± 2609	319 ± 69
Stand climate (mean ± SD)		
Mean winter temperature (°C)	2 ± 9	1 ± 4
Mean summer temperature (°C)	20 ± 5	22 ± 5
Precipitation sum winter (mm)	183 ± 164	152
Precipitation sum summer (mm)	356 ± 259	293 (+ 350*)
Net radiation winter (W /m2)	150 ± 100	9 ± 93
Net radiation summer (W/m2)	425 ± 78	162 ± 258
Mean winter air humidity (%)	79 ± 11	72 ± 23
Mean summer air humidity (%)	77 ± 5	62± 23
Mean C fluxes (mean ± SE)		
GPP	1375 ± 12 (n=22)	1263 ± 189
NPP	738 ± 8 (n=52)	956 ± 70
fNPP	235 ± 2 (n=32)	106 ± 5
wNPP	329 ± 10 (n=21)	173 ± 53
rNPP	207 ± 3 (n=52)	139 ± 28
fNPP	~	495 ± 35
uNPP	~	42 ± 3
NEP	311 ± 7 (n=29)	380 ± 29
Reco	1048 ± 13 (n=24)	883 ± 160
Ra	673 ± 22 (n=15)	307 ± 202
Rh	387 ± 4 (n=40)	563 ± 45
Re/GPP (before balance closure)	0.77 ± 0.04	0.70 ± 0.16
CUE	0.54 ± 0.01	0.68 ± 0.10

CHAPTER 3

Environmental and physiological factors governing C fluxes in an apple orchard

1. INTRODUCTION

Terrestrial ecosystems are known to interact with atmosphere exchanging heat, moisture, and trace gases at different timescales (Pielke et al., 1998). The annual exchange of carbon between global vegetated land and the atmosphere is about 120 Gt of C y^{-1} with creation of organic matter by photosynthesis almost balanced by the release of CO_2 from respiration and decomposition (Schimel et al., 1996; IPCC, 2007). Despite a great concern exists at the global scale regarding the terrestrial biomass being destroyed by deforestation, burning and other land use changes, it appears that the overall contribution of the terrestrial biosphere to the carbon balance of the atmosphere is to act as a sink of 1-2 Gt C y^{-1} (Schimel et al., 2001; IPCC 2007).

Temporal pattern of gross photosynthesis, respiratory processes and the resulting net ecosystem carbon fluxes are dependent on the fluctuating interaction between available radiation, air temperature, atmospheric vapor pressure deficit, water availability and the physiological status of the ecosystem, which can be described by leaf area index and leaf nitrogen content (Falge et al., 2002; Misson et al., 2006; Schulze 2006; Groenendijk et al., 2011).

Biosphere atmosphere interaction measurements and modeling are useful tools for understanding the carbon economy of plants (Chen at al.2003; Wang et al., 2004; Migliavacca 2009) and offer the potential to determine the atmospheric carbon dioxide sink effect of the studied ecosystem. In this topic are involved different scientific communities, ranging from physicists and meteorologists to ecologists and agronomists. On the way of ensuring long-term sustainability of agricultural practices, horticultural community merges the specific interests in understanding cultivated plant ecophysiology with the need to define potential CO_2 sink effect of horticultural crops.

Despite a growing amount of information comes from a wide range of natural ecosystems at different latitudes (FLUXNET), still scarce is the knowledge of biosphere-atmosphere interaction in cultivated orchards (Rossi et al., 2007, Testi et al., 2010, Liguori et al 2009, Navarro et al., 2008).

The major effort in fruit tree cultivation is commonly focused in increasing the harvest index (*HI*) intended as the fraction of dry matter allocated to fruits over total GPP (Forshey and McKee 1970) as well as the quality of fruits. High *HI* values are achieved in modern orchards systems using high-density plantation with small-sized trees obtained using dwarfing rootstocks and/or appropriate training and pruning systems which can maximize light interception (Robinson and Lakso, 1991; Caruso et al., 1999; Corelli Grappadelli 2003; Liguori et al., 2009).

In fruit tree ecosystems, some of the parameters influencing C cycle are maintained within optimal levels for improving *HI* (i.e. water and nutrients level), and others significant differences with natural ecosystems occur by the fixed tree density, by pruning and by the reduced biodiversity (Testi et al. 2010). Moreover, in woody tree crops such as apple orchards, where the fruits are the dominant sinks for photoassimilates, it has been demonstrated that both photosynthesis and transpiration are enhanced by fruit load throughout the growing season (Monselise and Lenz, 1980; Gucci et al., 1995, Wibbe and Blanke 1995, Giuliani et al., 1997) and also at the harvest time (Tartachnyk and Blanke, 2004).

Supporting the statement of Rossi et al. (2007) regarding the need of bridging the long-standing gap between ecology and agronomy in order to contribute at the cause of long-term sustainability of agricultural production, in the present study we reported the ecosystem carbon fluxes over an apple orchard for three continuous years using eddy covariance, the common methodology adopted in FLUXNET network. Apple trees are widely cultivated all around the World occupying a surface of more 4,7 million hectares and Italy is among the largest apple producer´s countries (FAOSTAT, 2010). Within Italy, the highest apple production comes from Alto Adige Province, where more than 18000 ha are dedicated to this land use type.

Objectives of this work were to quantitatively assess the carbon exchange fluxes of an apple orchard at different time scales (daily, seasonal and interannual), to partition the net carbon exchange, NEE, between its downward (Gross photosynthesis, Gp) and upward (Ecosystem Respiration, R*eco*) component and assess the influence of the main environmental and physiological parameters on the daily values of the three C fluxes.

2. MATERIALS AND METHODS

2.1 Study Site description

The study site is located in the bottom Valley of the Adige river (municipality of Caldaro, South Tyrol, Italy, 46°21’ N, 11°16’ E; 240 m a.s.l.), intensively cultivated for apple production. Apple trees (*Malus domestica* var. Fuji grafted on dwarfing M9 rootstock) have been planted in the year 2000 in a regular frame of 3x1 m, where 1 m is the distance between plants along the line and 3 m is the distance between two lines of trees. Training system is slender-spindle. Average tree height is 3.6 m. The orchard is managed according to organic production guidelines. Budburst occurs normally in the second half of March and the growing season ends commonly at the beginning of November when leaf fall starts. The historical data of mean precipitation of the area average 810 mm y^{-1}. Irrigation is practiced during the summer period with the sprinkler overhead method. Average marketable fruit production in the three considered years was 61 ± 15 t ha^{-1}. The soil is a Calcaric Cambisols according to FAO Soil Taxonomy, with a pH of 7.4, an organic carbon of 1.43 % and a total Nitrogen of 0.17 %. The soil bulk density is 1.49 In the upper 20 cm and 1.52 between 20 and 60 cm. Soil texture analysis in the upper 60 cm revealed that sand, lime and clay were respectively 44, 45 and 11 %. General hydraulic properties such as Permanent Wilting point (PWP), Field Capacity (FC) and Saturation Point (SP) were estimated on texture data (Saxton et al., 1986) and were 9.8, 24.0 and 43.8 % of volumetric soil water content (m^3/m^{-3}) respectively. Apple tree plantations with the same characteristics are present around the selected field for a minimum distance of 300 m in all directions. Apple trees are commonly pruned during the dormant season (December-February). In the present study, trees of the selected field were not pruned after the highly productive 2010 season, as a strategy to limit alternating problem by avoiding an excessive reduction of flower-buds load.

The inter-row alley, a stripe of 1.8m width between tree lines, was covered by grass which was cut 3-4 times per year. The most representative species are: *Poa annua, Poa trivialis, Taraxacum officinalis,Trifolium repens, Medicago sativa, Agrostis tenuis, Plantago major, Veronica hederifolia, Veronica agrestis, Cerastium holosteoides, Capsella bursa-pastoris, Anthriscus sylvestris, Galinsoga ciliate, Glechoma hederacea, Polygonum aviculare, Stellaria media, Rorippa silvestris.*

2.2 Continuous measurements

The site was selected based on the favorable conditions for eddy-covariance (EC) measurement in term of regular terrain and homogeneity of land surface cover. An 8 meter tower was settled up at the beginning of 2009. Instruments for EC measurements were installed at the top of it in March 2009. Additionally, a series of instruments were installed on or in the close proximity of the tower in order to monitor continuously the main environmental variables such as solar radiation, Air temperature (T*air*), relative humidity (RH), photosynthetically active photon flux density (PPFD), soil water content (SWC), precipitation, soil heat flux (G).

2.2.1 CO_2 fluxes

Net Ecosystem Exchange (NEE) of CO_2 was measured continuously by the eddy covariance technique since March 21, 2009. Measurements and calculation were performed following Euroflux methodology as described by Aubinet et al. (2000) with a 3D sonic anemometer (Gill R3-50, Gill-Instruments, Lymington, UK) at a height of 8 m above ground (4 m above the canopy) and a close path CO_2/H_2O infrared gas analyzer (IRGA, LI-7000, Li-Cor Biosciences, Lincoln, Nebraska, USA). Air was sampled trough a polyethylene tube (4 mm inner, 6 mm external diameter) at a distance of 0.3 m from the anemometer with a flux rate of 10 l min^{-1} provided by an external pump (N838 KNDC, KNF Nueberger GmbH, Freiburg, Germany). Calibration was performed bi-weekly with reference gases: Nitrogen and 380 ppm CO_2 flasks (produced by Messer, Grugliasco, Italy), were used to set the zero and the CO_2 span, respectively. Zero-level of CO_2 and H_2O in the reference cell of the analyzer was assured by the use of chemicals (respectively Ascarite II for CO_2 and magnesium perchlorate for water vapor), which were substituted bi-weekly. The software Eddysoft (Kolle and Rebmann, 2007; Mauder et al., 2008) was used to calculate eddy fluxes with the following criteria: no detrending, no high or low pass filtering corrections were used; a two-axis rotation of coordinates was applied each 30 minutes. The software automatically calculated the lag-time for CO_2 at each half-hour to maximize the covariance between fluctuations in vertical wind velocity and gas mole density. In addition, the analysis of stationary conditions for CO_2 turbulent flux and of Integral Turbulent Characteristic (ITC) following Foken and Wichura (1996) was performed.

2.2.2 Meteorological data

Solar radiation components were measured by a net radiometer (CNR1, Kipp & Zonen, Delft, Holland) placed on an horizontal pole at the top of the tower; air temperature and relative humidity data were collected at 8 meter above ground level by CS215, Campbell Scientific Incorporated, Logan, Utah, United States (CSI hereafter). Rainfall was collected by a professional rain gauge (RAIN-O-MATIC, Pronamic, Silkeborg, Denmark) also placed on the top of the tower. The amount of water provided by Irrigation, periodically carried out in the field during summer months, was estimated based on the duration of the intervention. Soil water content was assessed by multiple TDRs (CS616, CSI) placed within a 30 m radius from the tower. Soil heat flux (G) was measured by two soil heat flux plates (HFP01, Hukseflux, Delft, Holland). All meteorological data were logged by a CR3000 (CSI).

2.3 Periodic measurements

2.3.1 Biometric assessment of NPP

NPP assessment was conducted in 2010 and 2011 over six representative plots, each one composed of five trees, following Law et al. (2008) in order to assess Net Primary Production (NPP). Six components of NPP were considered separately: leaves (NPP*l*); fruits (NPP*f*); aboveground woody tissues ($\text{NPP}w_{\text{ag}}$) which include trunk, branches and shoots; belowground woody tissues ($\text{NPP}w_{\text{bg}}$) which include coarse roots and the belowground part of trunk, fine roots (NPP*fr*) and understory production (NPP*u*). Each of these fluxes was assessed directly and independently in the growing seasons 2010 and 2011 by a combination of non-destructive measurements on selected plots and destructive harvest of tree branches at regular intervals. We did not consider in this budget the volatile organic compounds (VOC), non CO_2 carbon emission and root exudates production. Data and samples were collected once a month and the following equation was used to calculate the total NPP produced within each sampling date and in the whole season:

$$\Delta NPP = (L_{t+1} + Sb_{t+1}) - (Sb_t) \qquad (1)$$

Where L_{t+1} is the litter collected from the nets placed under selected trees and *Sb* is the actual (*t*) and at the successive sampling date (*t+1*) standing biomass. Variations in C storage within tree organs were not considered beside their relevance. Details on the sampling procedures for each NPP component are described in the first part of the PhD thesis.

Excised branches were brought to laboratory for analysis. The collected material, after subdivision of the organs as specified at the beginning of this paragraph, was used to determine the dry weight per unit of mass of each organ (after drying in oven to a constant weight at 65°C), the mean carbon and nitrogen content of each NPP component (FlashEA™ 1112 Elemental Analyzer, Thermo Fisher Scientific, Germany) and the mean leaf surface (LI-3000 + LI-3050 Portable Area Meters, Li-Cor Biosciences, Lincoln, Nebraska, USA).

2.3.2 LAI assessment

In the first month after budburst (April 2010 and 2011), we numbered and tagged all the branches and counted the number of leaves of each branch present in 3 levels of height (low= 0 – 120 cm, medium = 120 – 240 cm, high=240-360 cm) to represent within tree vertical variability (e.g. Rayment et al., 2002). Three branches per plant level were then chosen from each tree, and from May till November, the number of leaves was monthly counted, avoiding any sampling collection avoiding any sample collection in the monitored plants. We used the complete characterization done in April to determine a multiplicative factor, specific for each plant level, to upscale measured number of leaves to the whole plant. The derived total number of leaves per plant was multiplied by the mean leaf surface at each respective sampling date to obtain the seasonal course of the Leaf Area Index (LAI). Only LAI of the apple trees was considered in the present study. Between each sampling date, LAI was linearly interpolated to obtain a daily value used in the regression modeling approach.

2.4 Gap filling and flux partitioning of CO_2 fluxes

Gap-filling of NEE fluxes was performed using the on-line standard tool ({HIPERLINK: "http://www.bgc-jena.mpg.de/bgc-mdi/html/eddyproc/index.html"}}. Only values that passed the Foken and Wichura test were provided as original data. The methodology is similar to Falge (2001) but accounts for both the temporal autocorrelation of fluxes with meteorological variables, and the temporal autocorrelation of the fluxes (Reichstein et al., 2005).This algorithm identifies three different conditions: i) in the case all meteorological data are available the missing value is replaced by the average value under similar meteorological conditions within a time-windows of 7 days. Meteorological conditions are considered similar when Air Temperature (Tair), global radiation (Rg) and Vapour Pressure Deficit (VPD) do not deviate more than 2.5°C, 50 W m^{-2}, and 5.0 hPa respectively. If no similar conditions are present in the same time window, the averaging window is increased to 14 days; ii) In the case only Rg is available among the meteorological data, the same approach is applied, with similar meteorological conditions defined only by an Rg deviation lower than 50 W m^{-2}, and windows size is not increased; iii) when also Rg is not available, the missing data are replaced by the average value of the same time of the day of adjacent days. Filled data are classified into three categories (A = best, B = acceptable, C = dubious) based on the method and the windows size used. The classification is based on the notion that the estimation of the missing data improves with the knowledge on meteorological conditions and with the use of the temporal auto-correlation of the variables that favors smaller time-windows. The output file contains a variable *fqc* with values 0: no gap-filled; 1-3: gap-filled category A-C.

Partitioning of NEE flux into GPP and R*eco* is provided by the already mentioned online tool. In this case the procedure foresees that NEE night-time data, according to a Rg threshold ratio of 20 Wm^{-2}, are defined as ecosystem respiration (R*eco*). Data are then split into consecutive periods of 10 days length and each period is checked to see if there are larger than six points available and whether the temperature range is more than 5°C, since only under this condition a reasonable regression of R*eco* versus temperature can be expected. For each of those periods where the criteria are met, the Lloyd and Taylor (1994) regression model

$$\mathrm{R}_{eco}(T) = \mathrm{R}_{eco,ref}\; e^{E_0 \left\{ \frac{1}{T_{ref}-T_0} - \frac{1}{T-T_0} \right\}} \qquad (2)$$

is fitted to the scatter of R*eco* versus Air Temperature (T). Parameters T_{ref} and T_0 (10 °C and -46.02°C respectively) are kept constant as in the original model, while the activation energy (E_0) which essentially determines the temperature sensitivity is allowed to vary. The three estimates of E_0 with the smallest standard error are assumed to best represent the short-term temperature response of R*eco* and are averaged, resulting in a $E_{0,avg}$ values for the dataset. Subsequently, the respiration at the reference temperature (R*eco*$_{,ref}$) is estimated from the night time data for consecutive intervals of 4 days using the non-linear regression of the R*eco* data versus temperature according to equation *(2)* , where E_0 is fixed to $E_{0,avg}$ value. The estimated values of R*eco*$_{,ref}$ is then assigned to the central time point of the period and linearly interpolated between periods. The results is that for each half hour the parameters E_0 and R*eco*$_{,ref}$ are available and are used to estimate R*eco* as a function of that Air Temperature that have also been used to derive the parameters.

A large gap in the measurements of the CO_2 net ecosystem exchange occurred in the first five months of 2011 due to a wrong signal provided by the anemometer. This malfunctioning happened during the winter season where no clear daily pattern of NEE occurred and thus it was difficult to identify. The size of the gap impeded to fill the missing values of this period with the procedure described above.

2.5 Light response curve

A rectangular hyperbole model was fitted to the light response curves for Gp (A_g) measured during the three summer months (June, July and August) of each year. These months were selected because of the high photosynthetic activity which characterizes that period:

$$A_g = \frac{A_{\max}\alpha Q}{\alpha Q + A_{\max}} \qquad (3)$$

Where Q is the incident PPFD (µmol $m^{-2}s^{-1}$), A_{max} is the maximum Gp (µmol $m^{-2}s^{-1}$) with unlimited PPFD, and α (mol CO_2 mol^{-1} of photons) is the initial slope of the light response curve that represents the apparent quantum yield. This equation was fitted using those half hourly day-time (PPFD > 25 µmol $m^{-2}s^{-1}$) values of GPP and PPFD for each month where the measured NEE values passed analysis of stationary conditions for CO_2 turbulent flux and of Integral Turbulent Characteristic (ITC) following Foken and Wichura (1996).

2.6 Interaction of C fluxes with environmental variables

On the attempt to assess a model that describes the daily NEE-GPP and R*eco* data (g C m^2d^{-1}), we selected five explanatory variables due to their mechanistic relation with the response variable. Four of them describe environmental aspects: Tair, °C (mean daily value), SWC, m^3m^{-3} (mean daily value), PPFD, µmol $m^{-2}s^{-1}$ (mean daily value), VPD, hPA, (mean daily value), while the last one, leaf area index (LAI, m^2m^{-2}, daily value linearly interpolated from periodic measurements) reflects physiological conditions. A correlation among the considered variables (both response and explanatory) was carried out through a series of plots using function pairs in the R software. An analysis of the complex interaction between explanatory variable and their relative importance on the response variable was performed assessing a tree model for each response variable. Tree model is fitted using binary recursive partitioning in which each explanatory variable is assessed in turn and the variable explaining the greatest amount of deviance in *y* is selected. Deviance is calculated on the basis of a threshold in the explanatory variable; this threshold produces two mean values for the response: a high value is the mean above the threshold and low value is the mean below the threshold. This approach was chosen essentially because of the efficiency of tree models in providing a clear picture of the structure of the data (Crawley, 2007).

Since all the explanatory variables were continuous, we proceeded to identify the minimum adequate model to describe daily values of NEE, GPP and R*eco* (g C $m^{-2}d^{-1}$) with the multiple regression approach:

$$y_i = \sum \beta_i x_i + \varepsilon_i \qquad (4)$$

Where the i^{th} data point y_i is determined by the level of the linear predictor (summation term) which can involve many explanatory variables, non linear terms and interactions. In our case, we started by fitting the maximal model which included the five explanatory variables discussed above, their respective quadratic term and all the possible interaction among them. We carried out the modeling process on a reduced dataset constituted of months 1-3-5-7-9-11 (2010) and months 6-8-10-12 (2011), for a total of 273 data points. The 2009 year was not considered because LAI was not measured. Following the *principle of parsimony* (Occam´s razor), which requires that a model should be as simple as possible, we then carried out a simplification of the complex model by stepwise deletion of non-significant terms. To account for the fact that the order in which variables are deleted from the model will influence the explanatory power attributed to them, we began the stepwise deletion process removing first non-significant interaction terms, then the non-significant quadratic terms and finally the non-significant explanatory variables. Within each group, the parameter with the highest *p* factor was eliminated first. The deletion process continued until all parameters left were significant ($p < 0.05$) and a significant increase in deviance was observed when removing another variable from the current model.

At this point the assumptions of constancy of variance and normality of errors were checked by plotting apposite model checking plots. In the case in which heteroscedasticity and non normality were observed, we continued improving the model by transforming either the response or the explanatory variables. A way to find the optimal transformation of the response variables is the Box-Cox transformation which aims to find the power transformation, λ (*lambda*), that maximizes the likelihood when a specific set of explanatory variables is fitted to

$$\frac{y^{\lambda} - 1}{\lambda} \qquad (5)$$

as the response (Crawley, 2007).

When two or more models were established for the same response variable, i.e after that several kinds of transformations were applied to response or explanatory variables, the Akaike´s Information Criterion (AIC) was used to select the model which ensured the best fit.

The complementary dataset (months 2-4-6-8-10-12, 2010 and 7-9-11, 2011) was used to test the performance of the minimum adequate model established for each response variable (NEE, GPP and Reco) trough plotting measured versus modeled values and assessing the modeling efficiency (MEF) defined as

$$MEF = 1 - \frac{\sum_{i=1}^{N}(OBS_i - SIM_i)^2}{\sum_{i=1}^{N}(OBS_i - \overline{OBS})^2} \qquad (6)$$

Where OBS_i and SIM_i are the corresponding observed and simulated values (Janssen and Heuberger, 1995). In contrast to the r^2 value, the modeling efficiency not only measures the association (or correlation) between modeled and observed data but also their coincidence, and it is sensitive to systematic deviations between model and observation (Smith et al., 1996, Reichstein et al., 2003).

The entire inspection process of all the correlations between the considered variables and their complex interactions as well as the modeling procedure, was carried out with *R* statistical software (R development core team, 2008).

3. RESULTS

3.1 Environmental conditions

Variation in weather conditions for the growing seasons 2009 – 2011 (March-November) is summarized in Table 1. Mean temperature of the growing season was 15.7 ± 0.45 °C (mean ± SD), 0.7 ° C above the historical mean (HM). A higher difference (+ 1.1°C) occurred between actual and historical minimum mean daily temperature, with peaks in April (+ 1.5°C), August (+ 1.8°C) and November (+ 2.2°C). Historically, the warmest month of the year is July, while for 2009 and 2011 it was August. 2009 was the warmest growing season of the considered period.

Total solar radiation, with small differences among years, reached its maximum in July (700 ± 29 MJ m^{-2}), while the annual sum was 4497± 107 MJ m^{-2}. Mean daily maximum VPD reached its highest value in July for the growing season 2010 and 2011 (respectively 29.8 and 24.1 hPa) and in August for the growing season 2009 (27.1 hPa). Historical precipitation for the considered 9 months was 709 mm. Roughly 180 mm above HM values were measured in 2010, 2011 was close to HM value while in 2009 rainfall was approximately 150 mm below HM with the highest discrepancies occurred in May (-80 mm) and in October (-50 mm). The differences in the precipitation pattern that were observed during the 3 years did not reflect the variation in soil water content, which was much less pronounced since irrigation was practiced in order to maintain the volumetric SWC at high levels. Considering that Permanent Wilting Point and the Field Capacity of the field were respectively 9.8, 24.0 % of volumetric SWC, it appears clear from figure 1 how soil water availability was in general not limiting factor for tree growth and productivity.

3.2 NPP and LAI trends

Figure 2 shows daily NPP accumulation in each considered ecosystem components. NPP*fr* and NPPw_{bg} was added together to form the NPP belowground (NPP*bg*) component (Fig 2 D). Total daily NPP is reported in figure 2-E. Net primary production started after budburst, which happened earlier in 2011 respect to 2010 (12 and 18 March respectively). At the beginning of the growing season (April and May), the rate of net C accumulation in leaves was higher in 2011 respect to 2010. A similar trend was found in April for NPP*f*, while, later in the season, the allocation rate to this component was lower in 2011 than

2010. Allocation to woody organs was higher in 2011, while no clear distinction appeared in the allocation pattern to belowground organs and understory. From the summation of all the considered NPP components, total daily NPP resulted to be higher in 2011 respect to 2010 in the early stage of the season, and lower from the beginning of the summer till leaf fall, with the highest differences occurring in July, (for both seasons the month with the highest NPP, 6.6 ± 1.1 and 6.0 ± 1.0 g C $m^{-2}d^{-1}$ in 2010 and 2011 respectively). Total yearly NPP was 960 ± 70 g C m^{-2} in 2010 and 988 ± 58 g C m^{-2} in 2011. Total NPP allocated to fruits was 495 ± 35 g C m^{-2} y^{-1} in 2010 and 468 ± 52 g C m^{-2} y^{-1} in 2011. In 2009, 2010 and 2011, marketable fruit production exported from the ecosystem was 45.2 ± 5.1, 74.4 ± 5.5 and 62.9 ± 7.0 t fresh weight ha^{-1} respectively.

The seasonal trend of leaf area index (figure 3), reflected the fact that trees were not pruned in 2011 so LAI was constantly higher respect to 2010. In both seasons we observed a sharp increase of LAI from budburst till mid May followed by a less steep increase until July where the maximum LAI was reached (2.8 ± 0.1 m^2m^{-2} in 2010 and 3.3 ± 0.2 m^2m^{-2} in 2011). A sharp LAI decline was observed from mid October till December, when leaf fall was completed.

3.3 Energy balance (evaluation of eddy covariance measurements)

We calculated the surface energy balance of the apple orchard on a daily basis in order to assess the accuracy of the eddy covariance measurements as follow:

$$R_n = H + \lambda E + G \tag{7}$$

Where R_n is net radiation, H is sensible heat flux, λE is the latent heat flux and G is the soil heat flux. The linear correlation between the sum of sensible and latent heat flux and available energy had a slope of 0.757, indicating that the eddy covariance measurements, also considering the amount of short wave radiation used for the metabolism of the plants, likely underestimates the sensible and/or latent heat fluxes.

3.4 Diurnal trend of NEE and environmental variables

Figure 4 shows the mean diurnal pattern of NEE and Gp (Gross photosynthesis) and the environmental variable Tair, VPD and PPFD of every month in which eddy covariance measurements were carried out. Following common micrometeorological sign convention, positive values of NEE represent a release of CO_2 from the ecosystem surface (upward fluxes) and negative values represent an uptake by the surface (downward fluxes). NEE started to become negative on average when the flux of available photosynthetic radiation (PPFD) was above 250 µmol m^{-2} s^{-1} and returned positive around 6-7 pm during the summer months and 5-6 pm in September – October in close relation to available photosynthetic radiation (PPFD between 200 and 300 µmol m^{-2} s^{-1}). Negative peaks of NEE occurred between hours 11 and 14 with the absolute mean highest values recorded always August (14.9 ± 4.0 µmol CO_2 m^{-2} s^{-1} for 2009; 16.2 ± 7.3 µmol CO_2 m^{-2} s^{-1} for 2010 and 17.8 ± 7.8 µmol CO_2 m^{-2} s^{-1} for 2011). Gross photosynthesis followed the same diurnal pattern of NEE with absolute mean highest values always recorded in August in the same day time period of NEE peaks (19.1 ± 4.0 µmol CO_2 m^{-2} s^{-1} for 2009; 20.6 ± 7.7 µmol CO_2 m^{-2} s^{-1} for 2010 and 23.5 ± 8.0 µmol CO_2 m^{-2} s^{-1} for 2011). A well distinct time lag (approximately 3 hours) was observed between maximum VPD and Tair (which occurred normally around 3 pm) and peaks of NEE and Gp in every months in which the ecosystem was photosynthetically active, while a less pronounced time lag occurred between C fluxes peaks and the available photosynthetically active light (PPFD peaks between hours 12 and 13, Fig 4).

On yearly basis, the months in which a clear pattern of daylight ecosystem CO_2 absorption from the atmosphere was observed were April-October, while from November until March, the apple orchard acted as source of carbon to the atmosphere.

3.5 Light response curve

The light response curve during the three summer months (June – July and August) was calculated using equation (3). No apparent light saturation of photosynthesis was observed. The highest A_{max} in 2009 was observed during August (-27.5 µmol CO_2 m^{-2} s^{-1}), in 2010 during July (-37.0 µmol CO_2 m^{-2} s^{-1}), and in 2011 during August (-38.2 µmol CO_2 m^{-2} s^{-1}, Figure 5). On average, a higher GPP at maximum PPFD (*Amax*) was observed in the 2010 summer months (-34.0 µmol CO_2 m^{-2} s^{-1}) respect to 2011 and 2010 (respectively -28.0 and -23.6 µmol CO_2 m^{-2} s^{-1}). The apparent quantum yield (α) was similar for 2009 and 2010, with an average of the measured values of respectively -0.0243 and -0.0256, while differed for 2011 where an average value of -0.0436 was observed for the three summer months.

3.6 Interaction of C fluxes with environmental variables

3.6.1 NEE

Correlations among NEE and all the considered explanatory variables are shown in figure 6a. The response variable NEE is shown on the *y* axis of the top row of panels: there is a strong negative relationship with PPFD, VPD, Tair and LAI, while a rather unclear but positive relationship appeared with SWC.

From the analysis of the fitted tree model, it emerged a rather simple structure of interaction between explanatory variables, with variation in NEE explained by only LAI and PPFD (Fig. 6b). The most important explanatory variable was LAI, and the threshold separating high and low NEE was a LAI value of 1.16 m^2m^{-2}. In the left hand branch of the tree a subtle effect of PPFD exists on mean NEE value. When PPFD (daily average) is lower than 11.31 $\mu mol\ m^{-2}s^{-1}$, average NEE is 1.26 $g\ C\ m^{-2}d^{-1}$, when, on the contrary, it is above, NEE is 0.45 $g\ C\ m^{-2}d^{-1}$. For LAI values > 1.16 m^2m^{-2} (right hand limb), PPFD has again a significant impact on NEE. When the daily average photosynthetic active photon flux density is below 13.20 $\mu mol\ m^{-2}s^{-1}$, average NEE is 0.52 $g\ C\ m^{-2}d^{-1}$, when PPFD is comprised between 13.20 and 22.93 $\mu mol\ m^{-2}s^{-1}$, average NEE was -1.41 $g\ C\ m^{-2}d^{-1}$. When PPFD is above 22.93 $\mu mol\ m^{-2}s^{-1}$, LAI has again a significant impact on NEE: if it is below 2.85 m^2m^{-2}, average NEE was -2.76 and if above average NEE was -3.88 $g\ C\ m^{-2}s^{-1}$.

The minimum adequate model obtained for NEE after stepwise deletion of all non-significant parameters was the following:

$$\mathrm{NEE}_{\mathrm{mod}} = a + b\sqrt{PPFD} + c\sqrt{VPD * PPFD * SWC} + d\sqrt{PPFD * SWC * LAI} \qquad (8)$$

Estimated parameters (*a, b, c and d*) are presented in table 2. A square root transformation of PPFD, LAI, VPD and SWC was performed to improve variance and normality distribution of residual of the fitted model. The presented minimum adequate model describing NEE data had an intercept plus only three highly significant parameters: transformed PPFD, a three way interaction between transformed PPFD, VPD and SWC and a second three way interaction between transformed PPFD, VPD and LAI. The NEE model explained almost 80% of the variance in observed NEE (adj r^2 =0.797). Four plots assessing model performances (residuals against fitted values; a normal QQ-plot, a scale-location plot of square rooted residuals against fitted values and a plot of residuals against leverages) are presented in figure 7a. Conditions of homogeneity distribution of the residuals and normality of errors were verified by the 2 plots of figure 7a.

Modeling efficiency (MEF), assessed with equation (6) on the complementary dataset, was 0.788 and indicates a good predictive power of the model. The measured versus predicted values obtained using the complementary dataset is reported in figure 7b. The coefficient of determination of the linear relationship (adj r^2 = 79%) showed a good correlation between measured and predicted values while the slope of the reported equation (0.79) indicates a conservative prediction of the model with and underestimation of both positive and negative fluxes of NEE in a way that may balance out and reduce cumulative errors.

3.6.2 GPP

Exploration of correlations among GPP and all the considered explanatory variables was conducted in the same way as for NEE (fig 8a). Strong positive correlations were found with Tair and LAI. A positive correlation with a hint of saturation emerged with PPFD and VPD while a negative correlation with SWC was observed.

The most important explanatory variable was LAI and the threshold value separating high and low values of GPP is close to 2 m^2m^{-2} (Fig 8b). When LAI is below 0.8, average daily GPP is 0.35 gC $m^{-2}d^{-1}$, When LAI is between 0.8 and 2, GPP is 2.70 g C $m^{-2}d^{-1}$. The right hand branch of the tree indicates that PPFD has a significant effect on GPP. At low values of PPFD (< 25.3 µmol $m^{-2}s^{-1}$), Tair is a significant explanatory variables with GPP being on average 2.49 if Tair < 15.5 °C, and 4.90 g C $m^{-2}d^{-1}$ if Tair is above that threshold. At high values of PPFD (> 25.3 µmol $m^{-2}s^{-1}$), GPP is described by different levels of LAI (2.19, 2.82, 2.84, 3.01).

The minimum adequate model describing daily GPP was the following:

$$\begin{aligned} GPPt_{\text{mod}} &= a + bVPD + cPPFD + dLAI + ePPFD^2 + fLAI^2 + g(VPD*PPFD) + \\ &+h(Tair*PPFD) + i(VPD*LAI) + j(VPD*Tair*PPFD) + \\ &+k(VPD*PPFD*SWC) + l(VPD*Tair*LAI) + m(VPD*LAI*SWC) \end{aligned} \tag{9}$$

Coefficients for all the significant parameters retained in the model are listed in table 3. In order to optimize the variance and normality distribution of the residuals, a Box Cox transformation was applied to the response variable following equation (5). The λ value that maximized likelihood of GPP was 0.43 which need to be considered before to obtain the true value of modeled GPP:

$$GPP_{\text{mod}} = (1 + GPPt_{\text{mod}} * 0.43)^{\frac{1}{0.43}} \tag{10}$$

Twelve significant parameters were kept after the stepwise deletion process was completed: three linear terms, two quadratic terms, three two-ways interactions and four three-way interactions. No trend in the size or degree of scatter of the residual was observed (Fig 9a). Normality of error condition was also ensured by the same series of plots of figure 9a. In figure 9b, the linear relationship original GPP (GPP_{fp}) and modeled GPP (GPP_{mod}) obtained using the complementary dataset is showed. Almost 90% of the deviation was explained by the model (adj $r^2 = 0.894$) with a slope of 0.946 ± 0.013. Modeling efficiency was also calculated using the complementary dataset and was 0.894 indicating a good predictive power of the model.

3.6.3 Reco

Ecosystem respiration showed a positive correlation with Tair and LAI while it was negatively correlated with SWC (Fig 10a). The correlation of R*eco* with both PPFD and VPD is positive but it saturates between 30 and 40 mean daily µmol $m^{-2}s^{-1}$ of PPFD and between 10 and 15 hPa of mean daily VPD.

From the tree model´s analysis, Tair was explanatory variable which explained the highest amount of variance of R*eco* data, with a threshold value separating low and high value of R*eco* of 14.2 °C (Figure 10b). The model showed also significant impacts of LAI and SWC on ecosystem respiration, with the lower mean R*eco* value (0.74 g C $m^{-2}d^{-1}$) occurring in days with Tair < 14.2 °C and LAI close to zero, and the higher mean R*eco* value (5.51 g C $m^{-2}d^{-1}$) occurring when LAI is between 2.8 and 3.0 m^2m^{-2} and air temperature above 20 °C.

The minimum adequate model describing R*eco* daily data was

$$\mathrm{Re}co\,\mathrm{t}_{\mathrm{mod}} = a + bPPFD + cLAI^{2} + d(PPFD*VPD) + e(PPFD*Tair) + \ f(Tair*LAI) +$$

$$+g(PPFD*VPD*Tair) + h(PPFD*VPD*SWC) + \ i(VPD*Tair*LAI) + \qquad (11)$$

$$j(Tair*LAI*SWC) + k(PPFD*Tair*LAI)$$

Ten parameters out of the 37 of the initial model were kept at the end of the stepwise deletion process due to their high significance in explaining R*eco* variation. Coefficients of the parameters are listed in table 5. The model explained 82 % of the variance in R*eco*. A BoxCox transformation (eq. 5) was carried out to improve model fitting to the data and the λ value which maximized the likelihood of R*eco* was 0.69. In order to obtain true value of modeled ecosystem respiration, the R*eco*t$_{\mathrm{mod}}$ was modified as follows:

$$\mathrm{Re}co_{\mathrm{mod}} = (1 + \mathrm{Re}co\mathrm{t}_{\mathrm{mod}} * 0.69)^{\frac{1}{0.69}} \qquad (12)$$

The absence of trends in residuals was verified (Fig 11a). QQ plot showed a curvature in the lowest part, but further transformation of explanatory variables did not improve model performances. The model was kept as the best minimum adequate model describing R*eco* data based on the lower AIC number. Relationship of predicted versus original R*eco* values is showed in figure 11b (adj r^2 = 0.836; slope = 0.839 ± 0.013). It was assessed on the complementary dataset similarly to the modeling efficiency, which was 0.836.

3.7 Seasonal and interannual C fluxes

The C fluxes measured (NEE$_{\mathrm{meas}}$) and derived via flux partitioning of night–time NEE value (R*eco*$_{\mathrm{fp}}$ and Gp$_{\mathrm{fp}}$) during the three year considered in the present study, are reported in figure 12 integrated over a daily base (g C $m^{-2}d^{-1}$). A large gap occurred from January 1 till May 31, 2011 due to instrument failure. Predicted values obtained using the multiple regression models described above for each of the three C fluxes are also presented in figure 13 and these values were used to fill the mentioned gap occurred in 2011. GPP is reported in a negative form (Gp) in respect to micrometeorological convention of downward fluxes (as photosynthesis) as previously reported by Flanagan et al. (2002).

NEE fluxes were higher in 2010 and 2011 respect to 2009. The maximum daily NEE in 2009 was -3.6 g C $m^{-2}d^{-1}$ and occurred three times along the summer season (June 14, July 22 and August 02). In 2010 there was a peak on NEE fluxes around the end of June where a maximum daily NEE of -6.9 g C $m^{-2}d^{-1}$ was reached. In 2011, the maximum daily NEE occurred on an isolated day in September (-6.4 g C $m^{-2}d^{-1}$) with an anomalous high air temperature, while a more prolonged peak of high NEE was observed between the end of July and the first week of August, with values ranging from – 5 to -5.5 g C $m^{-2}d^{-1}$).

The maximum gross photosynthesis (Gp) in 2009 occurred quite homogeneously throughout the summer months with values ranging from -6.5 and -7.5 g C $m^{-2}d^{-1}$, with a maximum of -8.4 g C $m^{-2}d^{-1}$ (21/08). Gp fluxes were generally higher in 2010, with a peak of -10.1 g C $m^{-2}d^{-1}$ reached in August. In 2011 the peak of Gp was the highest of the three considered years (-11.8 g C $m^{-2}d^{-1}$) and occurred at the beginning of August within a period of high Gp activity.

Differences in the ecosystem respiration (R*eco*) were not so marked among the three considered years. Maximum R*eco* occurred in the second half of August in 2009 (5.9 g C $m^{-2}d^{-1}$) and at the beginning of August in both 2010 and 2011 (5.7 and 6.3 g C $m^{-2}d^{-1}$ respectively). An anomalous peak of R*eco* took place in November 2011 with values close to those registered in summer. Yearly cumulated data of the three C fluxes described are listed in table 5 along with the total NPP assessed through biometric measurements in 2010 and 2011.

In figure 13, the cumulated value of the Net Ecosystem production over the three years is presented. On average, the ecosystem starts to be a net sink of Carbon between full budburst and full bloom, which happened in the first half of April for 2009 and 2010 and in the second half of March for 2011. The “sink-period” lasted on average 220 ± 7 days (mean ± SD) and ended in the first half of November, when major leaf fall occurred. The “source-period” lasted 141 ± 7 days (mean ± SD). Data of cumulated NEP for each sink-source season is presented in table 6. On average, during the sink season, the ecosystem was able to capture 450 ± 110 g C m^{-2}; 2011 was the year with the highest NEP, approximately 100 g C m^{-2} above the mean. Only two complete source-periods were monitored, and during this winter time the ecosystem lost on average 95 ± 30 g C m^{-2}.

4. DISCUSSION

4.1 Environmental conditions, NPP and LAI over the considered period

Light is known to be the most important environmental factor affecting photosynthesis an consequently dry matter production and partitioning (Corelli Grappadelli and Sansavini, 1988; Blanke and Notton 1992). In fruit orchards it also influences flower bud differentiation, fruit set, fruit color and quality and it may induce both anatomical and physiological differences in leaves formed in shade or in light conditions (Tustin et al., 1992, Corelli Grappadelli et al., 1994, Wünsche et al., 1996). Modern orchards designs, intended as tree form, planting density and row spacing and orientation, were developed in order to ensure an elevated capacity for light interception and a good distribution of light throughout the canopy, and thus maximize tree efficiency (Corelli Grappadelli, 2003). The orchard in which the present work was conducted meets these conditions of high density planting (3300 trees ha^{-1}) and tree height (3.6 to 4.0 m) and thus has the potential for high photosynthetic response.

No particular differences were observed in the environmental conditions of the three considered growing seasons and mean values of the considered parameters were close to the historical average data of the area (tab 1). It is worth to stress here the fact that availability of photosynthetic active radiation is crucial in orchard productivity because other fundamental environmental parameters such as nutrient and water availability are artificially kept within optimal ranges by irrigation and nutrient supply, contrary to what happens in natural ecosystems, where they may represent limiting factors for the optimal growth.

Periodic measurements, carried out in 2010 and 2011 seasons, reflected the fact that the apple trees were not pruned during the latter year as a strategy to avoid alternate bearing following the highly productive 2010 season. This led to some important differences in the structure of the trees between the monitored seasons which were observable in both NPP and LAI measurements. Pruning is an agronomic practice which is commonly carried out during the dormant season in apple orchard to keep the correct balance between vegetative and reproductive organs. It influences the ability of the tree to acquire necessary resources such as water, light and nutrients, to produce dry matter and to partition the carbon and nutrients to vegetative and reproductive organs (Lakso and Corelli Grappadelli, 1992). The higher number of buds left on 2011 caused a development of a higher leaf biomass right after budburst and a higher LAI respect to 2010, which was monitored during the whole season. The presence of a higher number of growing points reduces individual shoot vigor and consequently their demand for carbon, and induces more shoots to terminate the growth early (Lakso and Corelli Grappadelli, 1992). Despite no distinction between spur and shoot leaves were made in the present study, it is arguable from figure 2 that the higher number buds left in 2011 due to the absence of pruning, caused a higher net primary productivity at the early stage of the growing season (probably due to a higher number of well exposed spur leaves) which decreased in later stage when a likely mutual shading effect of leaves occurred (Palmer, 1977; Blanke and Notton 1992) and contributed to the overall lower total NPP observed in 2011 after DOY 150.

Along with light efficiency, fruit load is another important aspect which is known to influence the photosynthetic capacity of the apple trees, with a general increase in photosynthetic efficiency of leaves present in trees with high yields (Fujii and Kennedy,1985; Palmer 1992, Wibbe and Blanke 1995; Giuliani et al., 1997; Wünsche et al., 2000, Tartachnyk and Blanke, 2004). In our case, fruit production was very high in 2010 (74 t ha^{-1} of fresh weight) and 2011 (63 t ha^{-1} of fresh weight), and lower in 2009 (45 t ha^{-1} of fresh weight), a fact that might contribute to explain the lower GPP values of 2009

4.2 Variation of C fluxes over the season and response to light

Half hourly values of the C fluxes and environmental variables were averaged for each month. The resulted diurnal pattern plotted on figure 4 gave a picture of the evolution of the Net ecosystem carbon exchange and Gross photosynthesis in relation with available active radiation (PPFD) at both daily and seasonal time scale.

On a daily basis, at a given rate of PPFD, higher fluxes of Gp and NEE occur during morning hours respect to the afternoon, when, in spite of high levels of light intensity, a decrease after the diurnal peak (approximately at noon) was observed. In the morning, the threshold rate of PPFD above which the orchard acts as net sink of CO_2 from the atmosphere appeared to be on average approximately 250 µmol of photon m^{-2} s^{-1}, although small variations were observed among the different months. Diurnal patterns of similar shape were reported previously for apple orchard (Wünsche et al., 2000, Corelli Grappadelli 2003) and are similar among different ecosystems (Steduto and Hsiao 1997; Röser et al., 2002; Tang et al., 2005; Ribeiro et al., 2006, Rossi et al., 2007).

On a seasonal time scale, clear diurnal patterns of C fluxes were observed starting from April, the first month after budburst, increased their amplitude until August and ceased in October, when leaf fall commonly begin and coherently with the known occurrence of leaf senescence after fruit harvest (Tartachnyk and Blanke, 2004).

Patterns of both environmental conditions and C fluxes among the same months of different year were surprisingly similar. Small differences were imputable to slightly different monthly environmental condition and to the higher LAI measured in 2011.

4.3 Light response curve

Comparing the data of photosynthesis obtained within this study with the available literature dealing with photosynthesis in fruit tree species, is not easy due to the intrinsic differences in the methodological approaches and their respective assumptions, which may also determine conceptual differences relative to what it is really measured. The two major techniques that have been adopted in previous studies included measurements obtained by analyzing single leaves (usually by portable instruments) or systems that enclose the entire tree canopy (Corelli Grappadelli e Magnanini, 1993, Giuliani et al., 1997). The latter system, considering leaf photosynthesis as well as the respiration of photosynthetic and not -photosynthetic above ground organs, provides, over time, values that are equal to the sum of the NPP and the root respiration, thus overestimating NPP. If we, in turn, measure over time the of C exchange from one single leaf exposed at the light, we obtain an estimation of the net photosynthesis which is however not easy to upscale to the entire canopy considering the different structural and physiological properties of “sun” and “shade” leaves (Doud and Ferree, 1980; Flore and Lakso, 1989).

The approach used in this study allowed instead to measure parameters relative to the whole soil-plant system at an ecosystem scale. At this stage it is therefore important to clarify that only less than 7% of total NPP was accounted by the herbaceous plants present in the orchard soil among tree rows, while the remaining can be attributed to the apple trees. We make therefore a relatively low error in attributing most of the results we observed to the performances of apple trees.

The relationship between photosynthesis and PPFD was analyzed by fitting a Michaelis-Menten rectangular hyperbola model (4) using data from the three summer months of each year. As expected, photosynthesis never reached the saturation point even at PPFD close to the values of about 2000 μmol $m^{-2}s^{-1}$. This is in line with findings obtained in apple trees with systems that enclose the whole canopy (Corelli Grappadelli, 2003) and that differ substantially from typical light saturation curves obtained by single leaves, showing saturation at values of PPFD generally close, in apple, to 800 µmol $m^{-2}s^{-1}$, and even lower in other fruit crops. In all the three summer months, at similar values of light intensity, higher values of assimilation were observed in 2011, as a likely consequence of higher LAI values. The same reason could also explain the higher (in absolute terms) quantum yield (alfa values) always found in 2011, a fact that suggests that not-pruned trees were more efficient in using light at low intensity levels (Corelli Grappadelli, 2003).

4.4 Multiple regression approach

The availability of a large dataset allowed us to study which parameter have the major effect on the carbon fluxes. In this respect, the "Tree models" approach proved to be a useful tool. The levels of light intensity and of LAI, as expected, controlled largely the NEE and GPP. The highest NEE and GPP values were obtained with LAI above 2.8 m^2m^{-2} and with a mean daily PPDF values above 25 µmol $m^{-2}s^{-1}$. Maximum LAI values above 3 are not the case in modern apple orchards, but is should be noticed that "Fuji" is a vigorous variety of apple, able to develop relatively high LAI values, even if grafted on low vigorous rootstocks.

Temperature was the environmental parameter with the strongest effect on ecosystem respiration, a fact that agrees with current scientific knowledge (Lloyd and Taylor, 1994) albeit it is important to recall that R*eco* values may be influenced by the adopted flux partitioning method described above.

Within the multiple regression approach that was undertaken to assess the best minimum adequate model to describe NEE, GPP and R*eco* values, the initial point contemplated all the explanatory variables (linear terms) their quadratic values and all the possible interactions among them, for a total of 37 parameters plus the intercept. The assumption that requires that the number of observations (217) are at least three times higher than the number of parameters (Crowley, 2007) was respected. After that progressive stepwise deletion of non-significant terms and transformations was carried out as explained above, we ended up with three models which were able to predict the carbon fluxes in a satisfactory way. NEE model (8) was the one with the lowest number of parameters, only four, while for GPP and Reco models, a relatively high number of parameters (respectively 13 and 11) resulted highly significant at the end of the modeling process. The complexity of the models, due to the presence of transformed variables, a high number of parameters and up to three way interaction parameters, makes it hard to interpret the model and understand the relative weight of each single explanatory variable, which in turn were described by the "tree model" discussed above. The equation, in turn, showed an elevated predictive power which was firstly successfully tested on a large complementary dataset and then used to estimate daily C fluxes that we lost during the first five months of 2011.

4.5 Cumulative C fluxes

Among the three monitored years, the highest cumulated C fluxes for each component (NEP, GPP and R*eco*) were observed in 2011, the lowest in 2009 (tab. 5). In 2009 the dataset is not complete for all the months, but it is unlikely that accounting for the period January 1st to late March could have increased the absolute values of NEE and GPP. Fruit production was higher in 2010 (74 t ha^{-1}) and lowest in 2009 (45 t ha^{-1}). In 2011 fruit production was 63 t ha^{-1}. NPP and LAI measurements were carried out only in 2010 and 2011. Harvest index, the ratio of fruit NPP over total NPP was 0.52 and 0.47 in 2010 and 2011 respectively. Since total NPP was slightly higher in 2011, *HI* indicates a different partitioning of photosynthates, which were allocated with a larger proportion to wood and leaves in 2011 respect to 2010. This reflected the fact that trees were not pruned in the latter season.

The ratio between NEP and GPP was constant in 2010 and 2011 (0.32), while the carbon use efficiency (CUE, NPP over GPP) was higher for 2010 respect to 2011. Considering that R*eco* is given by the sum of autotrophic (Ra) and heterotrophic (Rh) respiration, it is likely that the presence of a higher quantity of vegetative organs in 2011 increased the maintenance costs (> Ra) as compared to 2010. These findings support the consideration made on the first part of this thesis (see chapter 2) where it was stated that an elevate fruit production (high *HI*) increases the CUE of the apple orchard.

From the time in which eddy covariance measurements were initiated in late March 2009 till end of December 2011, the ecosystem showed a net assimilation a total of 1160 g di C m^2. As expected, a marked seasonally variable sink/source behavior of the orchard was observed, coherently with the phenological phases indicated in figure 13. The apple orchard starts to act as a sink of carbon approximately 10 to 20 days after bud-burst and continued for about 2-3 weeks after harvest when the upward respiratory fluxes return to be higher respect to GPP. Important not-CO_2 derived ecosystems carbon loss occurs at harvest when the fruit production leaves the ecosystem for commercial purposes. On averages over the three years, this lateral C flux accounted for 385 ± 93 g C m^2 y^{-1}, which approximately balanced out the yearly NEP.

5. CONCLUSIONS

The net ecosystem carbon exchange fluxes of an apple orchard and the main environmental factors which may influence them were monitored in the present study for three growing seasons using the eddy covariance technique. In two of them (2010 and 2011) also NPP and LAI were assessed with periodic biometric samplings. A higher LAI and a larger allocation of photosynthates to vegetative organs were observed in 2011 respect to the previous year, likely reflecting the fact that trees were not pruned during the latter season.

A pronounced diurnal pattern of the C fluxes was observed in those months in which the orchard acts as a net sink of carbon to the atmosphere (April-October). A distinct time-lag of approximately three hours occurred between daily peak of photosynthesis and maximum air temperature and VPD, suggesting a limiting effect of these environmental variables on the photosynthetic capacity of apple trees.

The light response curve fitted to Gp data of the three summer months, revealed that apple trees canopy never reached the saturation point even at the maximum photosynthetically active radiation values. Among the three considered years, the quantum yield as well as the actual photosynthesis at a given available PPFD, was higher in 2011, probably because of the higher foliar biomass observed.

The importance of light among the other environmental parameters was verified for both the daily integrated fluxes of NEE and for the GPP data, using the “Tree model” approach, although the most important explanatory variable was the leaf area index. The highest amount of deviance for ecosystem respiration was instead explained by air Temperature variation. A Multiple regression model with good predictive performances was assessed for each C flux (NEE, GPP and R*eco*) on a daily basis.

As a response to the increased concern about the GHG emission from agricultural land, measurements carried out in the present work allowed to quantitatively assess the cumulated net ecosystem production of the orchard over three seasons, a value that approximately balanced the amount of carbon annually exported with the harvested apples. The models could also be used to simulate future scenarios resulting from changes in environmental factors. The data would support the hypothesis that, if we do not consider the direct or indirect C emissions due to orchard management, the production of apple fruits implies a minimal or null impact on net C emissions to the atmosphere from the orchard ecosystem.

References

Aubinet M., Grelle A., Ibrom A., Rannik Ü., Moncrieff J. B., Foken T., Kowalski, A.S., Martin, P.H., et al., 2000. Estimates of the annual net carbon and water exchange of forests: The EUROFLUX methodology. *Advances in Ecological Research*, 30: 113–175.

Blanke M.M., Notton B.A, 1992. Light transmission into apple fruit and leaves. *Scientia Horticulturae*, 51: 43-53.

Caruso T., Inglese P., Marra F.P., Sottile F., et al., 1999. Effect of planting system on productivity, dry matter partitioning and carbohydrate content in aboveground components of "Flordaprince" peach trees. *Journal of American Society of Horticultural Sciences*, 124: 39-45.

Chen X.Y., Hutley L.B., Eamus D., 2003. Carbon balance of a tropical savanna in a Northern Australia. *Oecologia*, 137(3): 405-416.

Corelli Grappadelli L., Sansavini S., 1989. Light interception and photosynthesis related to planting density and canopy management in aple. *Acta Horticulturae*, 243: 159-174.

Corelli Grappadelli L., Lakso A.N., Flore J.A. , 1994. Early season Patterns of Carbohydrate Partitioning in Exposed and Shaded Apple Branches. *Journal of American Society of Horticultural Sciences*, 119: 596-603.

Corelli Grappadelli, 2003. Apples: Botany, Production and Uses; Light relations. *Eds. D.C. Ferree and I.J. Warrington,* chapter 9: 195-216.

Crawley M.J., 2007. The R Book. *Eds John Wiley and Sons Ltd,* England.

Doud D.S., Ferree D.C., 1980. Influence of altered light levels on growth and fruiting of mature "Delicious" apple trees. *Journal of American Society of Horticultural Sciences*, 105: 325-328.

Falge E., Baldocchi D., Olson R., et al., 2001. Gap filling strategies for defensible annual sums of net ecosystems exchange. *Agricultural and Forest Meteorology*, 107: 43-69.

Falge E., Baldocchi D., Tenhunen J., Aubinet M., Backwin P., Berbigier P., et al., 2002. Seasonality of ecosystem respiration and gross primary production as derived from FLUXNET measurements. *Agricultural and Forest Meteorology*, 113: 53-74.

FAOSTAT, 2010. Statistical databases. Agriculture Data Collection. FAO, Food and Agricultural Organization of the United Nations, Rome, {HIPERLINK http://faostat.fao.org/site/567/DesktopDefault.aspx?PageID=567}

Flanagan L.B., Wever L.A., Carlson P.J., 2002. Seasonal and interannual variation in carbon dioxide exchange and carbon balance in a northern temperate grassland. Global Change Biology, 8: 599-615.

Flore J.A., Lakso A.N., 1989. Environmental and Physiological regulation of photosynthesis in fruit crops. *Horticultural Reviews*, 11: 111-157.

FLUXNET, A Global Network Integrating Worldwide CO_2, Water and Energy Measurements. {HYPERLINK http://www.fluxnet.ornl.gov/}

Foken T., Wichura B., 1996. Tools for quality assessment of surface-based flux measurements. *Agricultural and Forest Meteorology*, 78: 83-105.

Forshey C.G., McKee M.W., 1970. Production efficiency of a large and small “McIntosh” apple tree. HortScience 5, 164-165.

Fujii J.A., Kennedy R.A.,1985. Seasonal Changes in the Photosynthetic Rate in Apple Trees, a comparison between fruiting and non fruiting trees. *Plant Physiology*, 78: 519-524.

Giuliani R., Nerozzi F., Magnanini E., Corelli Grappadelli L., 1997. Influence of environmental and plant factors on canopy photosynthesis and transpiration of apple trees. *Tree Physiology* 17: 637-645.

Groenendijk M., Dolman A.J., Ammann C., Arneth A., Cescatti A., Dragoni D., Gash J.H.C., Gianelle D., et al., 2011. Seasonal variation of photoshynthetic model parameters and leaf area index from global fluxnet eddy covariance data. *Journal of Geophysical Research*, 116, G04027: 1-18.

Gucci R., Corelli Grappadelli L., Tustin S., Ravaglia G., 1995. The effect of defruiting at different stages of fruit development on leaf photosynthesis of “Golden Delicious” apple. *Tree Physiology*, 15: 35-40.

Intergovernmental Panel on Climate Change, 2007. AR-4, Climate Change, Synthesis Report. *Contribution of Working Groups I, II and III to the Fourth Assessment Report of the Intergovernmental Panel on Climate Change*. IPCC, Geneva, Switzerland, pp 104.

Janssen P.H.M., Heuberger P.S.C., 1995. Calibration of process oriented models. *Ecological Modelling*, 83: 55-66.

Kolle O., Rebmann C., 2007. Eddysoft – Documentation of a Software Package to Acquire and Process Eddy Covariance Data. Technical Reports, pp. 88, Max-Planck Institut für Biogeochemie, Jena, Germany.

Lakso A.N., Corelli Grappadelli L., 1992. Implication of pruning and training practices to carbon partitioning and fruit development in apple. *Acta Horticulturae*, 322: 231-239.

Law B., Arkebauer T., Campbell J.L., Chen J., Sun O., Schwartz M., van Ingen C., Verma S., 2008. Terrestrial Carbon Observations: Protocol for Vegetation Sampling and Data Submission. TCO panel of the Global Terrestrial Observing System (GTOS - 55), {HYPERLINK http://www.fao.org/gtos/ }.

Liguori G., Gugliuzza G., Inglese P., 2009. Evaluating carbon fluxes in orange orchards in relation to planting density. *Journal of Agricultural Science*, 147: 637-645.

Lloyd J., Taylor J.A., 1994. On the temperature dependence of soil respiration. *Functional Ecology*, 8, 315-323.

Mauder M., Foken T., Clement R., Elbers J.A., Eugster W., Grünwald T., Heusinkveld B., Kolle O., 2008. Quality control of CarboEurope flux data – Part II: Inter-comparison of eddy-covariance software, *Biogeosciences,* 5: 451-462.

Migliavacca M., Meroni M., Manca G., Matteucci G., Montagnani L., Grassi G., Zenone T., Teobaldelli L., Goded I., Colombo R., Seufert G., 2009. Seasonal and interannual patterns of carbon and water fluxes of a poplar plantation under peculiar eco-climatic conditions. Agricultural and Forest Meteorology 149: 1460-1476.

Misson L., Tu K.P., Boniello R.A., Goldstein A., 2006. Seasonality of photosynthetic parameters in a multi-specific and vertically complex forest ecosystem in Sierra Nevada in California. *Tree Physiology* 26: 729-741.

Monselise S.P., Lenz F., 1980. Effects of fruit load on stomatal resistance, specific leaf weight and water content of apple leaves. Gartenbaumwissenshaft 45: 220-224.

Navarro M.N.V., Jourdan C., Sileye T., Braconnier S., Mialet-Serra I., Saint-Andre L., Dauzat J., Nouvellon Y., Epron D., Bonnefond J.M., Berbigier P., Rouziere A., Bouillet J.P., Roupsard O., 2008. Fruit development, not GPP, drives seasonal variation in NPP in a tropical palm plantation. *Tree Physiology*, 28:1661-1674.

Palmer J.W., 1977. Light transmittance by apple leaves and canopies. *Journal of Applied Ecology*, 14: 505-513.

Palmer J.W., 1992. Effects of varying crop load on photosynthesis, dry matter production and partitioning of Crispin/M.27 apple trees. *Tree Physiology*, 11:19-33.

Pielke R.A., Avissar R., Raupach M., Dolman A.J., Zeng X., Denning S., 1998. Interaction between the atmosphere and terrestrial ecosystems: influence on weather and climate. *Global Change Biology*, 4: 461-475.

R Development Core Team, 2008. R: A language and environment for statistical computing. *R Foundation for Statistical Computing*. Vienna, Austria. ISBN 3-900051-07-0, {HYPERLINK http://www.R-project.org }.

Rayment M.B., Lousau D., Jarvis P.G., 2002. Photosynthesis and respiration of black spruce at three organizational scales: shoot, branch and canopy. *Tree Physiology*, 22:219-229.

Reichstein M., Falge E., Baldocchi D., Papale D., Aubinet M., Berbigier P., Bernhofer C., Buchmann N., et al., 2005. On the separation of net ecosystem exchange into assimilation and ecosystem respiration: review and improved algorithm. *Global Change Biology*, 11: 1424-1439.

Reichstein M., Tenhunen J., Roupsard O., Ourcival J.M., Rambal S., Miglietta F., Peressotti A., Pecchiari M., Tirone G., Valentini R., 2003. Inverse modeling of seasonal drought effects on canopy CO_2/H_2O exchange in three Mediterranean ecosystems. *Journal of Geophysical Research*, 108: D23, 4726, ACL 6.

Ribeiro R.V., Lyra G.B., Santiago A.V., Pereira A.R., Machado E.C., Oliveira R.F., 2006. Diurnal and seasonal patterns of leaf gas exchange in a bahiagrass (*Paspalum notatum* Flügge) growing in a subtropical climate. Grass and Forage Science, 61:293-303.

Robinson T.L., Lakso A.N., 1991. Bases of yield and production efficiency in apple orchard systems in apple orchard systems. *Journal of American Society of Horticultural Sciences*, 116: 188-194.

Röser C., Montagnani L., Schulze E.D., Mollicone D., Kolle O., Meroni M., Papale D., Belelli M., Federici S., Valentini R., 2002. Net CO_2 exchange rate in three different successional stages of the "Dark Taiga" of central Siberia. *Tellus*, 54B: 642-654.

Rossi F., Facini O., Georgiadis T., Nardino M., 2007. Seasonal CO2 fluxes and energy balance in a kiwifruit orchard. *Italian Journal of Agrometeorology*, 2007(1): 44-56.

Saxton K.E. et al., 1986. Estimating generalized soil-water characteristics from texture. *Soil Science Society American Journal*, 50(4):1031-1036.

Schimel D., Alves D., Enting I., et al., 1996. Radiative forcing of climate change. In Climate Change 1995: The Science of Climate Change (eds Hougton J.T., Meira-Filho L.G., Callander B.A., Harris N., Kattemberg A., Maskell H.), pp. 65-132. IPCC/ Cambridge University Press, Cambridge.

Schimel D.S., House J.I., Hibbard K.A., Bousquet B., Ciais P., Peylin P., Braswell B.H., et al., 2001. Recent pattern and mechanisms of carbon exchange by terrestrial ecosystems. *Nature,* 414: 169-172.

Schulze E.D., 2006. Biological control of the terrestrial carbon sink. Biogeosciences 3: 147-166.

Smith J.U., Smith P., Addiscott T.M., 1996. Quantitative method to evaluate and compare soil organic matter (SOM) models, in *Evaluation of Soil Organic Matter Models Using Existing Long-Term Datasets, Global Environmental Change*, Nato ASI Ser. 1, vol 38, edited by D.S. Powlson, P.Smith and J.U. Smith, pp 181-199, Springer-Verlag, New York, 1996.

Steduto P., Hsiao T.C., 1997. Maize canopy under two water regime. I. Diurnal patterns of energy balance, carbon dioxide flux, and canopy conductance. *Agricultural and Forest Meteorology,* 89: 169-184.

Tang J., Baldocchi D.D., Xu L., 2005. Tree photosynthesis modulates soil respiration on a diurnal time scale. *Global change biology* 11: 1298-1304.

Tartachnyk I.I., Blanke M.M., 2004. Effect of delayed fruit harvest on photosynthesis, transpiration and nutrient remobilization of apple leaves. New Phytologist, 164: 441-450.

Testi L., Orgaz F., Villalobos F., 2008. Carbon exchange and water use efficiency of a growing, irrigated olive orchard. *Environmental and Experimental Botany*, 63: 168-177.

Tustin S., Corelli Grappadelli L., Ravaglia G., 1992. Effect of previous season and current radiant environments on early season spur development and assimilate translocation of “Golden Delicious” apple. *Journal of Horticultural Science,* 67: 351-360.

Wang K.G., Kellomaki S., Zha T.S., Peltola H., 2004. Component carbon fluxes and their contribution to ecosystem carbon exchange of a pine forest: an assessment based on eddy covariance measurements and an integrated model. *Tree Physiology*, 24(1): 19-34.

Wibbe M.L., Blanke M.M., 1995. Effects of defruiting on sink-source relationship, carbon budget, leaf carbohydrate content and water use efficiency of apple trees. *Physiologia Plantarum*, 94: 529-533.

Wünsche J.N., Lakso A.N., Robinson T.L., Lenz F., Denning S.S., 1996. The base of productivity in apple production systems: the role of light interception by different shoot types. *Journal of American Society of Horticultural Sciences*, 125: 93-99.

Wünsche J.N., Palmer J.W., Greer D.H., 2000. Effects of Crop Load on Fruiting and Gas-exchange Characteristics of Breaburn /M.26 Apple Trees at Full Canopy. *Journal of American Society of Horticultural Sciences*, 125: 93-99.

FIGURE captions

Figure 1. Seven day moving average of the Soil Water Content along the 3 considered years.

Figure 2. Annual course of the daily NPP for each considered ecosystem component for the 2 years in which biometric measurements were carried out (*A*-*F*). Fine and coarse root NPP were considered together (*D*). Yearly trend of daily total NPP accumulation for 2010 and 2011 (*E*).

Figure 3. Yearly trend of leaf area index (LAI) in 2010 and 2011.

Figure 4. Mean diurnal trend of NEE and Gp (µmol CO_2 $m^{-2}s^{-1}$), PPFD (µmol $m^{-2}s^{-1}$), VPD (hPa) and Tair (°C). For simplicity, the figures are assembled in three periods: January-April (a); May-August (b); September-December (c). NEE is missing in the first five months of 2011 (c) due to instrument failure. Gp values of may 2011 were obtained from partitioning of reconstructed NEE data with acceptable quality (fqc = 2).

Figure 5. Relationship between photosynthetic active radiation (PPFD) and Gross photosynthesis (Gp) for the three summer months of each year. A rectangular hyperbole model was fitted to assess the light response curve of the orchard and parameter of A_{max} and α reported in each plot. Only Gp data with a quality label ≤ 1 were used to assess model´s parameters.

Figure 6. (a) Exploration of all the possible correlations among NEE (g C $m^{-2}d^{-1}$) and the explanatory variables used in the multiple regression model: PPFD (µmol $m^{-2}s^{-1}$), VPD (hPa), Tair (°C), SWC(m^3m^{-3}), LAI(m^2m^{-2}). (b) The tree model used to assess interactions between explanatory variables in explaining variation of NEE.

Figure 7. Evaluation plots for the NEE multiple regression model (7a) after transformation of explanatory variables. Data of months 1,3,5,7,9,11 (2010) and 6,8,10,12 (2011) were used in the proposed modeling approach. The model was used to predict NEE values of the complementary dataset (months 2,4,6,8,10,12 (2010) and 7,9,11 (2011)). (7b) Measured versus predicted values are plotted along their linear relation (blue line). Dotted line represent the 1:1 relation.

Figure 8. (a)Exploration of all the possible correlations among GPP (g C $m^{-2}d^{-1}$) and the explanatory variables used in the multiple regression model: PPFD (µmol quanta $m^{-2}s^{-1}$), VPD (hPa), Tair (°C), SWC(m^3m^{-3}), LAI(m^2m^{-2}). (b) The tree model used to assess interactions between explanatory variables in explaining variation of GPP

Figure 9. Evaluation plots for the GPP multiple regression model (a) after BoxCox transformation of the response variable GPP. Model testing approach was the same as for NEE so the linear relation between measured versus predicted values is plotted (green line, fig b). Dotted line represents the 1:1 relation.

Figure 10. (a) Exploration of all the possible correlations among R*eco* (g C $m^{-2}d^{-1}$) and the explanatory variables used in the multiple regression model: PPFD (µmol quanta $m^{-2}s^{-1}$), VPD (hPa), Tair (°C), SWC(m^3m^{-3}), LAI(m^2m^{-2}). (b) The tree model used to assess interactions between explanatory variables in explaining variation of R*eco*.

Figure 11. Evaluation plots for the R*eco* multiple regression model (a) after BoxCox transformation of the response variable. Model testing approach was the same as for NEE so the linear relation between measured versus predicted values is plotted (red line, fig b). Dotted line represent the 1:1 relation.

Figure 12. Overall course of the Carbon fluxes for the considered time period. Measured daily data of NEE , Gp and R*eco* data (g C $m^{-2}d^{-1}$) derived from flux partitioning are presented with black bars. Predicted values for NEE, Gp and R*eco* obtained through the proposed models are plotted with a blue, green and red line respectively.

Figure 13. Cumulative net ecosystem production (g C m^{-2}) of the studied apple orchard for the period 2009-2011. Occurrence of the main phenological phases are indicated (BB= budburst; FB=full bloom; H = harvest).

Fig. 1

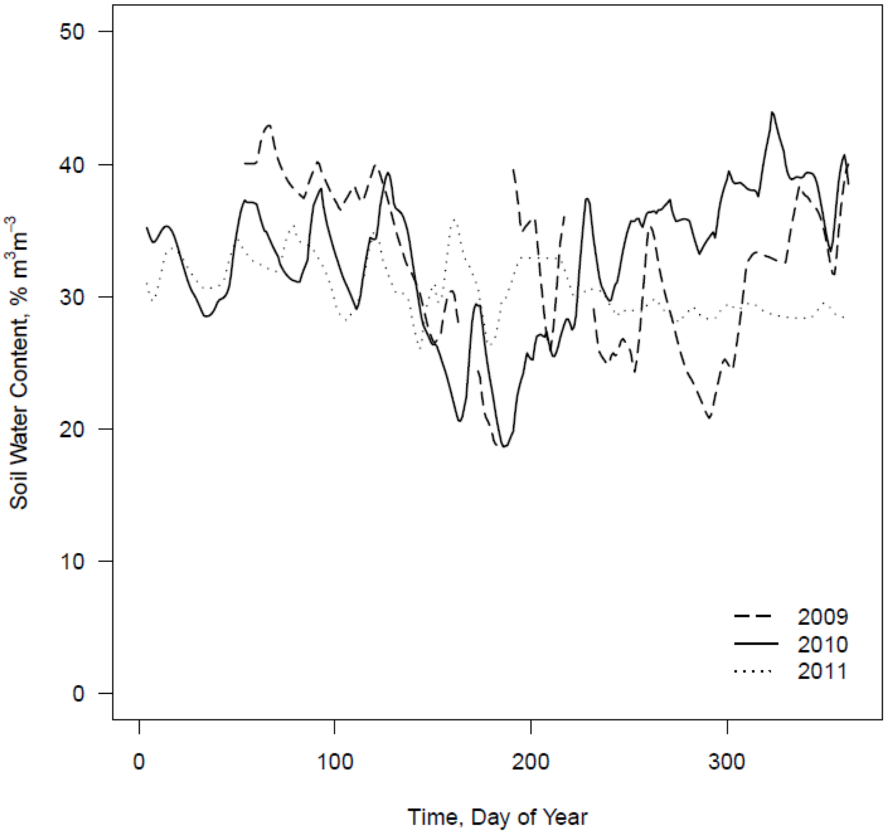

Soil Water Content, % m^{3}m^{-3}
50
40
30
20
10
0
0
100
200
300
Time, Day of Year
2009
2010
2011

Fig. 2

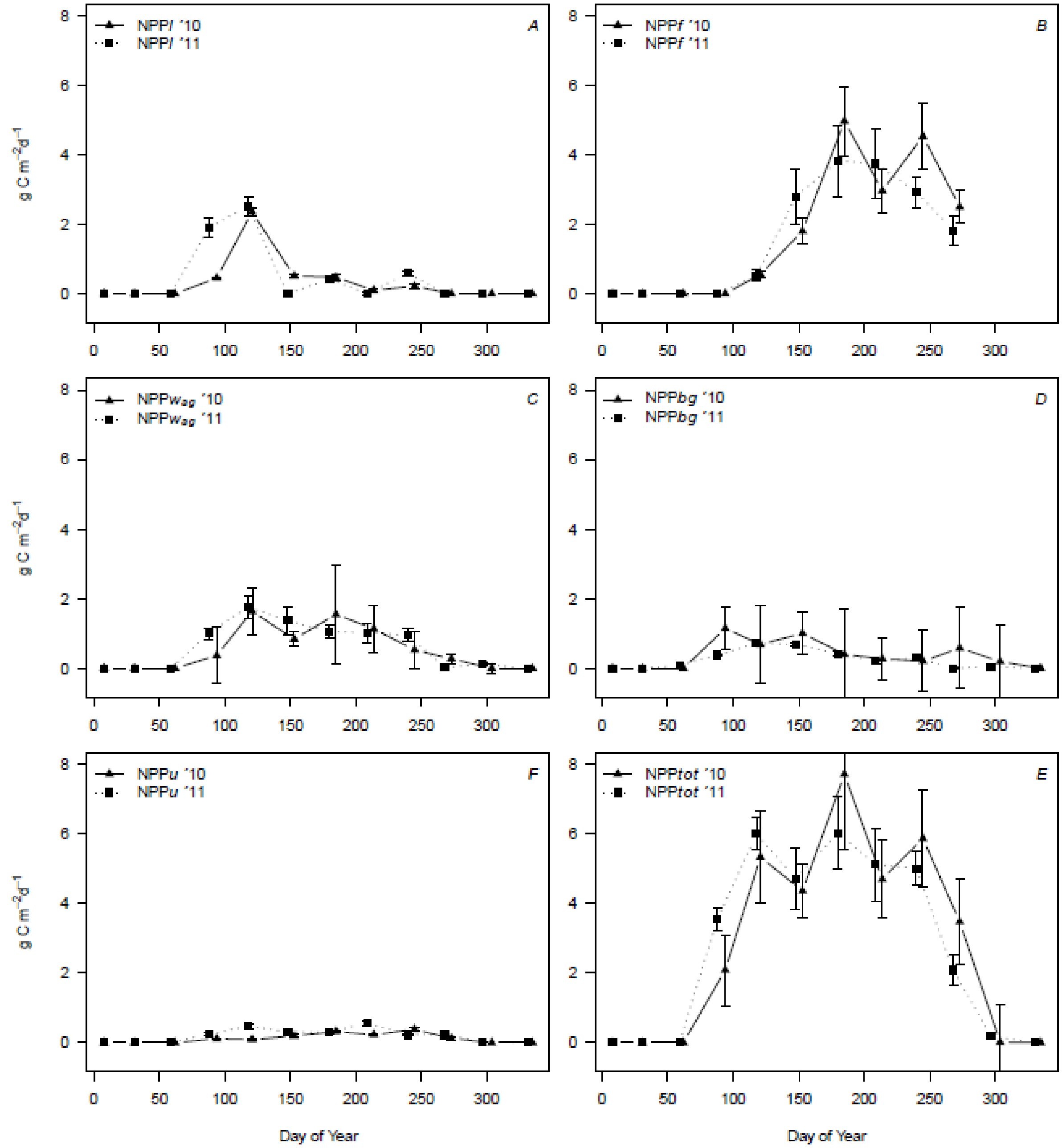
NPP*l* '10
NPP*l* '11
A
NPP*f* '10
NPP*f* '11
B
NPP*w*$_{ag}$ '10
NPP*w*$_{ag}$ '11
C
NPP*bg* '10
NPP*bg* '11
D
NPP*u* '10
NPP*u* '11
F
NPP*tot* '10
NPP*tot* '11
E
g C m^{-2}d^{-1}
0
2
4
6
8
0
50
100
150
200
250
300
Day of Year

Fig. 3

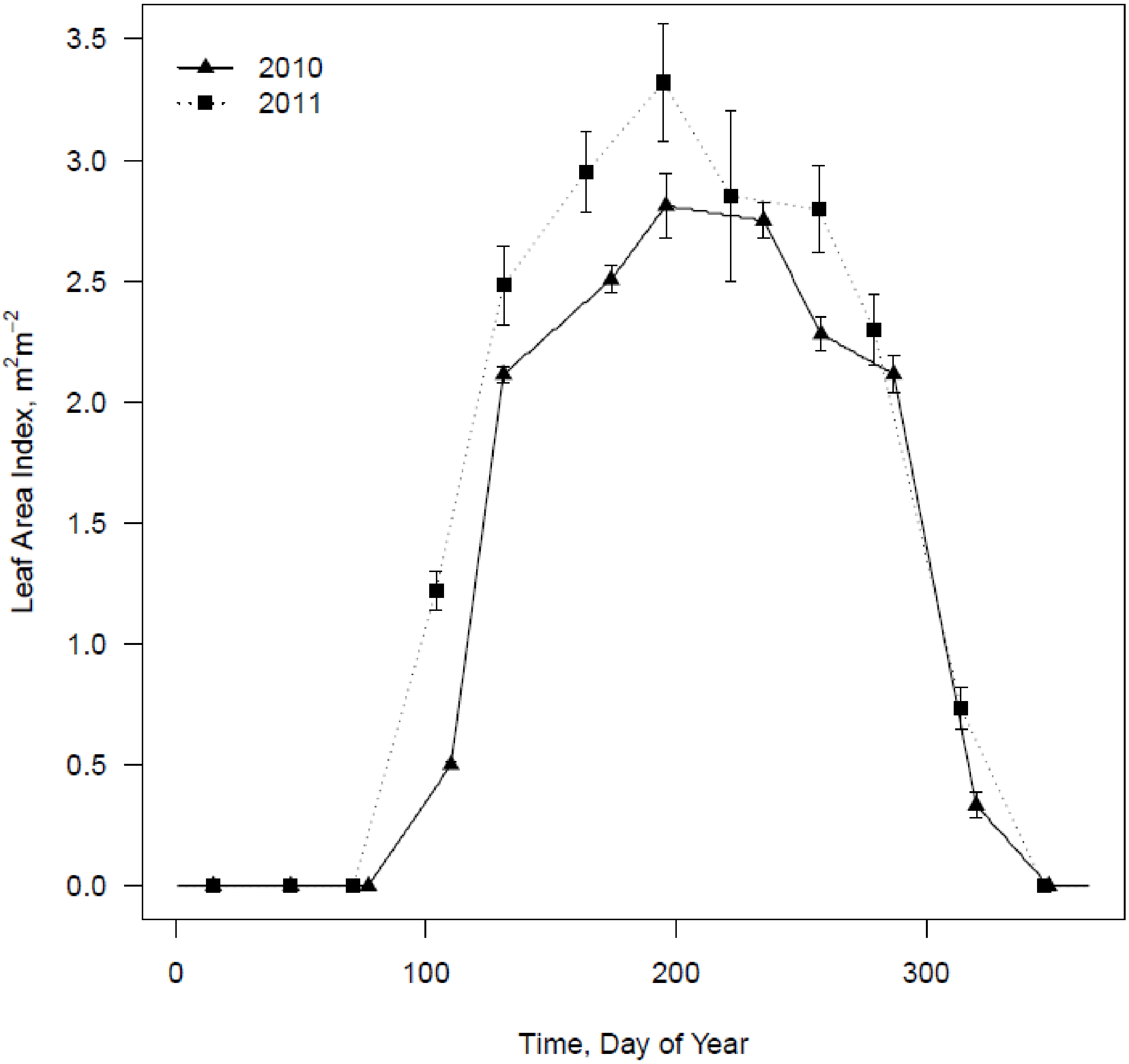

2010
2011
3.5
3.0
2.5
2.0
1.5
1.0
0.5
0.0
Leaf Area Index, m^2m^{-2}
0
100
200
300
Time, Day of Year

Fig. 4a

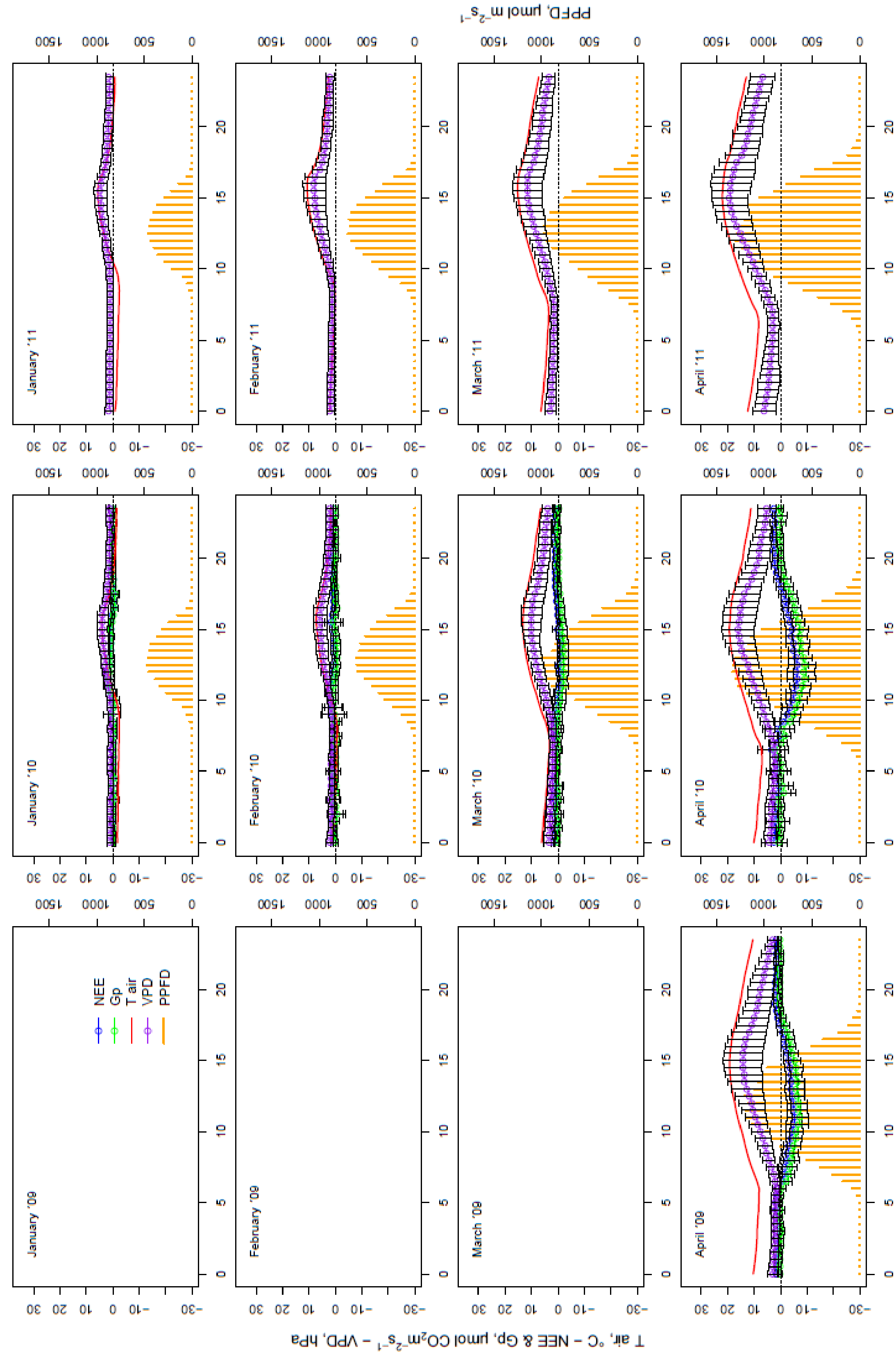
January '09
February '09
March '09
April '09
January '10
February '10
March '10
April '10
January '11
February '11
March '11
April '11
NEE
Gp
T air
VPD
PPFD
T air, °C – NEE & Gp, μmol CO$_2$m^{-2}s^{-1} – VPD, hPa
PPFD, μmol m^{-2}s^{-1}
-30
-10
0
10
20
30
0
500
1000
1500
0
5
10
15
20

Fig. 4b

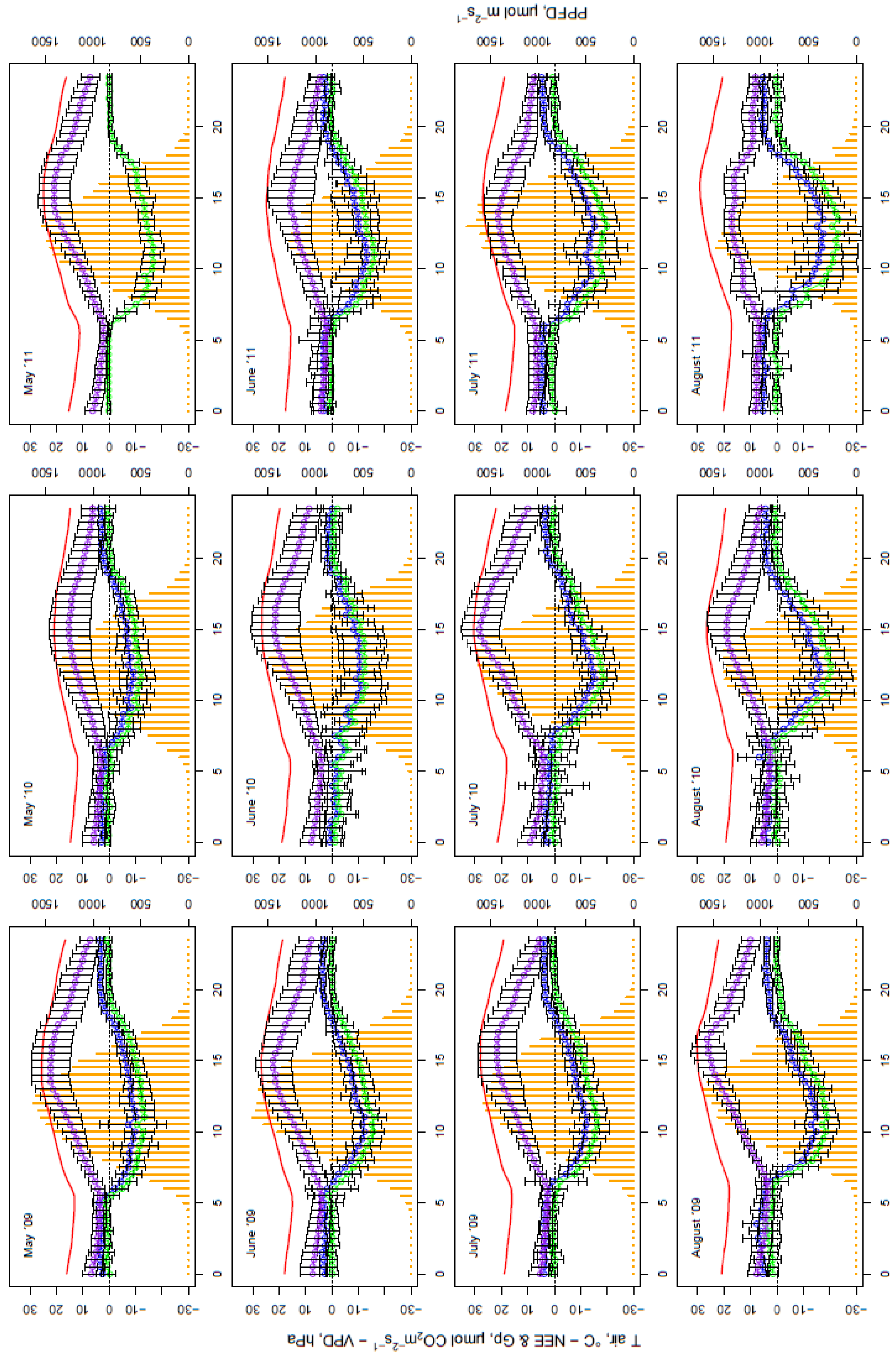

May '09
May '10
May '11
June '09
June '10
June '11
July '09
July '10
July '11
August '09
August '10
August '11
PPFD, µmol m^{-2}s^{-1}
T air, °C – NEE & Gp, µmol CO$_2$m^{-2}s^{-1} – VPD, hPa
0
500
1000
1500
30
20
10
0
−10
−30
0
5
10
15
20

Fig. 4c

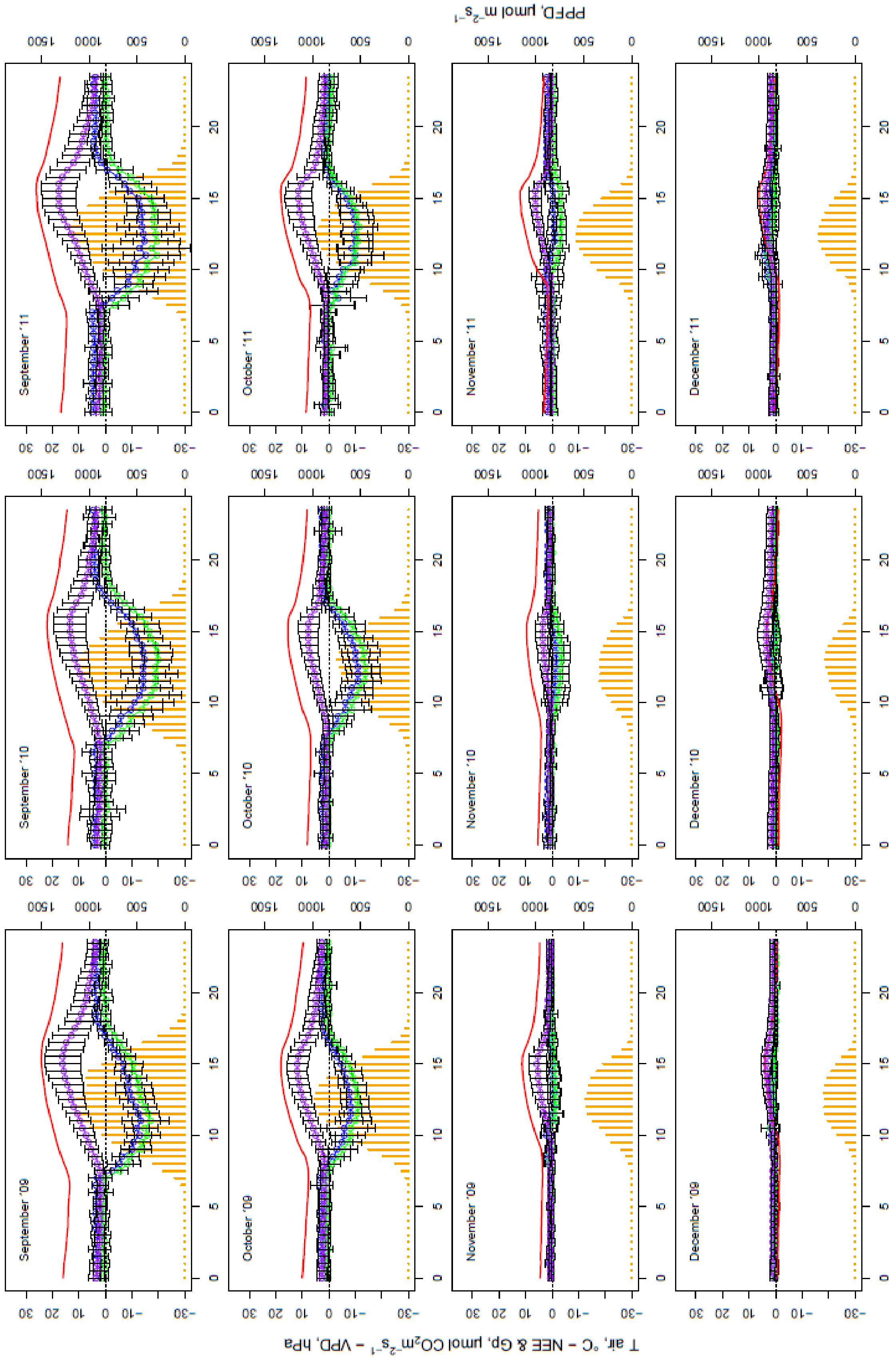
September '11
October '11
November '11
December '11
September '10
October '10
November '10
December '10
September '09
October '09
November '09
December '09
PPFD, μmol m⁻²s⁻¹
T air, °C – NEE & Gp, μmol CO₂m⁻²s⁻¹ – VPD, hPa
0
500
1000
1500
30
20
10
0
−10
−30
0
5
10
15
20

Fig. 5

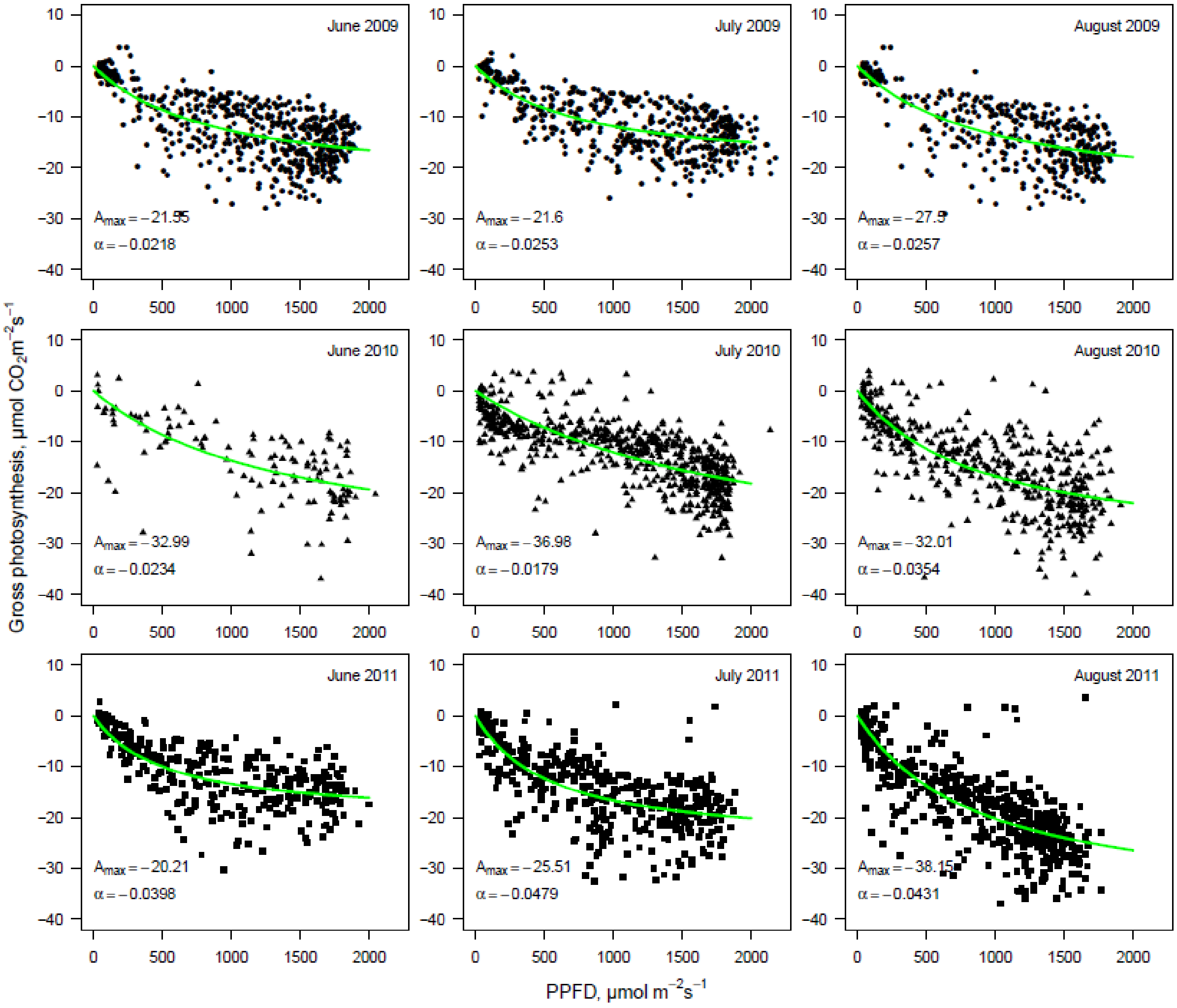
June 2009
$A_{max} = -21.95$
$\alpha = -0.0218$
July 2009
$A_{max} = -21.6$
$\alpha = -0.0253$
August 2009
$A_{max} = -27.9$
$\alpha = -0.0257$
June 2010
$A_{max} = -32.99$
$\alpha = -0.0234$
July 2010
$A_{max} = -36.98$
$\alpha = -0.0179$
August 2010
$A_{max} = -32.01$
$\alpha = -0.0354$
June 2011
$A_{max} = -20.21$
$\alpha = -0.0398$
July 2011
$A_{max} = -25.51$
$\alpha = -0.0479$
August 2011
$A_{max} = -38.15$
$\alpha = -0.0431$
Gross photosynthesis, µmol $CO_2 m^{-2}s^{-1}$
10
0
−10
−20
−30
−40
0
500
1000
1500
2000
PPFD, µmol $m^{-2}s^{-1}$

Fig. 6a

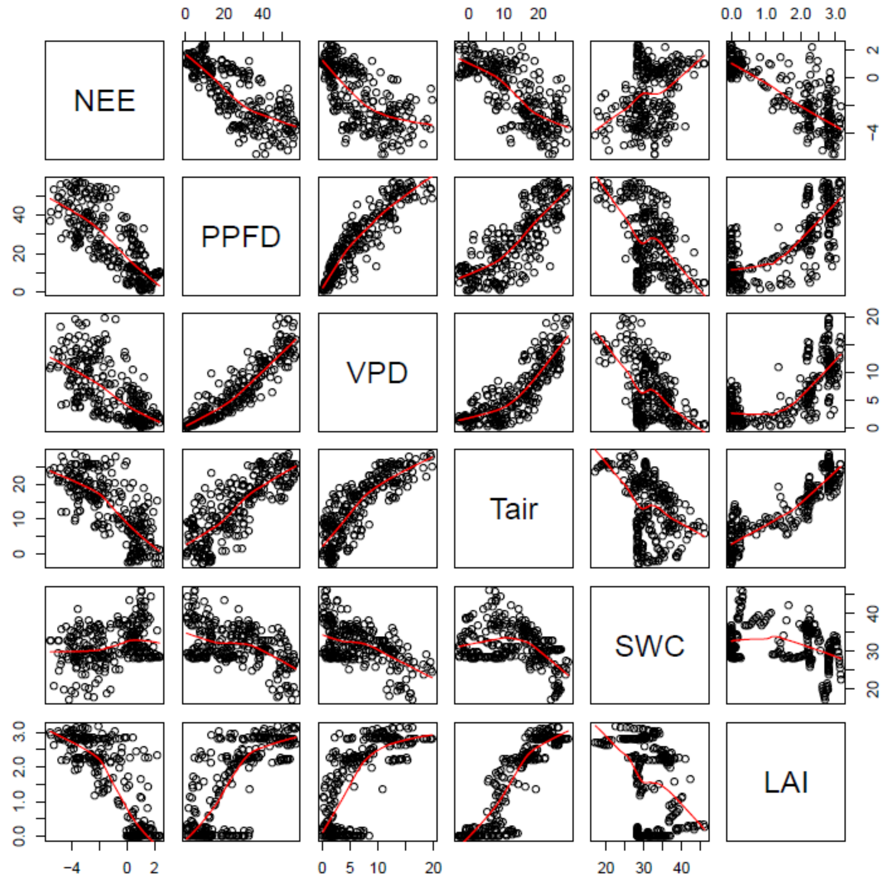
NEE
PPFD
VPD
Tair
SWC
LAI
0 20 40
0 10 20
0.0 1.0 2.0 3.0
2 0 −2 −4
0 20 40
20 15 10 5 0
0 10 20
40 30 20
3.0 2.0 1.0 0.0
−4 0 2
0 5 10 20
20 30 40

Fig. 6b

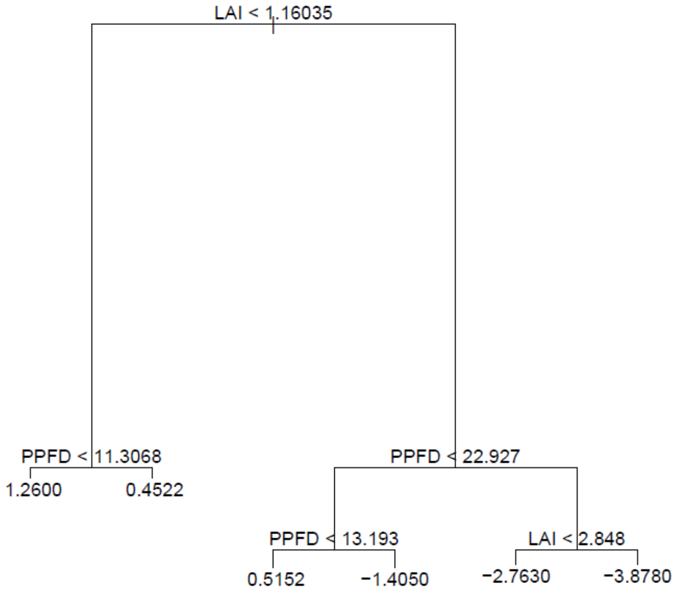
LAI < 1.16035
PPFD < 11.3068
1.2600
0.4522
PPFD < 22.927
PPFD < 13.193
0.5152
−1.4050
LAI < 2.848
−2.7630
−3.8780

Fig. 7a

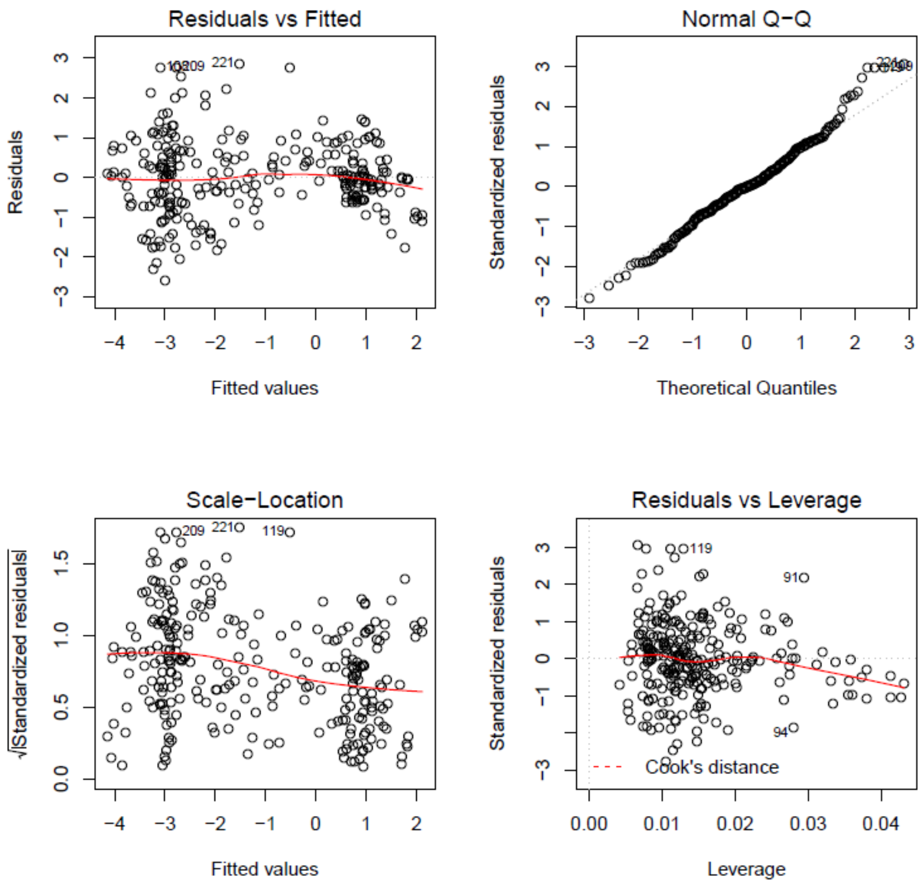

Residuals vs Fitted
Residuals
Fitted values
209
221
Normal Q−Q
Standardized residuals
Theoretical Quantiles
221
Scale−Location
√|Standardized residuals|
Fitted values
209
221
119
Residuals vs Leverage
Standardized residuals
Leverage
119
91
94
Cook's distance

Fig. 7b

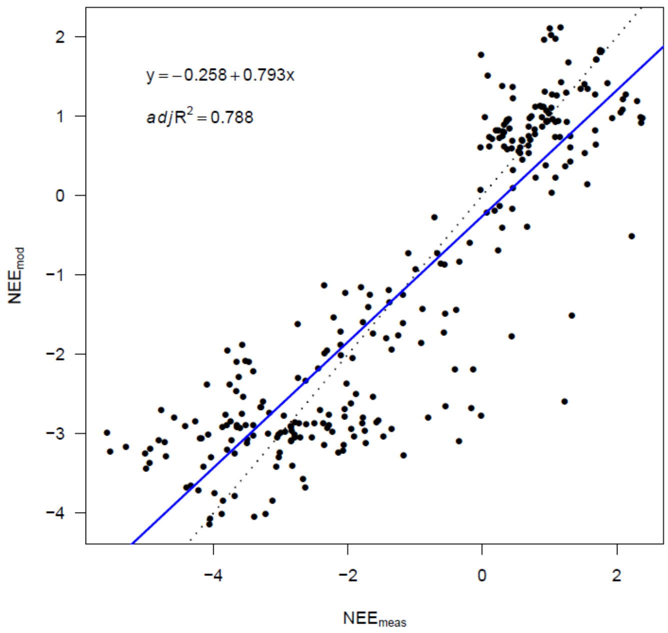

y = −0.258 + 0.793x
adjR² = 0.788
NEEmod
NEEmeas
−4
−2
0
2

Fig. 8a

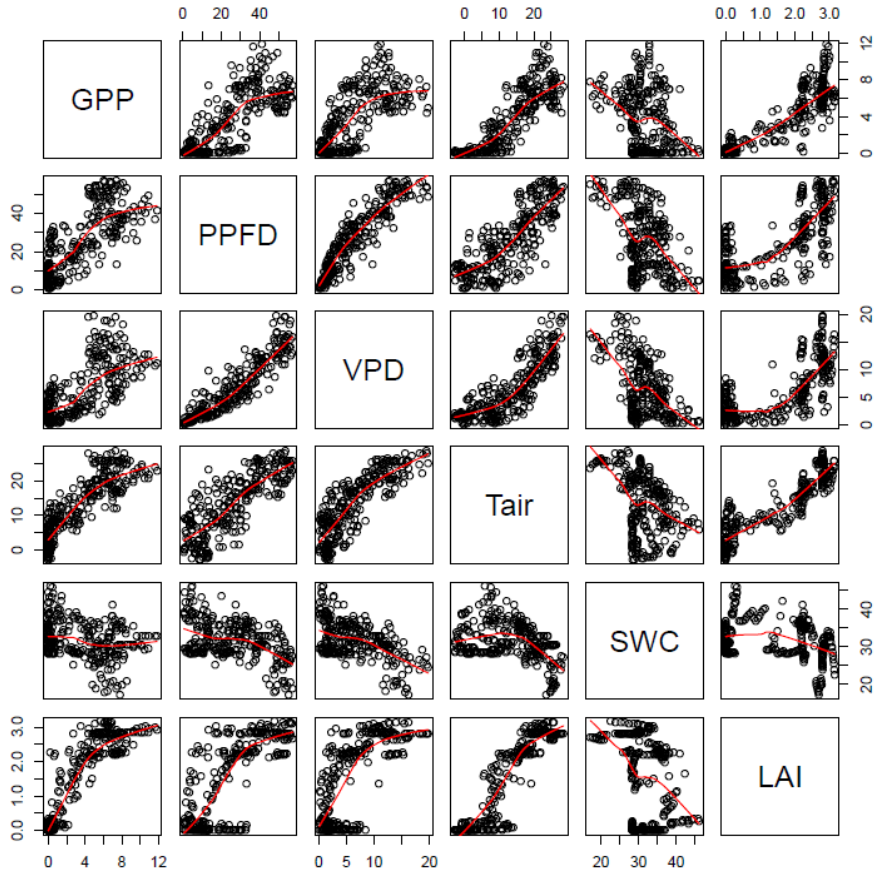

GPP
PPFD
VPD
Tair
SWC
LAI
0 20 40
0 10 20
0.0 1.0 2.0 3.0
0 4 8 12
0 20 40
0 5 10 20
0 10 20
0 5 10 15 20
20 30 40
0.0 1.0 2.0 3.0
0 4 8 12
0 5 10 20
20 30 40

Fig. 8b

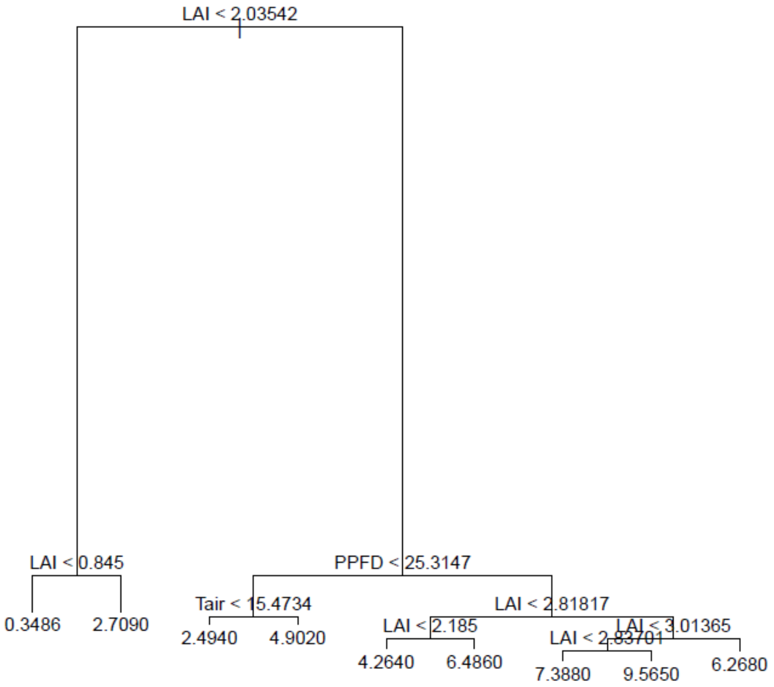

LAI < 2.03542
LAI < 0.845
PPFD < 25.3147
0.3486
2.7090
Tair < 15.4734
LAI < 2.81817
2.4940
4.9020
LAI < 2.185
LAI < 3.01365
LAI < 2.83701
4.2640
6.4860
7.3880
9.5650
6.2680

Fig. 9a

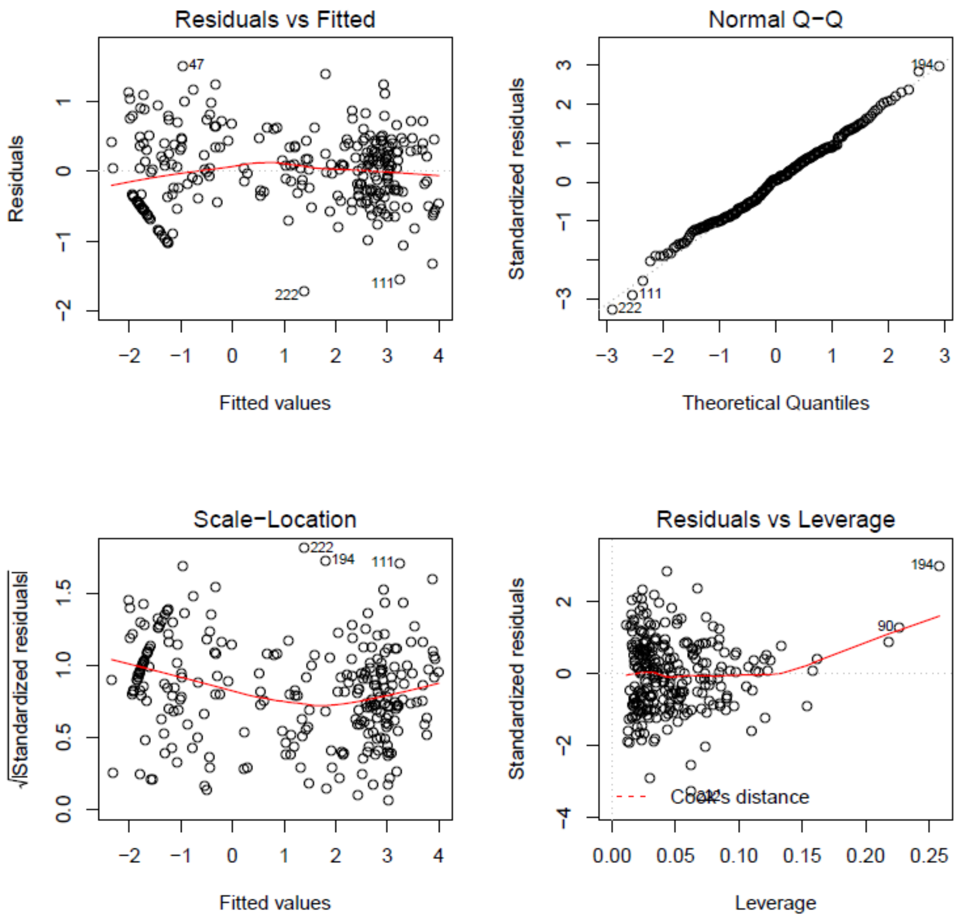
Residuals vs Fitted
Residuals
Fitted values
47
222
111
Normal Q−Q
Standardized residuals
Theoretical Quantiles
194
111
222
Scale−Location
√|Standardized residuals|
Fitted values
222
194
111
Residuals vs Leverage
Standardized residuals
Leverage
194
90
Cook's distance
−2
−1
0
1
2
3
4
−3
0.00
0.05
0.10
0.15
0.20
0.25
0.0
0.5
1.0
1.5

Fig. 9b

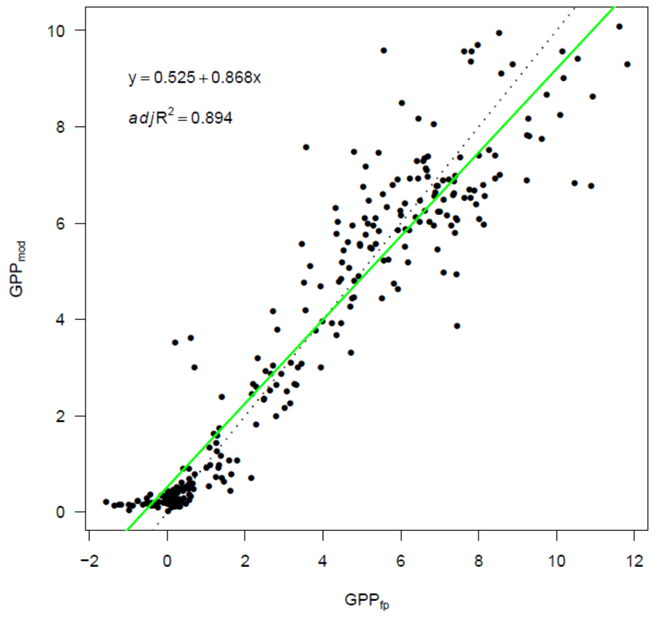
y = 0.525 + 0.868x
adjR² = 0.894
GPP_mod
GPP_fp
−2
0
2
4
6
8
10
12

Fig. 10a

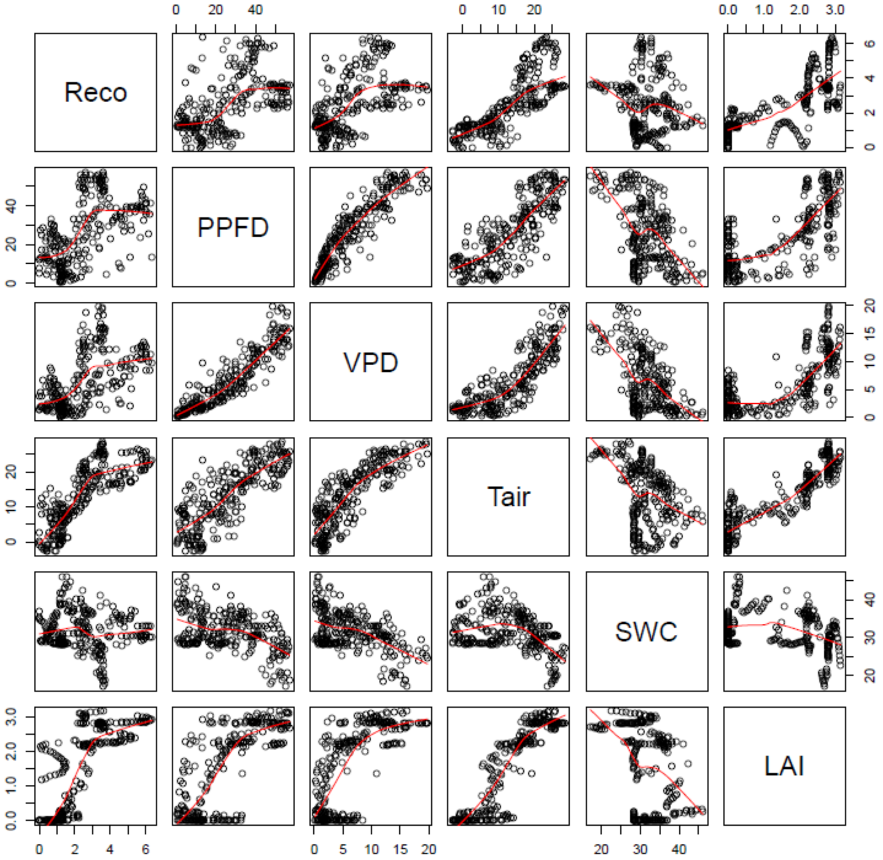

Fig. 10b

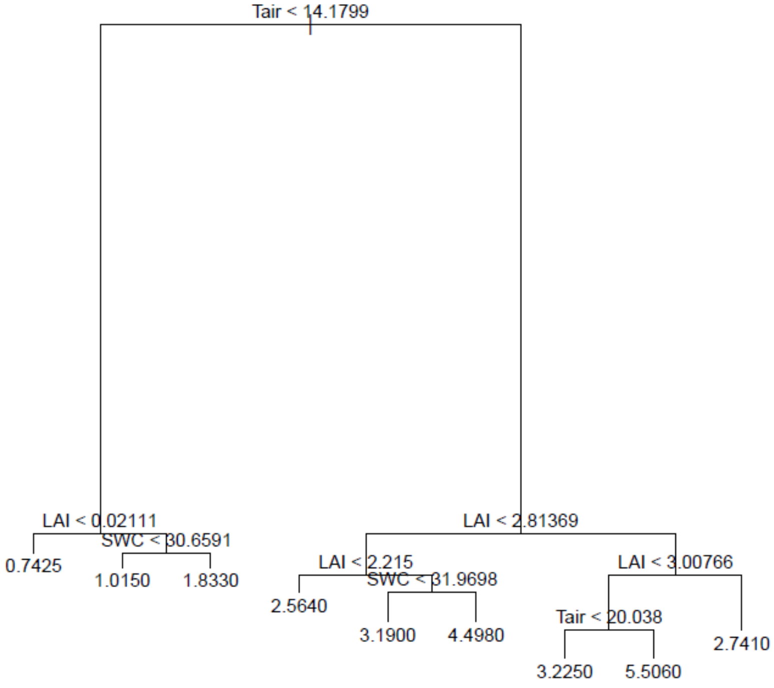

Fig. 11a

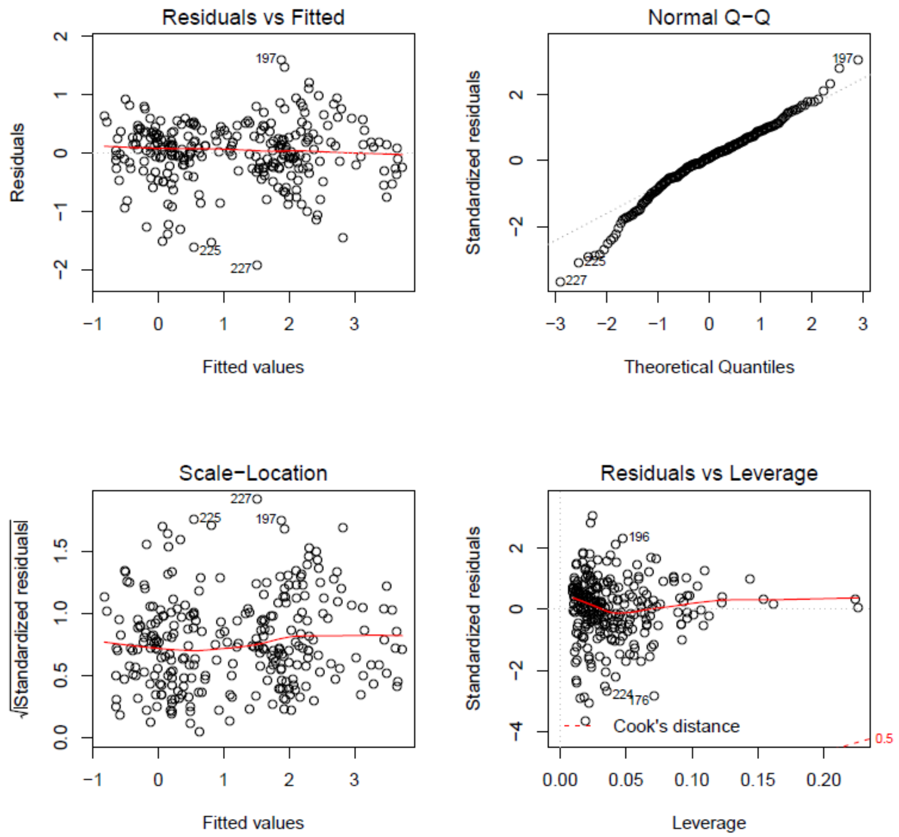

Fig. 11b

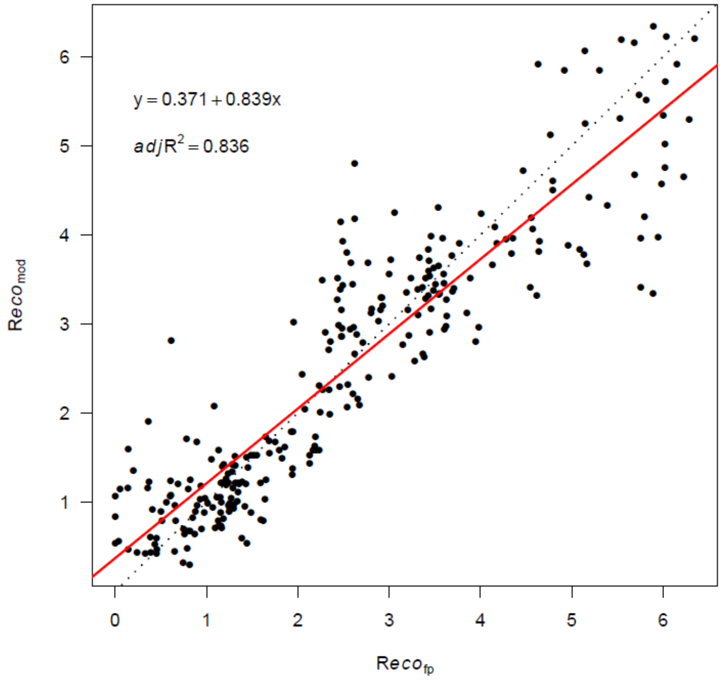

Fig. 12

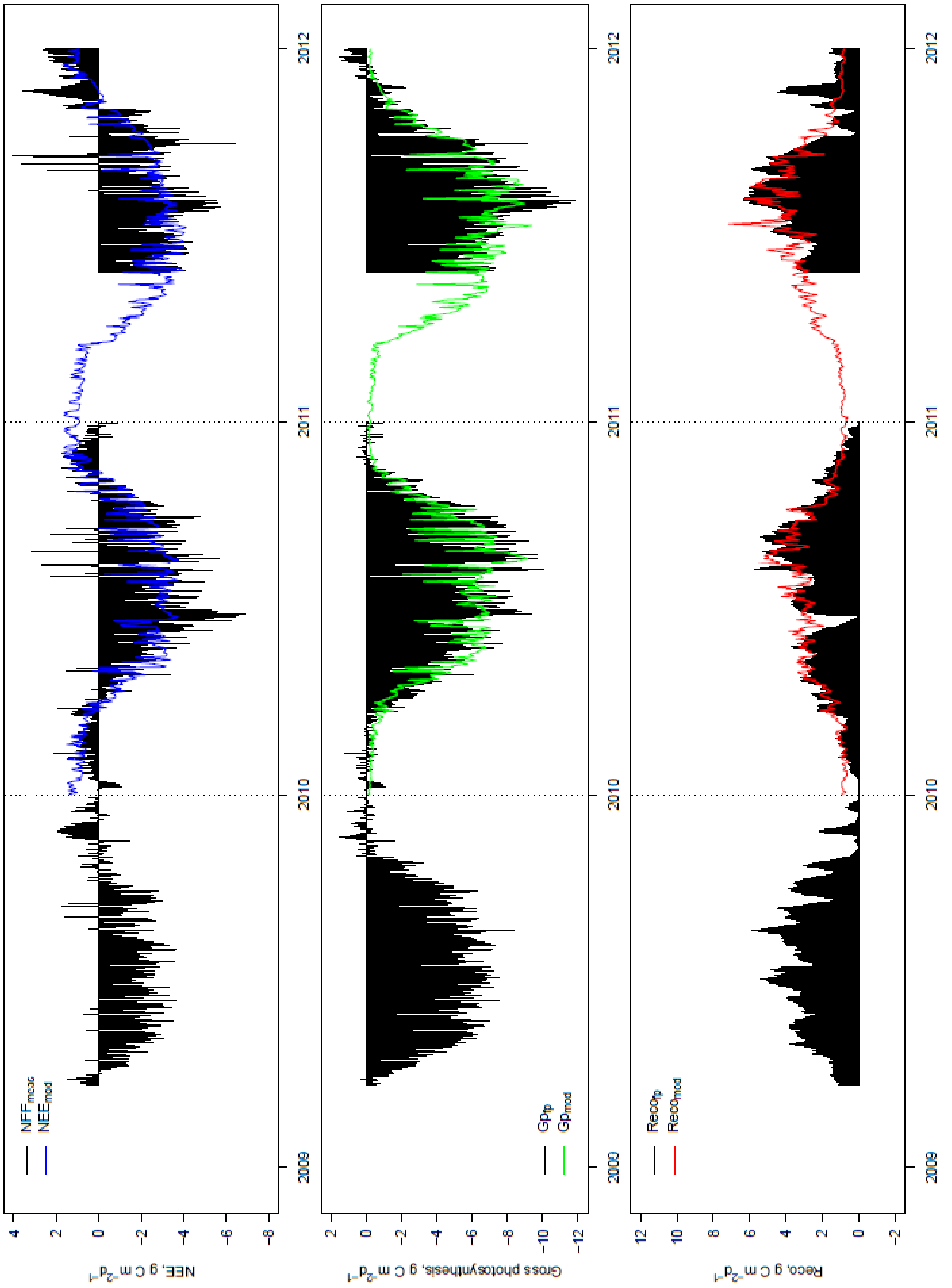

NEE, g C m⁻² d⁻¹
4
2
0
-2
-4
-6
-8
NEE_meas
NEE_mod
Gross photosynthesis, g C m⁻² d⁻¹
2
0
-2
-4
-6
-8
-10
-12
Gp_fp
Gp_mod
Reco, g C m⁻² d⁻¹
12
10
8
6
4
2
0
-2
Reco_fp
Reco_mod
2009
2010
2011
2012

Fig. 13

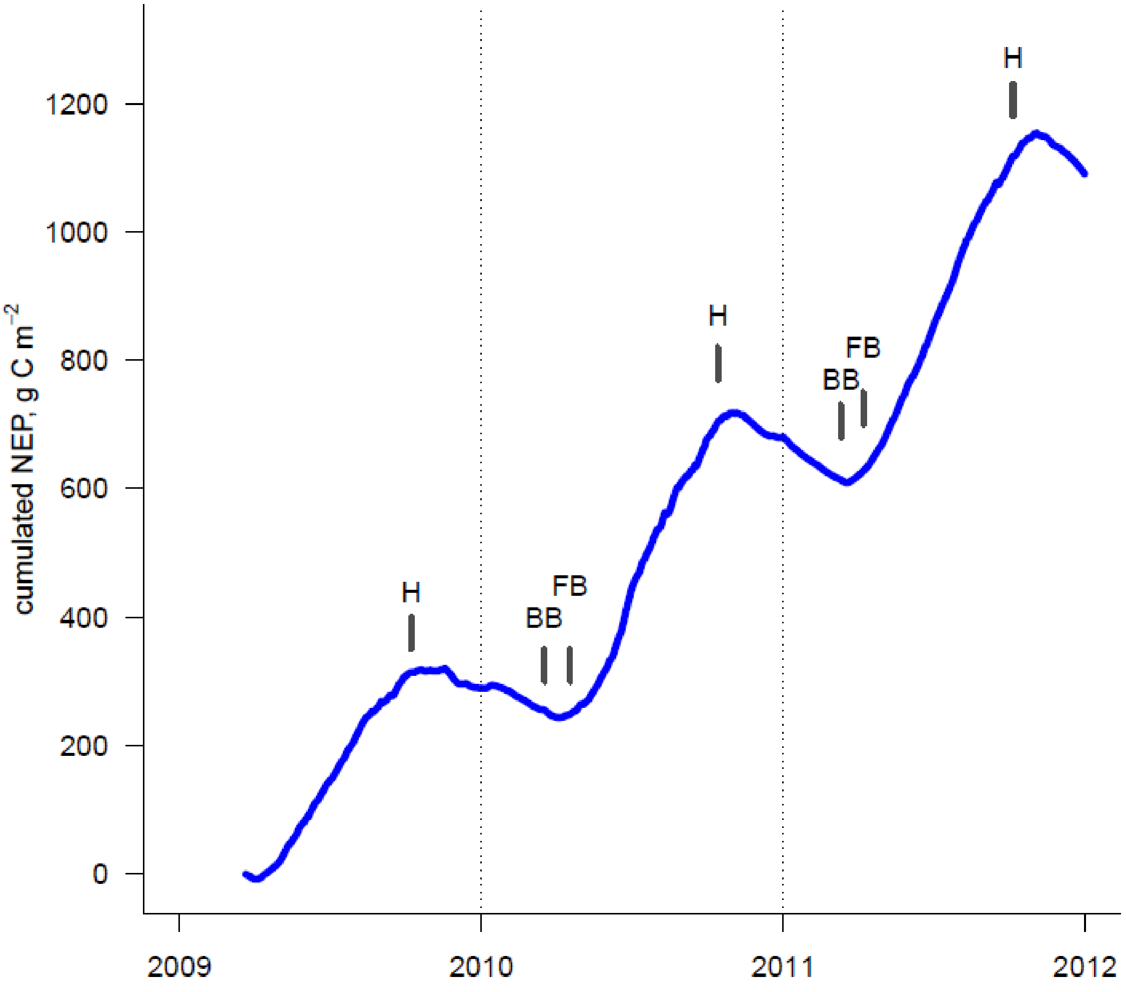

cumulated NEP, g C m^{-2}
1200
1000
800
600
400
200
0
2009
2010
2011
2012
H
BB
FB
H
BB
FB
H

TABLES

Table 1. Comparison of environmental conditions during growing season in Caldaro for the period 2009-2011. Historical Mean data (1980-2009) were collected by the meteorological station of the Laimburg research center for Agriculture and Forestry, close to our study site.

Variable	Year	Mar	Apr	May	Jun	Jul	Aug	Sep	Oct	Nov	*Mar-Nov*
Temperature, °C											
Mean daily temperature	2009	8.4	13.4	19.7	20.9	22.1	23.9	18.3	12.0	6.2	*16.1*
	2010	8.0	13.0	16.5	21.3	24.4	21.3	16.4	9.9	6.2	*15.2*
	2011	8.9	15.1	18.5	20.1	21.1	22.9	19.5	10.9	5.2	*15.8*
	HM	8.5	12.3	16.8	20.1	22.2	21.4	17.5	11.7	4.7	*15.0*
Mean daily minimum	2009	1.7	7.6	12.5	14.4	15.6	17.8	13.0	7.0	2.6	*10.3*
	2010	2.7	6.4	11.4	15.1	17.6	16.1	11.3	5.8	3.5	*10.0*
	2011	3.3	7.8	10.9	15.0	14.8	16.4	14.0	5.9	0.8	*9.9*
	HM	1.9	5.8	10.3	13.5	15.4	15.0	11.2	6.7	0.1	*8.9*
Mean daily maximum	2009	14.6	19.7	26.4	27.3	28.6	30.7	24.7	18.6	11.5	*22.4*
	2010	13.8	19.9	21.5	27.1	31.0	27.3	22.5	15.7	9.9	*21.0*
	2011	15.5	22.5	25.7	25.7	27.6	29.7	26.5	18.3	12.4	*22.6*
	HM	15.7	18.9	24.1	27.0	29.3	28.9	24.4	18.4	11.1	*22.0*
Total solar radiation, MJ m^{-2}	2009	425.3	481.3	680.1	701.0	690.8	652.7	442.5	336.1	161.1	*4571.0*
	2010	382.4	568.5	609.6	682.0	732.3	568.8	442.5	255.8	131.9	*4373.8*
	2011	398.3	599.8	706.1	575.1	676.8	618.3	450.9	323.8	195.5	*4544.7*
	HM	380.2	472.1	577.5	607.0	652.0	564.4	417.6	264.3	163.2	*4098.3*
Mean daily max. VPD, hPa	2009	*n.a.*	15.2	24.0	23.7	23.7	27.1	17.0	12.5	5.7	*18.6*
	2010	10.8	17.0	16.0	23.0	29.8	20.6	14.7	8.3	3.9	*16.0*
	2011	11.8	20.0	22.8	17.7	24.1	19.3	18.9	11.6	6.7	*17.0*
	HM	*n.a.*	*n.a.*	*n.a.*	*n.a.*	*n.a.*	*n.a.*	*n.a.*	*n.a.*	*n.a.*	*n.a.*
Total precipitation, mm	2009	65.1	64.3	6.6	50.6	92.0	69.4	81.2	30.6	93.0	*552.8*
	2010	62.8	49.6	100.4	70.4	47.4	175.6	126.8	124.8	141.0	*898.8*
	2011	41.8	42.6	77.6	107.0	30.6	173.4	136.2	124.4	15.2	*748.8*
	HM	44.1	58.3	87.1	89.4	98.2	96.9	79.6	81.7	74.1	*709.4*
Soil Water Content, m^3m^{-3}	2009	*n.a.*	38.1	32.8	25.9	31.2	30.6	29.4	23.7	32.4	*30.5*
	2010	33.3	33.1	33.4	24.7	23.6	30.9	35.7	35.8	39.9	*32.3*
	2011	33.4	30.7	30.1	31.0	32.0	30.6	29.0	28.8	28.9	*30.5*
	HM	*n.a.*	*n.a.*	*n.a.*	*n.a.*	*n.a.*	*n.a.*	*n.a.*	*n.a.*	*n.a.*	*n.a.*

Table 2. Estimated parameters for the minimum adequate model describing NEE data.

NEE_{mod}	**Estimate**	**Std.Error**	**Pr(>|t|)**
a	2.74030	0.25277	< 0.001
b	-0.71101	0.10530	< 0.001
c	0.02400	0.00426	< 0.001
d	-0.06919	0.00449	< 0.001

Table 3. Estimated parameters for the minimum adequate model describing GPP data

$GPPt_{mod}$	**Estimate**	**Std.Error**	**Pr(>|t|)**
a	-2.02519	0.11738	< 0.001
b	-0.23151	0.06396	< 0.001
c	0.06576	0.01411	< 0.001
d	2.38615	0.18108	< 0.001
e	-0.00246	0.00046	< 0.001
f	-0.52398	0.07233	< 0.001
g	0.03054	0.00596	< 0.001
h	0.00538	0.00074	< 0.001
i	-0.40244	0.08309	< 0.001
j	-0.00064	0.00013	< 0.001
k	-0.00049	0.00012	< 0.001
l	0.00667	0.00184	< 0.001
M	0.00973	0.00219	< 0.001

Table 4. Estimated parameters for the minimum adequate model describing R*eco* data

R*eco*t$_{mod}$	**Estimate**	**Std.Error**	**Pr(>|t|)**
A	0.26520	0.10150	< 0.01
B	-0.06279	0.01124	< 0.001
C	-0.29890	0.07537	< 0.001
D	0.01598	0.00250	< 0.001
E	0.00675	0.00097	< 0.001
F	-0.08499	0.02286	< 0.001
G	-0.00049	0.00007	< 0.001
H	-0.00036	0.00006	< 0.001
I	0.00352	0.00085	< 0.001
J	0.00475	0.00053	< 0.001
K	-0.00091	0.00022	< 0.001

Table 5. Comparison of net ecosystem carbon productivity (NEP, g C m^{-2}y^{-1}) and the component terms gross primary productivity (GPP, g C m^{-2}y^{-1}) and total ecosystem respiration (R*eco*, g C m^{-2}y^{-1}). Total net primary productivity (NPP) biometrically measured in 2010 and 2011 is also reported.

C fluxes, g C m^{-2}y^{-1}	**2009**	**2010**	**2011**
NEP	290*	371	430**
GPP	1010*	1164	1347**
Reco	720*	815	917**
NPP	*n.a.*	960	988

* measurements started the 22th of March 2009

** cumulated data of the first five months of 2011 are obtained from modeled data

Table 6. Successive periods in which the ecosystem acted as net sink or source of C to the atmosphere and quantification of the relative NEE cumulated. The average values (mean of day of switch ± 3 days, (*SD*)) of the main environmental variables in the days in which the apple orchard switches from being a net source to a net sink of C and viceversa are listed.

Data	**ecosystem status**	**length of period (*days*)**	**cumulative NEE (*g C m^{-2}*)**	**day of switch (*DOY*)**	**mean daily Air Temp (*°C*)**	**mean daily PPFD (*µmol m^{-2} s^{-1}*)**	**mean daily VPD (*hPa*)**
7/04/2009	sink	218	-326	97	14.5 *(0.8)*	36.7 *(6.4)*	8.5 *(1.0)*
13/11/2009				315	6.0 *(2.3)*	11.0 *(5.5)*	2.4 *(0.8)*
	source	146	75				
6/04/2010	sink	213	-475	96	11.6 *(2.6)*	35.1 *(9.9)*	7.4 *(3.1)*
5/11/2010				309	9.0 *(1.3)*	9.8 *(6.2)*	1.3 *(0.7)*
	source	136	116				
20/03/2011	sink	227	-550	80	9.4 *(1.5)*	24.7 *(11.5)*	6.4 *(2.9)*
3/11/2011				307	9.0 *(1.9)*	8.7 *(6.2)*	1.2 *(0.6)*

CHAPTER 4

General conclusions

Conclusions

The main findings of the first part of this thesis (chapter 2) are that the main ecosystem carbon fluxes of a fruit tree ecosystem have a comparable magnitude with respect to deciduous forest growing at the same climate conditions, while the allocation pattern is strongly different. Approximately half of the net primary productivity of the orchard is allocated into fruits while allocation to vegetative organs such as leaves, wood and roots is preponderant in forests. Carbon use efficiency of the orchard is higher respect to forest, allowing us to reject, for this ecosystem type, the hypothesis that wants maintenance costs (autotrophic respiration) being half of the gross primary production.

In the second part, the Carbon fluxes of the apple orchard for three growing seasons are reported. Clear patterns of photosynthesis and net ecosystem exchange were observed at daily basis and results were consistent among months of different years. The relationship with the main environmental drivers were assessed, and light, as expected, resulted the most influential parameters governing the diurnal amount of carbon exchanged at a given value of leaf area index. After having taken into account the acclimation effects, the established models could also be used to simulate future scenarios resulting from changes in environmental factors.

As a response to the increased concern about the GHG emission from agricultural land, the cumulated net ecosystem production of the orchard over three seasons was quantitatively assessed in a value that approximately balanced the amount of carbon that annually was exported through the harvested apples. The presented data support the hypothesis that, if we do not consider the direct or indirect C emissions due to orchard management, the production of apple fruits implies a minimal or null impact on net C emissions to the atmosphere from the orchard ecosystem.

Summary

Carbon fluxes and allocation pattern in an apple orchard

In the present work, an apple orchard located in the Province of Bolzano (Alto Adige) was investigated with a micrometeorological and ecophysiological approach with the objectives to assess its carbon fluxes and allocation patterns and their relationship with the main environmental ad physiological parameters. In the first study, we combined three largely deployed methods, eddy covariance, soil respiration and biometric measurements, during a complete year (2010). We applied a measurement protocol optimized for quantifying monthly values of carbon fluxes in this ecosystem type, which allows a cross-check between estimates obtained from different methods. We also attributed NPP components to standing biomass increment, detritus cycle feeding and lateral export. In the second study, the eddy covariance measured net ecosystem carbon exchange and the derived GPP and R*eco* are reported for three complete growing seasons. The influence of environmental and physiological parameters on these three carbon fluxes were analyzed with a multiple regression model approach.

We found that in the apple orchard both net ecosystem production and gross primary production, were of magnitude comparable to those of natural forests growing in similar climate conditions, while large differences occurred in the allocation patterns and in the fate of produced biomass: the carbon sequestered from the atmosphere was largely allocated to production of fruits: 49% of annual NPP was taken away from the ecosystem as apple production. Organic material (leaves, fine root litter, pruned wood and early fruit drop) contributing to detritus cycle was the 46% of NPP and the 5% only went to standing biomass increment. The carbon use efficiency (CUE), with an annual average of 0.68 ± 0.10, was higher than the previously suggested constant values of 0.47-0.50. Low nitrogen investment in fruits and the optimal growth temperature (11.6°C) observed at the site are suggested as explanatory variables for the high CUE observed.

Light and LAI had the strongest influence on both NEE and GPP. On a diurnal basis, these two carbon fluxes reach their peak approximately at noon, while they appear to be limited by high value of VPD and air temperature in the afternoon. The proposed models can be used to explain and simulate current relations between carbon fluxes and environmental parameters at daily and yearly time scale. In a context of global change, ecosystem acclimation has to be considered in order to predict future scenarios.

At a seasonal scale, consistent sink/source behavior pattern was observed within the three years: the apple orchard begun to perform as a net sink of carbon between bud burst and full-bloom, while became a net carbon source approximately 2-3 weeks after fruit harvest. On average, the yearly net ecosystem production balanced the carbon annually exported with the harvested apples. This allows to support the hypothesis of a minimal or null impact on net C emission to the atmosphere from the apple orchard ecosystem.

Riassunto

Flussi e modalità di allocazione del carbonio in un meleto

Nel presente lavoro, sono state applicate tecniche micrometeorologiche ed ecofisologiche alla coltura del melo, con l´obiettivo di valutare i flussi di carbonio (C) propri di questo ecosistema, l´allocazione della biomassa prodotta e la relazione dei flussi giornalieri di carbonio con i principali parametri ambientali e fisiologici.

Il protocollo sperimentale adottato in un primo studio ha previsto l´uso sinergico di tre metodologie (misure eddy covariance, di respirazione del suolo e biometriche) per l´intero anno 2010, permettendo di ottenere un controllo incrociato delle stime di flusso di C derivanti dai diversi metodi. Attraverso misure biometriche è stata valutata l´allocazione dei prodotti della fotosintesi nelle diverse componenti dell´ecosistema meleto, individuando la quota di C destinata ai tre pools: biomassa vivente, ciclo di detrito ed asportazione dal frutteto.

In un secondo studio, lo scambio ecosistemico netto di cabonio (NEE) misurato con la tecnica dell´eddy covariance ed i valori derivati di produttività primaria lorda (GPP) e respirazione ecosistemica (R*eco*), sono riportati per tre intere stagioni vegetative (2009-2011). L´influenza delle principali variabili ambientali e fisiologiche su questi tre flussi a livello giornaliero è stata analizzata con l´approccio della regressione multipla.

Questo studio ha permesso di verificare che sia la produzione ecosistemica netta (NEP) che la GPP sono quantitativamente simili a quelle di foreste che crescono in condizioni climatiche simili, mentre sussistono sostanziali differenze nei pattern di allocazione e nel destino della biomassa prodotta. Nel 2010, il 49% del carbonio fissato è stato esportato dal meleto alla raccolta dei frutti, la quantità di biomassa che nello stesso anno ha contribuito ad alimentare il ciclo di detrito è stata il 46%, mentre solo il 5 % ha incrementato il volume della biomassa vivente. L´efficienza di uso del carbonio (CUE), intesa come il rapporto tra NPP e GPP, è stata di 0.68 ± 0.10, più alta rispetto a valori precedentemente proposti in letteratura (0.47-0.50) su altri ecosistemi vegetali. La bassa concentrazione di azoto nei frutti e l´ottimale temperatura di crescita rilevata nel frutteto sono ritenuti essere i fattori principali che giustificano questo risultato.

La radiazione fotosinteticamente attiva (PPFD) e l´indice di area fogliare (LAI) hanno avuto la maggiore influenza su GPP e NEE. Su base giornaliera, questi due flussi di carbonio raggiungono il loro picco verso mezzogiorno, mentre nel pomeriggio è stato osservato un effetto limitante possibilmente dovuto agli alti valori di VPD e temperatura dell´aria. I modelli proposti possono essere usati per spiegare e simulare le relazioni tra flussi di carbonio e parametri ambientali su scala temporale giornaliera ed annuale. Nel contesto del cambiamento climatico, l´acclimatazione dell´ecosistema deve essere considerata prima di poter usare tali modelli per simulare scenari futuri.

Su scala stagionale, la capacità dell´ecosistema di agire come assorbitore o sorgente di carbonio verso l´atmosfera nelle tre le stagioni monitorate è stata coerente con lo sviluppo delle fasi fenologiche: il meleto comincia ad essere un sink netto nel periodo compreso tra la rottura delle gemme e la piena fioritura, mentre i flussi di carbonio in uscita dall´agroecosistema superano di nuovo quelli in entrata a partire da circa 2-3 settimane dopo la raccolta. I risultati ottenuti permettono di sostenere l´ipotesi che l´ecosistema meleto ha un impatto minimo o nullo riguardo le emissioni nette di C in atmosfera.

Zusammenfassung

Kohlenstoffflüsse und Kohlenstoffverteilung in einer Apfelanlage

In folgender Arbeit, wurde mit Hilfe eines mikrometeorologischen und ökophysiologischen Ansatzes, ein Apfelanlage, die in der Provinz Bozen (Südtirol) liegt, auf dessen Kohlenstoffflüsse untersucht. Ziel war es, die Kohlenstoffflüsse innerhalb der Apfelanlage und die Verteilung der Biomasse zu bestimmen und deren Beziehungen zu den wichtigsten ökologischen ad physiologischen Parametern zu beurteilen. In der ersten Studie wurden dafür, während eines kompletten Jahres (2010), drei weitgehend gängige Methoden eingesetzt, nämlich Eddy-Covariance, Bodenatmung und biometrischen Daten. Wir haben ein für dieses Ökosystem optimiertest Messprotokoll für die Quantifizierung der monatlichen Kohlenstoffflüsse verwendet, welches eine Querverprobung zwischen den Schätzungen aus verschiedenen Methoden ermöglichte. Zusätzlich, wurden die einzelnen Komponenten der Primärproduktion (NPP), dem Zuwachs der stehenden Biomasse, dem „Detritus-Zyklus“ und dem seitlichen Abtransport zugewiesen.

In der zweiten Studie, wird der gemessen Eddy-Covariance-Netto-Öekosystem-Kohlenstoff-Austausch und die daraus abgeleitete Bruttoprimärproduktion (GPP) und Öekosystematmung (R*eco*), für drei komplette Vegetationsperioden, präsentiert. Der Einfluss von Umweltfaktoren und physiologischen Parametern auf diese drei Kohlenstoffflüsse wurden mit einem Multiple-Regression-Modell analysiert.

Wir fanden, dass sowohl die Werte der Nettoökosystemproduktion (NEP), als auch die der Bruttoprimärproduktion (GPP) der Apfelanlage, in der Größenordnung mit jenen von natürlichen Wäldern, mit ähnlichen klimatischen Bedingungen, vergleichbar ähnlich sind, während große Unterschiede in der Verteilung der produzierten Biomasse aufgezeichnet wurden: der aus der Atmosphäre entnommene Kohlenstoff ist weitgehend der Produktion von Früchten zugeordnet worden: 49% der jährlichen NPP wurde als Apfel-Produktion aus dem Öekosystem entfernt. Das organische Material (Blätter, tote Feinwurzeln, Schnittholz und Fallobst) das dem Detritus-Zyklus zugeordnet wird, machte 46% der NPP aus, und nur 5% der NPP ging in den Zuwachs der stehenden Biomasse. Die Kohlenstoff Nutzungseffizienz (Carbon Use Efficiency, CUE), lag mit einem Jahresdurchschnitt von 0,68 ± 0,10, etwas höher als die bisher vorgeschlagenen konstanten Werte von 0,47-0,50. Die geringe Stickstoffnachfrage der Früchte und die optimale Wachstumstemperatur (11,6°C) die in der Apfelanlage gemessen wurde, werden als jene Variablen vorgeschlagen die zur hohen CUE geführt haben.

Licht und LAI hatte den stärksten Einfluss, sowohl auf NEE, als auch auf GPP. Auf einer täglichen Basis, erreichen diese beiden Kohlenstoffflüsse ihren Höhepunkt etwa um die Mittagszeit, während sie durch die hohen VPD- und Lufttemperatur-Werte am Nachmittag begrenzt zu sein scheinen. Die vorgeschlagenen Modelle können verwendet werden, um auf täglicher und jährlicher Zeitskala die Beziehungen zwischen Kohlenstoffflüssen und Umgebungsparametern erklären und simulieren zu können. In einem Kontext des globalen Wandels, muss die Öekosystem-Akklimatisierung berücksichtigt werden, um zukünftige Szenarien vorhersagen zu können.

Auf saisonaler Skala wurden markante sink/source Verhaltensmuster innerhalb der drei Jahre beobachtet: Die Apfelanlage erwies sich im Zeitraum zwischen dem Knospenaufbruch und der Vollblüte als ein Netto-sink für Kohlenstoff, während sie ca. 2-3 Wochen nach der Obsternte zur Netto-Kohlenstoff-Quelle wurde. Auf einer jährlichen Basis, wurde im Durchschnitt der mit den geernteten Äepfeln exportierte Kohlenstoff, durch die Netto-Ökosystem-Produktion (NEP) ausgeglichen. Dies ermöglicht es, die Hypothese von einer minimalen oder gar null-Auswirkung des Apfelanlage-Oekosystems auf die Netto-Kohlenstoff-Emission in die Atmosphäre zu unterstützen.

Acknowledgements

The thesis project has been carried out with financial support from:

- Potenziale di fissazione della CO_2 atmosferica da parte di una coltura del melo in Alto Adige - *Provincia Autonoma di Bolzano/Bozen.*
- Flussi di carbonio nel meleto / Carbon fluxes in the apple orchard - *PRIN 2008.*

My warmest thanks go to Prof. Massimo Tagliavini and Dr. Leonardo Montagnani, they have been two independent and stimulating sources of inspiration and encouragement throughout the whole time of my research.

Special thanks go to Dr. Christian Ceccon, Dr.ssa Francesca Scandellari, Dr. George Wellington, Dr. Paulo Cassol, Dr.ssa Tanja Mimmo, Dr.ssa Maddalena Bolognesi, and to everybody else collaborated to some extend at this research project at the University of Bolzano, without their help this work would certainly not have been possible.

Sincere thanks go also to Prof. Alexander Knohl and to the bioclimatology group of the Georg-August University of Göttingen, for the positive scientific experience I could benefit during my period by them.

A fine thank to Dr. Martin Thalheimer (Research Centre for Agriculture and Forestry, Laimburg, BZ), to Dr. Giovanni Manca (CNR, Cosenza) and to Mr. Robert Sinn (owner of the experimental site) for their precious helpfulness throughout the whole research period.

A heartfelt thank goes to my family, their sympathy has been essential to go over the hardest times that occurred during the last three years.

Finally, I would like to extend my loving thanks to my girlfriend Ylenia, while I´m with her everything gets easier.